PHYSICAL & MECHANICAL PROPERTIES OF

NATURAL FIBER THERMOPLASTIC COMPOSITE

(PP MATRIX WITH PINEAPPLE FIBER)

RATCHAPHON TANGNOPPHAPATON

A THESIS SUBMITTED IN PARTIAL FULFILLMENT

OF THE REQUIREMENT FOR THE DEGREE OF

MASTER OF ENGINEERING IN AUTOMOTIVE ENGINEERING

(INTERNATIONAL PROGRAM)

INTERNATIONAL COLLEGE

KING MONGKUT'S INSTITUTE OF TECHNOLOGY LADKRABANG

2011

Thesis Title	Physical & Mechanical properties of Natural Fiber Thermoplastic Composite (PP matrix with Pineapple fiber)
Student	Mr. Ratchaphon Tangnopphapaton
Student ID	51061902
Degree	Master of Engineering
Program	Automotive Engineering (International Program)
Year	2011
Thesis Advisor	Asst. Prof. Dr. Surat Areerat
	Dr. Wuttipong Rungseesantivanon
	Prof. Isao Satoh
	Assoc. Prof. Takushi Saito

ABSTRACT

The study investigates the feasibility of using polypropylene (PP) and pineapple fiber to manufacture experimental thermoplastic composite. This investigation is focused on the effects of fiber content on physical and mechanical properties of this composite. The treatment method of fiber is applied to this research to improve efficiency and thermal properties of pineapple fiber. The main factor that influenced all the properties of pineapple fiber composite was adhesion surface. In order to improve the poor interfacial interaction between the hydrophilic natural fibers and the hydrophobic matrix PP, maleic anhydride (MA) grafted PP (PP-g-MA) was used as a compatibilizer. The surface adhesion between matrix and natural fiber increase which is increased percentage of compatibilizer. On the mechanical properties, the tensile strength of these composites was decreased 3.2% compared to pure polypropylene. On the other hand,

flexural strength and impact strength these composites were increased 10% and 42.3% respectively. The thermal properties were improved in the term of service temperature and processing temperature. Morphology and microstructure of fractured surfaces were analyzed and discussed using SEM. Moreover, the rheological behavior of short pineapple fiber reinforced polypropylene composites containing short pineapple fiber has been studied. The effect of fiber loading, shear rate, shear stress and temperature on the rheological behavior of the composites was studies.

The major objective is new composites materials having natural fiber as reinforcement in polypropylene based thermoplastic matrix were prepared by extrusion method. Moreover, this new composites material can applied to automotive part in the future.

ACKNOWLEDGEMENT

This thesis could not be completed without the assistance of many persons to whom I would like to express my sincere appreciation.

First, I would like to sincerely thank Dr. Wuttipong Rungseesantivanon who has given me many suggestions, fulfill discussions during the undertaken research.

I would like to sincerely thank Asst. Prof. Dr. Surat Areerat for kind advising and helping, Prof. Isao Satoh and Assoc. Prof. Takushi Saito for the suggestion of this thesis.

Moreover, I would like to acknowledge Mrs. Buapan Puangsin, Department of Forest Products, Kasetsart University, for providing the laboratory equipments and instruments. I would like to gratitude to National Metal and Materials Technology Center (MTEC), especially the plastic laboratory for support all equipments and instruments as well as financial supporting.

I am grateful to National Science and Technology Development Agency (NSTDA) which provided the full scholarship for studying in the master program.

Finally, I have special thanks to MTEC Plastic laboratory's members for helping me during the experiment and helpful for discussion.

Ratchaphon Tangnopphapaton

CONTENTS

Page

CONTENTS (CONT.)

Page

CONTENTS (CONT.)

Page

CONTENTS (CONT.)

Page

CONTENTS (CONT.)

Page

CONTENTS (CONT.)

Page

LIST OF TABLES

Table Page

LIST OF FIGURES

Figure Page

LIST OF FIGURES (CONT.)

Figure Page

LIST OF FIGURES (CONT.)

Figure Page

LIST OF FIGURES (CONT.)

Figure Page

LIST OF FIGURES (CONT.)

Figure Page

CHAPTER 1

INTRODUCTION

1.1 Significance and Background

Thermoplastic composite is a blend of plastic and natural fiber. There are widely used in many industries such as the aircraft, automobile, leisure, electronic, and medical industries [10]. The use of natural fibers in thermoplastics composite has recently attracted increased attention, due to the increasingly stringent government regulations and growing environmental awareness. The potential advantages of natural fibers, apart from their environmental benefits, are the abundant availability of the raw materials from renewable resources, rather than fossil sources, their low cost and light weight. Also, they have high specific strength due to their low density. Furthermore, it is possible to obtain a higher loading of natural fibers in compounding process.The main disadvantages of natural fibers are: their low permissible processing temperature, their tendency to form clumps, and their hydrophilic nature.

Currently, plenty of research material is being generated on the potential of cellulose based fibers as reinforcement for plastics [47]. The major component of natural fibers are consist of cellulose, such as seed fibers (cotton, kapok, etc.) and more complex materials where cellulose is associated with hemicelluloses, lignin, peptic cements, etc., such as leaf fibers, blast fibers or wood.

In fact, the most important problem in the thermoplastics composite compounding is the fiber matrix adhesion. The role of the matrix in a fiber reinforced composite is to transfer the load to the stiff fibers through shear through shear stresses at the interface. The process requires a good bond between the polymeric matrix and fibers. Poor adhesion at the interface means that the full capabilities of the composite cannot be exploited and leaves it vulnerable to

environmental attacks that may weaken it, thus reducing its life span. Also, the mechanical properties of natural fiber reinforced polymer composites are poor. These properties may be improved by physical treatments (cold plasma treatment, corona treatment) and chemical treatment (maleic anhydride, organosilanes, isocyanates, sodium hydroxide, permanganate and peroxide). Treatment process helps to increase mechanical property of fiber about 5-10 times of untreament fiber [9].

In this study, the thermoplastic polypropylene (PP) composite aim to the one choice of the customer that looking to light weight and high mechanical property material. Also, the parameter properties for injection molding process were investigated. This study makes the new natural fiber thermoplastic composite datasheet. The main problem with natural fiber thermoplastic composites has been the poor interfacial interaction between the hydrophilic natural fibers and the hydrophobic matrix PP. Therefore, maleic anhydride grafted PP (PP-g-MA), which is compatible with PP and can react with the hydroxyl groups of the fiber, was used as a compatibilizer in this study.

1.2 Objectives

1.2.1 To make the new composite materials having natural fiber as reinforcement in polypropylene based thermoplastic matrix were prepared by compounding process using twin-screwextrusion method.

1.2.2 To investigate the properties of PP/natural fiber composite for injection molding process.

1.3 Scopes

1.3.1 The first study was on the fiber extraction process by using various defibrator techniques. Also, the compounding process of polypropylene and pineapple fiber

was treated in various percentage of maleic anhydride grafted PP (PP-g-MA) and various percentage of pineapple fiber.

1.3.2 Furthermore, studied the physical properties, mechanical properties, thermal properties and rheological properties including morphological properties of the natural fiber thermoplastics composite.

CHAPTER 2

LITERATURE REVIEWS

2.1 Introduction to polypropylene

Polypropylene (PP) is a thermoplastic polymer, made by the chemical industry and used in a wide variety of applications, including packaging, textiles (e.g. ropes, thermal underwear and carpets), stationery, plastic parts and reusable containers of various types, laboratory equipment, loudspeakers, automotive components, and polymer banknotes [44]. An addition PP made from the propylene monomer, it is rugged and unusually resistant to many chemical solvents, bases and acids [38].

Structurally, it is a vinyl polymer, and is similar to polyethylene, only that on every other carbon atom in the backbone chain has a methyl group attached to it. Polypropylene can be made from the propylene monomer by Ziegler-Natta polymerization[19] and by metallocene catalysis polymerization[20]. The structure of polypropylene is shown in Figure 2.1.

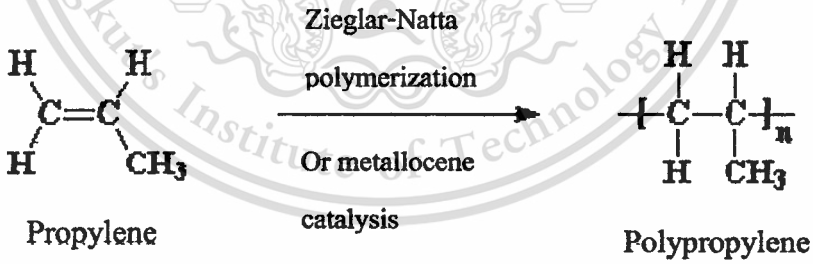

Figure 2.1 The structure of polypropylene

Most commercial polypropylene is isotactic and has an intermediate level of crystallinity between that of low-density polyethylene (LDPE) and high-density polyethylene (HDPE). Polypropylene is normally tough and flexible, especially when copolymerized with ethylene monomer. This allows polypropylene to be used as an engineering plastic, competing with materials such as ABS. Polypropylene is reasonably economical, and can be made translucent when uncolored but

is not as readily made transparent as polystyrene, acrylic, or certain other plastics. It is often opaque or colored using pigments. Polypropylene has good resistance to fatigue. Moreover, the thermal properties of polypropylene are also continually explained. The melting of polypropylene occurs as a range, so a melting point is determined by finding the highest temperature of a differential scanning calorimetry chart. Perfectly isotactic PP has a melting point of 171 °C (340 °F). Commercial isotactic PP has a melting point that ranges from 160 to 166 °C (320 to 331 °F), depending on atactic material and crystallinity. Syndiotactic PP with a crystallinity of 30% has a melting point of 130 °C (266 °F) [48].

The melt flow rate (MFR) or melt flow index (MFI) is a measure of molecular weight of polypropylene. The measure helps to determine how easily the molten raw material will flow during processing. Polypropylene with higher MFR will fill the plastic mold more easily during the injection or blow-molding production process. As the melt flow increases, however, some physical properties, like impact strength, will decrease.

There are three general types of polypropylene: homopolymer, random copolymer, and block copolymer. The comonomer used is typically ethylene. Ethylene-propylene rubber or EPDM added to polypropylene homopolymer increases its low temperature impact strength. Randomly polymerized ethylene monomer added to polypropylene homopolymer decreases the polymer crystallinity and makes the polymer more transparent.

Polypropylene is liable to chain degradation from exposure to heat and UV radiation such as that present in sunlight. Oxidation usually occurs at the tertiary carbon atom present in every repeat unit. A free radical is formed here, and then reacts further with oxygen, followed by chain scission to yield aldehydes and carboxylic acids. In external applications, it shows up as a network of fine cracks and crazes that become deeper and more severe with time of exposure.

For external applications, UV-absorbing additives must be used. Carbon black also provides some protection from UV attack. The polymer can also be oxidized at high temperatures, a common problem during molding operations. Anti-oxidants are normally added to prevent polymer degradation.

2.2 Introduction to pineapple fiber [7]

Pineapple fiber is one of the most widely used natural fibers in yarns, ropes, twines, cords, rugs, carpets, mattresses, mats, and handcrafted articles. During the past two decades pineapple fibers have also been used as reinforcement in cement and polymer based composites. The pineapple reinforcement can be used as short randomly distributed fibers, long oriented fibers, or as a fiber fabric. Pineapple fibers (Agave sisalana) are extracted from pineapple plant leaves (see Figure 2.3a) in the form of long fiber bundles. A pineapple plant produces between 200 and 250 leaves before flowering, each of which contains approximately 700–1400 fiber bundles with a length of about 0.5–1.0 m. The pineapple leaf consists of a sandwich structure composed of approximately 4% fiber, 1% cuticle, 8% dry matter, and 87% water.

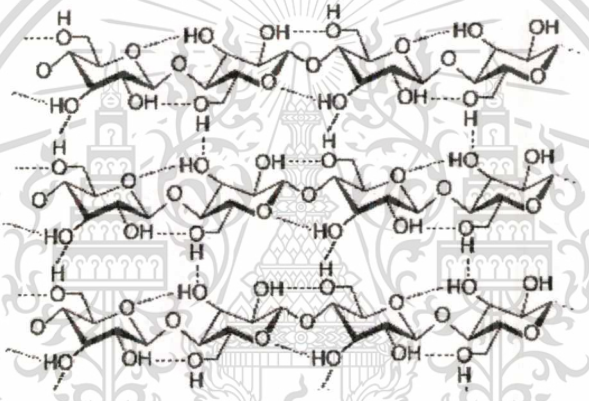

Figure 2.2 Chemical structure of cellulose

Figure 2.3 The pineapple: (a) its plant, (b) cross-section view, and (c) optical microscopy of region selected in (b).

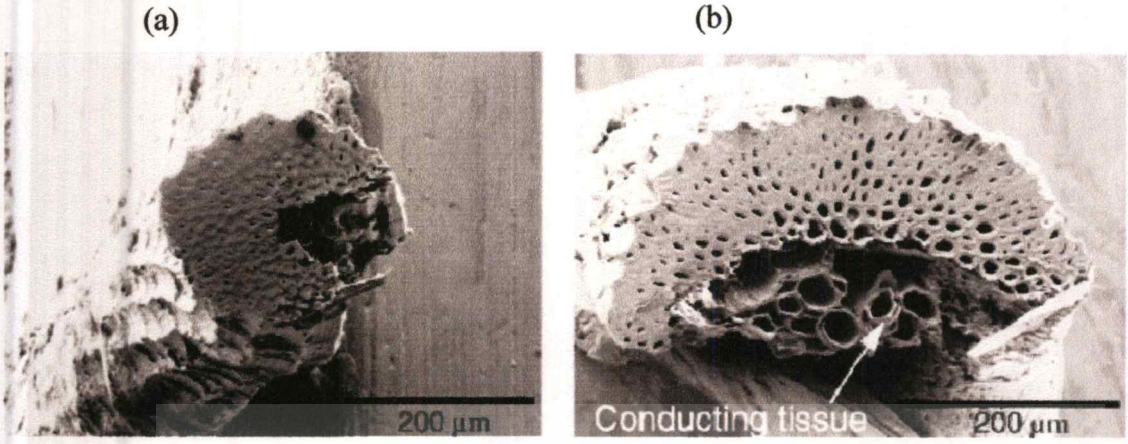

Figure 2.4 Different pineapple fiber types: (a) structural fiber with a horse shoe shape geometry and (b) arch fiber.

Within the leaf, there are three basic types of fibers: structural, arch, and xylem fibers. The structural fibers give the pineapple leaf its stiffness and are found in the periphery of the leaf (see Figure 2.3b and c). The equivalent diameter of the fibers is around 200 µm and the cross-section is rarely circular and usually has a ''horseshoe" shape (see Figure 2.4a). The structural fibers are of great importance commercially because they almost never split during the process of extraction. The arch fibers grow in association with the conducting tissues of the plant (see Figure 2.4b) and are usually found in the middle of the leaf (see Figure 2.4b). These fibers run from base to tip of the plant and have good mechanical strength. The xylem fibers grow opposite to the arch fibers and are connected to them through the conducting tissues. According to Nutman[21], they are composed of thin walled cells, and are invariably broken up and lost during the process of fiber extraction.

It is interesting to note that the pineapple fiber has a hierarchical structure. Every fiber contains numerous elongated individual fibers, or fiber-cells, which are about 6–30 µm in diameter. Each fiber-cell is made up of four main parts, namely the primary wall, the thick secondary wall, the tertiary wall, and the lumen (see Figure 2.5). The fiber-cells are linked together by means of the middle lamellae (ML), which consist of hemicellulose and lignin (see Figure 2.5). The lumen varies in size but is usually well-defined. The walls consist of several layers of fibrillar structure consisting of fibrillae which are linked together by lignin. In the primary wall, the fibrillae have a

reticulated structure, while in the outer secondary wall the fibrillae are arranged in spirals. The thin, innermost, tertiary wall has a parallel fibrillar structure and encloses the lumen. The fibrillae are, in turn, built of micro-fibrillae with a thickness of about 20 nm. The micro-fibrillae are composed of cellulose chains with a thickness of around 0.7 nm and a length of a few micrometer and are linked together by means of hemicelluloses[22].

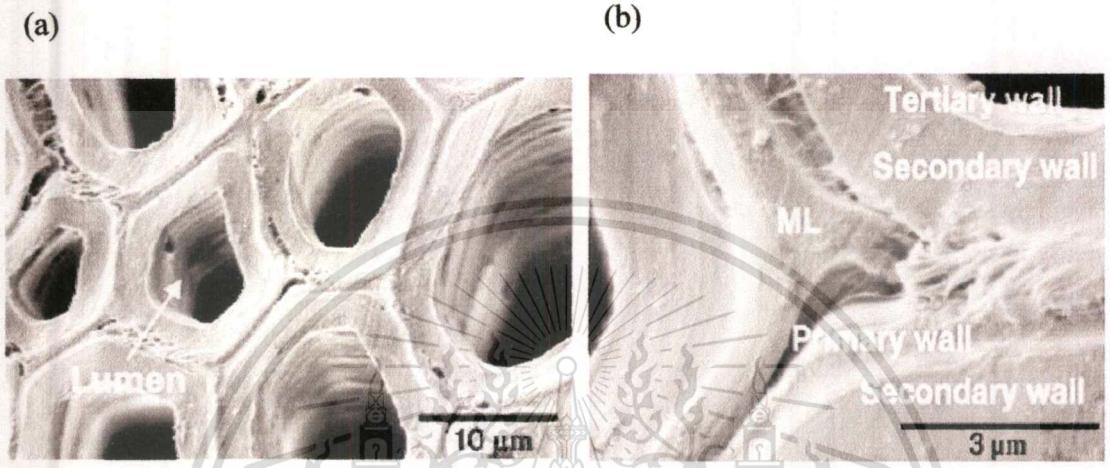

Figure 2.5 Pineapple fiber microstructure showing (a) fiber-cells with lumen and middle lamellae and (b) detail of ML and cell-walls.

2.3 Introduction to composite material [14]

The definition of a composite is that a composite material contains a chemically and/or physically distinct phase distributed within another continuous phase and exhibits properties that are different from both of these.

Historically, composite materials have been used for centuries in one form or another, for example, straw reinforced mud bricks, paper and concrete. Wood and bone are an example of naturally occurring composites. Artificial composites are based on fibrous materials bound together with resins, one of the earliest synthetic types being glass reinforced polyester.

Composites are especially attractive for their high specific strength (stress/density or σ/ρ) and modulus (stress/stiffness or σ/E) and low density (mass/volume or m/v). This has led to great interest in their research and development in the past few decades, particularly for aero

applications where additional payload capacity and engine efficiency are paramount. In more recent times the automotive industry has shown interest in structural (primary load carrying members) composite materials for similar reasons, although the effects of exhaust emissions on the environment has provided the impetus for the lightweight vehicle of the future. Composites also offer numerous advantages over many traditional materials like metals, including low density and enhanced corrosion and temperature capability.

2.3.1 Why add fibers to the matrix?[17, 18]

Some monolithic (consisting of a single material) materials that are isotropic (havinguniform physical properties in all directions) and homogeneous, such as thermosetting polymers, e.g., epoxies, polyesters, and phenolics, intermetallics, e.g., titanium aluminideand molybdenum disilicide, and ceramics, would make ideal engineering materials in terms of strength or wear resistance, but often exhibit brittle behavior and low fracture toughness (as, for example, does window glass) leading to failure. In other words, such materials do not deform with a large degree of plasticity at room temperature. Failure typically occurs by propagation of cracks nucleated from processing defects such as pores or from surface abrasions such as scratches or machining marks. Failure of brittle materials has been well characterised after the Griffith theory of 1920 which identified that the strength of a material was dependent on the size of the flaws it contained.

2.3.2 The importance of fracture toughness [44]

The resistance of a material to crack propagation is described by its fracture toughness (Kc) and is the value of critical stress necessary to propagate a crack. The lower value of this parameter is more brittle of the material. It is thus possible to enhance the ultimate tensile strength of a material (UTS) by either changing the critical flaw size through processing, for example, or by changing the fracture toughness via microstructural modifications to form a composite structure or toughening mechanism. Various toughening techniques have been utilized including phase transformation, microcrack, particle toughening and toughening by the addition of fibers and/or whiskers. Most of these are limited to specific materials or chemistries. The most versatile method by far of improving the fracture toughness is through the addition of fibers. Glass and polyester, for example, both have a Kc of ~ 0.7 $MPa\sqrt{m}$ whereas a 50% glass filled polyester composite has a fracture toughness of ~ 50 $MPa\sqrt{m}$. Fibrous composites may be manufactured

using a vast range of matrices and reinforcements and their properties can be altered substantially by changes in constitution and quantity of the respective components. When materials for use in composites are selected, the most important criteria's are thermal expansion matching, density, creep behavior, modulus and the chemical compatibility between the fiber and matrix. Of additional importance are the ability of the reinforcement to withstand the processing conditions and the ability of the matrix to infiltrate the fibers adequately. One of the most significant tests of composite quality is that the composite does not fail in a catastrophic manner but gracefully, in a tough manner, much as metals do. Figure 2.6 is a schematic stress/strain plot illustrating the desired failure characteristics of a composite in contrast to a brittle monolithic material.

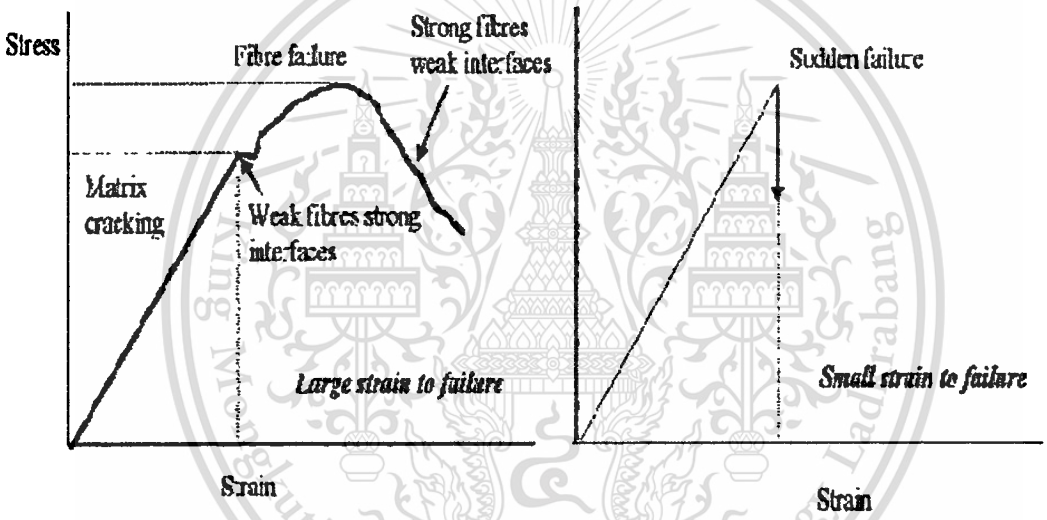

Figure 2.6 Schematic stress/strain plot for a composite with high fracture toughness [14]

It can be seen in Figure 2.6that initially, there is a linear portion to the curve and a subsequent load drop corresponding to the matrix cracking. It should be noted that this does not result in failure of the composite. As the stress is increased the matrix continues to crack and in so doing absorbs energy. Progressively more and more of the load is transferred to the fibers until at the maximum stress (σmax) they carry all of the load. After this maximum the fibers begin to break but continue to dissipate energy by pulling out of the matrix, resulting in a work of fracture many times that of its monolithic counterpart, as previously noted. The way in which load is transferred between the matrix and fiber in the composite is a very important parameter in attaining composite toughness.

2.3.3 Performance of the reinforcement [4, 9, 17]

Composites may be broadly classified according to the nature of the matrix phase – for example, metal matrix composite (MMC), polymer matrix composite (PMC) or ceramic matrix composite (CMC). The scope of this discussion will be limited to those composites that have brittle polymer matrices. Reinforcements may be in the form of single crystal whiskers, platelets, long fibers, short fibers, small particles or precipitates (or a combination of any of these) which are typically supported in a less brittle matrix. Materials in the fibrous form exhibit much greater strengths than in any other form, and furthermore the smaller the diameter of the fiber the greater the strength, see Figure 2.7.

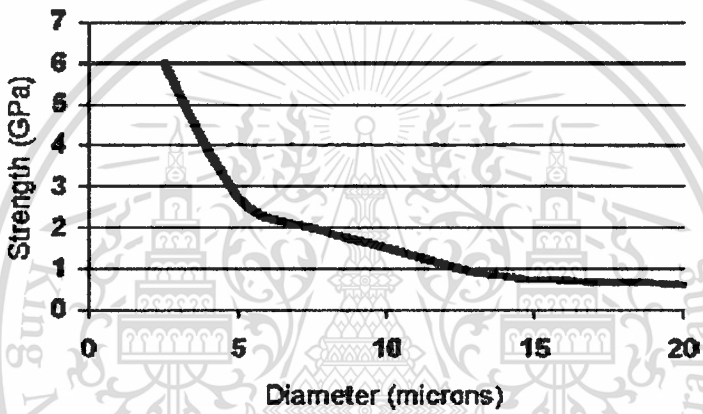

Figure 2.7 Reducing fiber diameter increases tensile strength [23]

This may be explained first by preferred orientation produced during drawing or spinning of fibers and secondly by considering failure as a statistical process induced by flaws (briefly mentioned in the introduction). Quite simply, the smaller of the fiber is the less likelihood of its containing a critical flaw.

In view of this fact, it is crucial to composite integrity that the surface of the fiber be protected from damage during fabrication. Hence, a sizing agent of some description is applied, which not only must be compatible with the fiber but also with the matrix material for optimum bonding. In polymer composites this protective coating is the foundation of the fiber/matrix interface which has a very important function.

The purpose of the matrix is to allow the fibers to be formed into a useful shape, to transport load to the fibers throughout the composite (via an interface) and to protect them from damage and corrosion.

Fibrous reinforcements are available in a variety of diameters but generally fall into the range of 5 to 100 μm. Reinforcements are available in the form of long or short fibers in a variety of architectures including continuous and discontinuous mats and woven roves as well as chopped and continuous strands or laminates. The diameter and length very much dictate the format of reinforcement (and properties). Large diameter fibers, such as silicon carbide or sapphire monofilaments are formed into shape by filament winding for example, where the bend radius on the fiber is shallow. Small diameter fibers such as glass can easily be formed directly into complex mold as mats or roves or if discontinuous may be injected into the cavity. Fibers will generally classify into four categories; glass, ceramic, metal or polymer, as do matrices. The processing route of the composite is usually dictated by the matrix material. Production of polymer composites invariably involves low temperature/low pressure compression and injection of resin into a cavity whereas metal and ceramic matrix composites require high pressure and/or temperature sintering or melting operations.

2.4 Properties of natural fiber reinforced composite material

2.4.1 Properties of short fiber reinforced composite materials[11-13]

The preceding analysis of composites has concentrated on the continuous fiber unidirectional or random fiber composites. Discontinuous fiber composites are most often used in injection molding, where the action of the screw in the injection molding barrel breaks down the fibers to lengths between 1 mm and 10 mm. Discontinuous fibers are also found in some compression molded composites such as glass mat thermoplastic (GMT) and sheet molding compound (SMC). For SMC and GMT compression moldings short glass fibers are used where greater flow lengths are required. Continuous fibers may block flow, whereas the shorter fibers will be transported along with the matrix to the extremities of the mold, thus giving higher quality moldings.

2.4.2 Fiber length distributions [11-13, 17, 45]

Fiber length distribution is important in short-fiber composites. Processing operations such as extrusion, commonly used for thermoplastic and metal matrix composites, can cause extensive fiber fracture, with strong effects on mechanical properties. The techniques used to determine the fiber length distribution can be classified broadly into indirect and direct methods. The indirect methods involve the measurement of some physical property of the composite, such as strength or modulus, which depends on the fiber length. This is an imprecise approach, although it may have some value in quality control. In direct methods, the fibers are separated from the matrix, since it is virtually impossible to make any useful measurements in situ. This is usually done by dissolving the matrix, so as to form a suspension of fibers, which are then deposited onto a suitable substrate for examination with the optical or scanning electron microscope[24]. An alternative approach involves filtering the fibers through a series of sieves to separate the different length fractions, but this is subject to errors by long fibers slipping through at steep angles to the sieve plane, or short ones becoming trapped by the presence of other fibers.

Direct measurement is straightforward, but can be time-consuming. An optical micrograph, such as that of Figure2.8(a), is examined, either manually or with an image analysis system, to give a series of fiber lengths. The data are plotted as a histogram, with each measured length allocated to a size bin, as shown in Figure 2.8(b). In this example, there is a pronounced skew to the distribution, with a tail at the long-fiber end. The fiber length before processing was 6 mm and the histogram shows that none of the fibers survived unbroken.

The definition of a meaningful average fiber length is difficult but two simple averages are commonly used. The number average fiber length is defined as:

$$L_N = \frac{\Sigma N_i L_i}{\Sigma N_i} \qquad \text{.....(2.1)}$$

Where N_i is the number of fibers of length L_i (i.e. within some specified range near L_i). The weight (or volume) average fiber length is defined as:

$$L_W = \frac{\Sigma W_i L_i}{\Sigma W_i} \qquad \text{.....(2.2)}$$

Where W_i is the weight of fibers of length L_i. For fibers of constant diameter, this can be expressed as:

$$L_W = \frac{\Sigma \alpha N_i L_i^2}{\Sigma \alpha N_i L_i} = \frac{\Sigma N_i L_i^2}{\Sigma N_i L_i} \quad \text{.....(2.3)}$$

Where $\alpha = \pi r^2 \rho$ ($2r$ = diameter of fibers, ρ = density). The difference between these two averages is shown in Figure 2.8(b). The number average L_N is lower than the weight average L_W. The length distribution based on weight is in many ways more meaningful, since it reflects the proportion of the total fiber content with any given length.

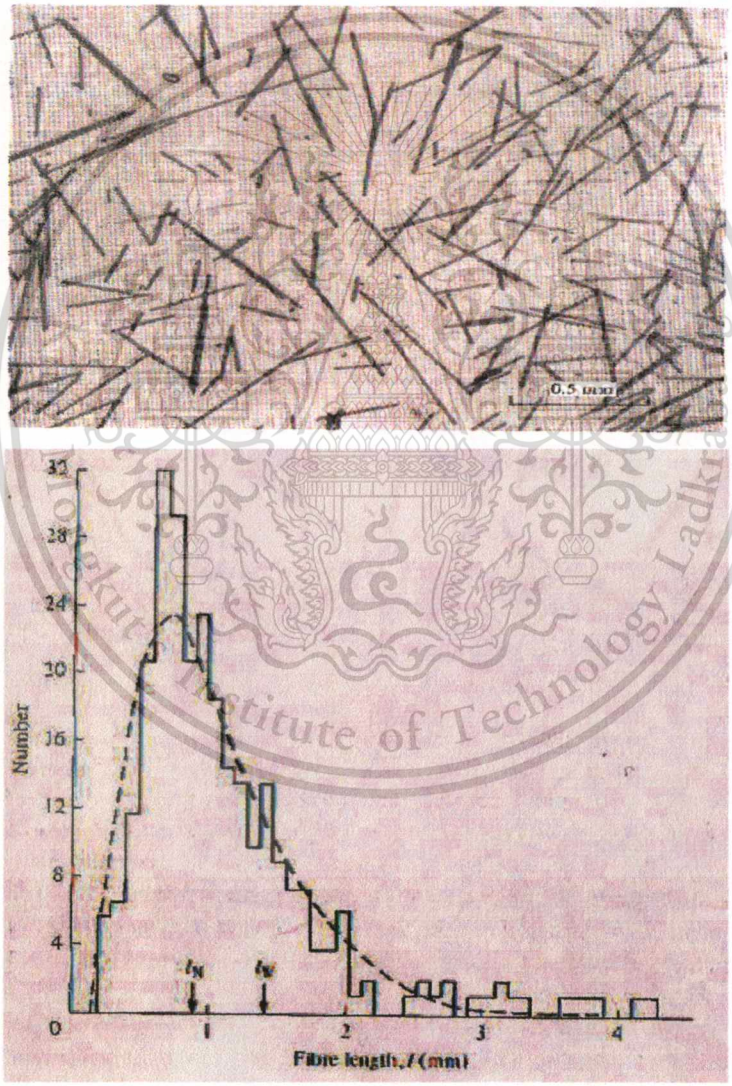

Figure 2.8 (a) Optical micrograph of short fibers separated from a thermoplastic matrix after an injection process. (b) Length histogram for fibers extracted from a thermoplastic injection molding. [25]

2.4.3 Stiffness of short fiber composites

In composites containing discontinuous reinforcements, stresses are transferred from thematrix to the fibers by shear forces at the fiber/matrix interface. The fibers may stillcarry a high proportion of the load on the composite, but there is a section at both endsof each fiber where the fiber tensile stress is still building up to it is maximum value andin which region it's reinforcing efficiency is diminished. In general this leads to short fiber composites being less stiff than continuous fiber composites. For most practicalcomposites, the stiffness of the short fiber composites is equal to that of a continuous fiber composite if the fibers are of the order of only 1 mm long (Figure 2.9).

It should be noted that in most practical short fiber composites, such as injection molded reinforced thermoplastics or dough molding compounds the fibers will usually not berandom but be slightly aligned by the fabrication process. This should be taken intoaccount during detailed design of components.

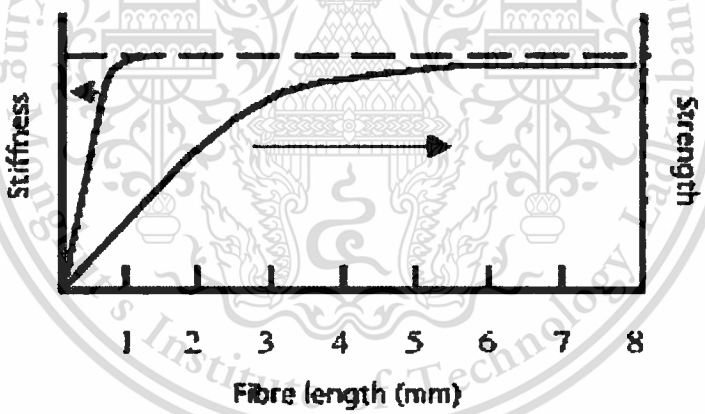

Figure 2.9 Fiber length effects

2.4.4 Strength of discontinuous fiber composites

As highlighted in section stiffness of short fiber composites, discontinuous fiber composites are loaded, throughor across the fiber matrix interface via shear forces, leading to an ineffective lengthof individual fibers at each end. Not only does this lead to a decrease in stiffness ofthe composites (when compared to continuous fiber composites) but also suffer areduction in

strength. As a guide, approximately 95% of the continuous fiber composite strength can be achieved in a short fiber composite with fibers only 8 mm-10 mm long (Figure 2.9).

One of the limiting factors on strength of short fiber composites is the fiber/matrixinterface strength. The higher the interfacial shear strength the more rapid the buildupof stress at the end of fibers therefore a stiff/strong composite requires stiff/stronginterfaces. Though as indicated previously stiffness and strength do not increase with fibers above 8 mm long, the impact properties of a material are improved through usinglonger fibers. It is generally accepted that a fiber length of approximately 20 mm isrequired in order to gain the impact properties of a continuous fiber composite (thisshould be regarded as a rule of thumb – the exact length depend on many things such asgeometry of the specimen, fiber/matrix interface strength,etc.).

2.4.5 Energy absorption and toughness

In section strength of discontinuous fiber composites on short fiber composites, it was noted that the strength of the composites can be improved with a stronger/stiffer interface. It is not always desirable for the fiber and matrix to be strongly bonded and some reasons for this will be discussed.

Fiber debonding and pull out is one of the important energy absorbing mechanisms during composite fracture. Figure 2.10illustrates a uni-directional (UD) composite which has undergone multiple fiber fracture and debonding in and around a matrix crack. Note that the matrix has failed in a brittle manner without yielding. It can also be seen that the fibers have pulled out of their 'sockets'. This mechanism increases the fracture toughness by dissipating energy. If the fiber/matrix interface is too strong, then it is possible that the composite would crack in a single fracture rather than the crack being diverted by the fibers. This single failure mechanism would reduce the toughness of the composite significantly. Other mechanisms operate in composites based on ductile matrices (such as thermoplastic polymers and metals) to dissipate energy. In most instances polymer matrix composites fail by delamination/debonding, an inherently tough mechanism. At present there exist no analytical means of deriving the energy absorption of composite structures. This topic remains the subject of research by academics and the major auto manufacturers alike.

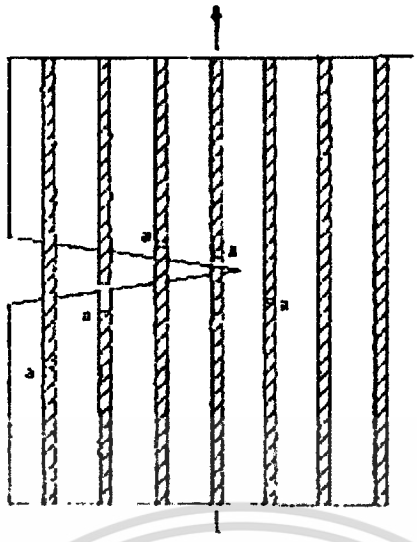

Figure 2.10 Multiple fracture and fiber pull out in a uni-directional composite.

2.4.6 Voids [26, 28, 31, 33]

Several types of voids may be present in composite materials. These can occur in all forms of composite, although there are variations in their incidence depending on fabrication route and matrix type. Large cavities can form during the manufacture of the component as a result of gross defects. Small voids often form adjacent to the fibers, either because of incomplete infiltration during processing or cavitation during deformation. Voids also form in matrix-rich pockets or fiber-free regions between laminae.

There are two main methods of evaluating the void content of materials (including composites). The first is to examine a polished section, identify the voids, either manually or automatically, and determine the area fraction, which is equal to the volume fraction in the absence of any sectioning bias. The sectioning method has the advantage of allowing the locations and shapes of the voids to be established. Examples of several types of voids are shown in Figure 2.11. The method is often inaccurate, since small voids are difficult to detect and even large ones are easily distorted by flow of matrix or loss of reinforcement fragments during polishing. It is also difficult to establish average void contents in a specimen without examining large numbers of sections.

The second technique, which is free from most of these problems, involves accurate measurement of the density of the sample. Some of the practical points involved in such measurements are

discussed by Pratten (1981). The density is determined by weighing the sample in air and then in a liquid of known density. Application of Archimedes' principle leads to the following expressing for the density (ρ) of the sample in terms of measured weights (W)

$$\rho = \left(\frac{W_a \rho_a - W_L \rho_a}{W_a - W_L} \right)$$

Where the subscripts a and$L$ refer to air and liquid. The liquid should have a high density and chemical stability and a low vapor pressure and surface tension. The most popular liquid currently in use is perfluoro-l-methyl decalin.

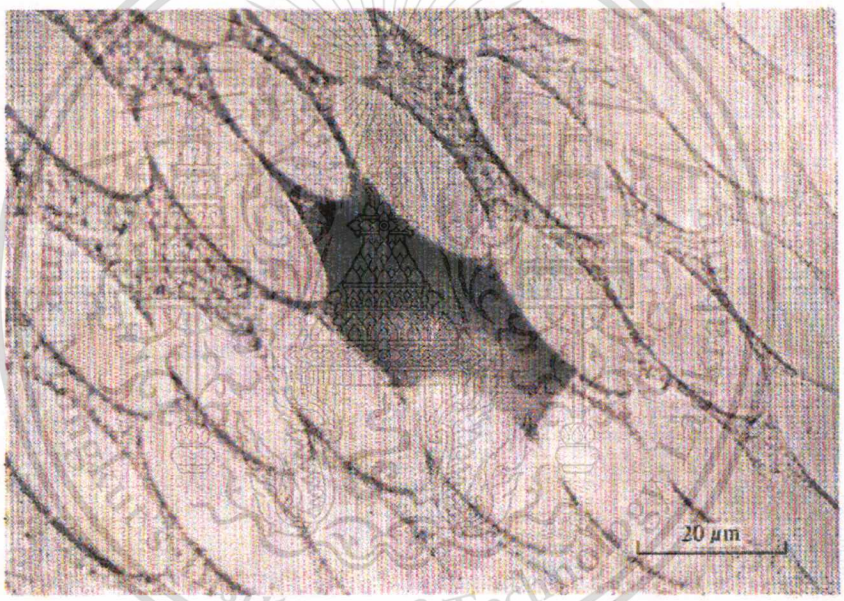

Figure 2.11 Void between fibers in a glass fiber-polyester resin lamina

2.5 The mechanism of adhesion [46]

The interaction, adhesion, between two different materials across an interface may involve either physical or chemical bonding. Chemical bonding consists of direct interlinking between molecules of the two materials, the adhesive and the substrate, by covalent or ionic bonds. Physical bonding may result from mechanical interlocking, or from the forces of physical absorption between adhesive molecules and substrate molecules, or by the penetration of adhesive

molecules into the substrate by diffusion. Thus, the mechanism of adhesive action is quite different for various types of adhesives and substrates.

2.5.1 Interdiffusion

Figure 2.12(a) shows the diffusion of free chain ends at the interface between two polymers, which leads to chain entanglements and a rise in the adhesive strength. This effect is employed in some coupling agents used on fibers in thermoplastic matrices. Interdiffusion can also take place in non-polymeric systems, particularly if it is accompanied by a chemical reaction. The adhesive strength is dependent on the nature of the resultant interatomic bonds.

2.5.2 Chemical reaction

Various types of chemical reaction may occur at the interface, either deliberately promoted or inadvertent. These can be represented, as in Figure 2.12(d), by new A-B bonds being formed as a result of interfacial chemical reactions. These bonds may be covalent, ionic, metallic, etc., and in many cases are very strong. There are many examples of the interfacial bond strength being raised by localized chemical reactions, but it is often observed that a progressive reaction occurs which results in the formation of a brittle reaction product.

2.5.3 Electrostatic attraction

If the surfaces carry net electrical charges of opposite sign, as illustrated in Figure 2.12(b), then a sustained adhesive force may result. This effect is utilized in certain fiber treatments, as in the deposition of coupling agents on glass fibers. The surface may exhibit anionic or cationic properties, depending on the oxide in the glass and the pH of the aqueous solution used to apply the coupling agents. Thus, if ionic functional silanes are used, it is expected that the cationic functional groups will be attracted to an anionic surface and vice versa (Figure 2.12(c)). Electrostatic forces are unlikely to constitute the major adhesive bond in a composite and they can readily be reduced, for example by discharging in the presence of a strongly polar solvent, such as water.

2.5.4 Mechanical keying

There may be a contribution to the strength of the interface from the surface roughness of the fibers if good wetting has occurred, as illustrated in Figure 2.12(e). The effects are much more significant under shear loading than for decohesion as a result of tensile stressed. Some improved resistance to tensile failure results if re-entrant angles are present and there is an increase in strength under all types of loading as a consequence of the increased area of contact.

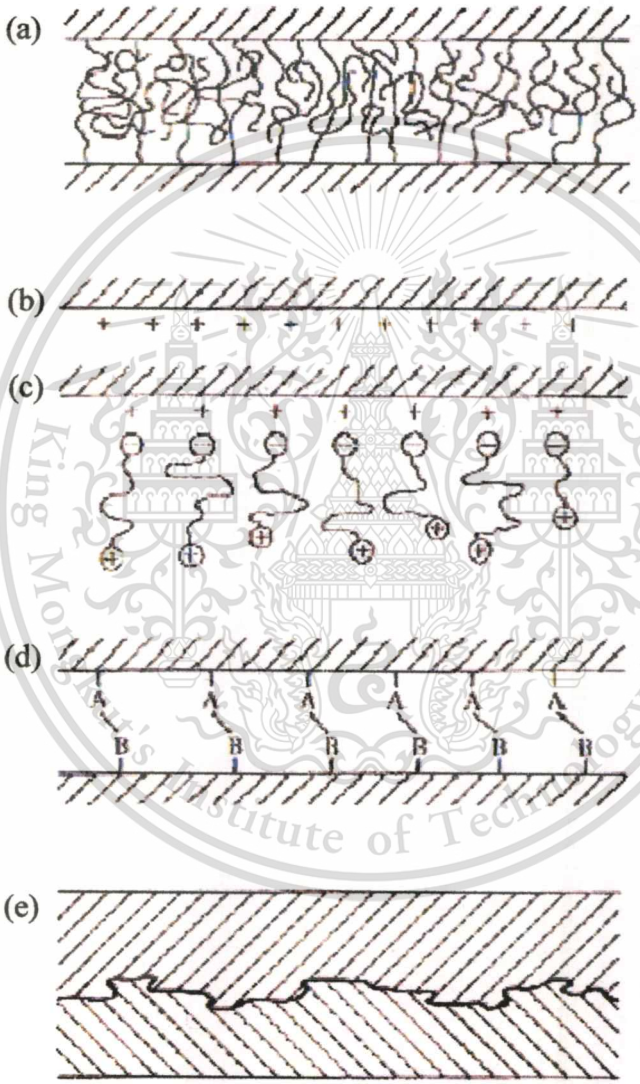

Figure 2.12 Interfacial bonds formed by (a) molecular entanglement following interdiffusion, (b) electrostatic attraction, (c) cationic groups at the end of molecules attracted to an anionic surface, resulting in polymer orientation at the surface, (d) chemical reaction and (e) mechanical keying.

2.6 Influence of MA-g-PP on abrasive wear behavior of chopped sisal fiber reinforced polypropylene composites [15]

The sisal fiber reinforce polypropylene composites with and without maleic anhydride grafted polypropylene (MA-g-PP) was developed by U.K. Dwivediand and N. Chand [15]. Different amounts of MA-g-PP, 1, 2 and 5-wt% were added to modify the composites. Abrasive wear and mechanical properties of sisal fiber reinforced polypropylene composites were determined. When increasing percentage of maleic anhydride grafted polypropylene, the tensile strength is increased. The improvement in the tensile strength is attributed to the increased adhesion between sisal fiber and PP that facilitates more stress transfer through bonding to the sisal fiber. Karnani et al. (1997) reported that this adhesion is due to the presence of MA-g-PP, which reacted with the hydroxyl group present in the sisal fiber surface. In another words, the addition of MA-g-PP increased the resistance to pullout the fiber from PP matrix. Percentage elongation of unmodified sisal fiber reinforced PP composite is highest as compared to other sisal fiber reinforced PP composites. Addition of MA-g-PP has reduced the elongation of the composite. Elongation of composites decreased with the increase of MA-g-PP contents. This decrease in elongation is due to the combined effect of (i) improvement in adhesion between fiber and matrix, and (ii) modification of matrix. Figure 2.13(a) shows the tensile fractured surface of unmodified sisal fiber reinforced PP composite. It can be seen that sisal fibers debonded easily and pulled out from matrix, which indicates poor bonding at inter face between sisal fibers and PP. Holes are created in the PP matrix as the fiber pullout and visible in Figure 2.13(a). Tensile fracture occurred in PP by the pulling of chains and the formation of voids in the bulk polymer material. Some fibers have fractured and broken after pullout. The easy pullout of fibers shows poor adhesion between sisal fibers and PP matrix. Figure 2.13(b) clearly shows the poor bonding at the fiber-matrix interface. Figure 2.13(c) exhibits the photograph of sisal fiber reinforced PP composite having 1-wt% MA-g-PP, which reflects the improved fiber-matrix interaction at interface. For more clarity at the interface, a micrograph (Figure 2.13(d)) of higher magnification of sisal fiber reinforced PP composite having 1-wt% MA-g-PP is incorporated to exhibit the

improved fiber-matrix interaction. In this figure, pullout of fibers has reduced due to the increased adhesion. Karnani et al. (1997) and Qiu et al. (2005) have investigated that the improvement of tensile strength on the addition of MA-g-PP is a common phenomenon observed with natural fibers.

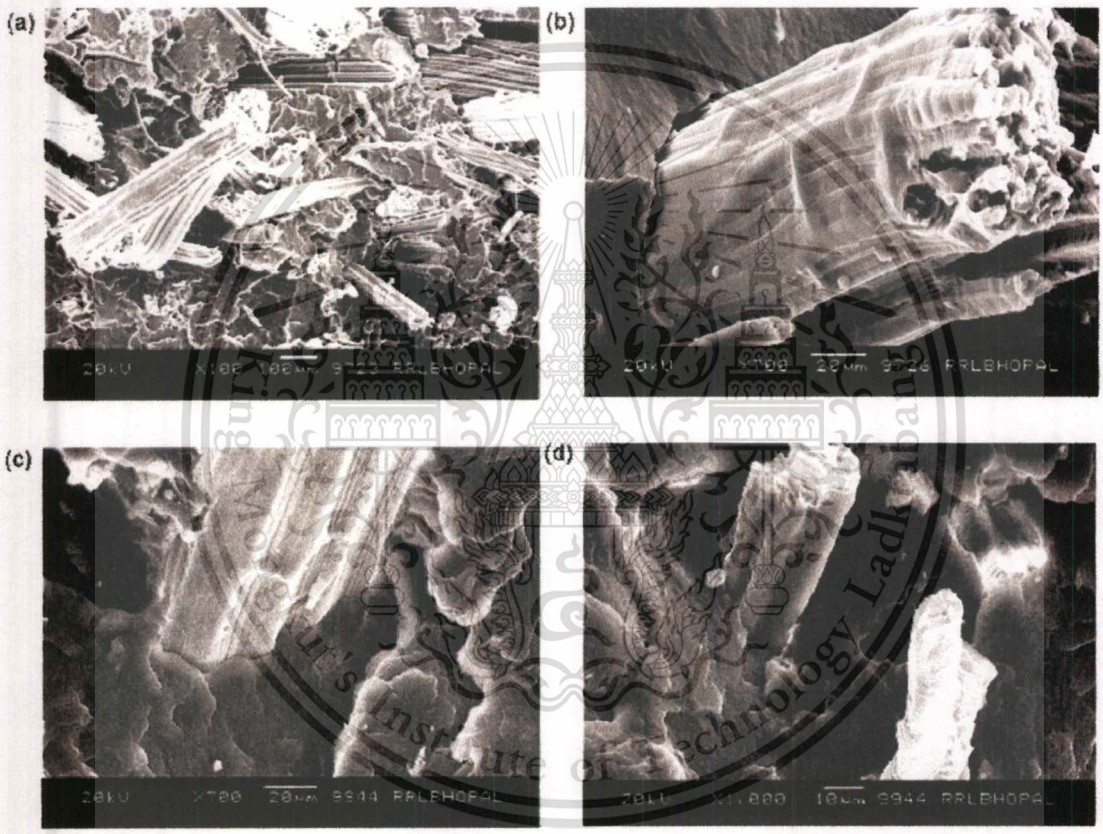

Figure 2.13 (a) shows SEM of tensile fractured surface of unmodified sisal fiber reinforced PP composite. (b) Shows magnified SEM of tensile fractured surface of unmodified sisal fiber reinforced PP composites. (c) SEM of tensile fractured surface of 1-wt% MA-g-PP modified sisal fiber reinforced PP composites. (d) Another SEM shows improved fiber–matrix interaction at interface with more clarity of 1-wt% MA-g-PP modified composite.

2.7 Rheological behavior of short sisal fiber-reinforced polystyrene composites [16]

K.C.M. Nair, R.P.Kumar and S. Thomas have studied the rheological behavior of short sisal fiber-reinforced polystyrene composites containing short sisal-fiber. The effect of fiber length, fiber loading, shear rate, shear stress and temperature on the rheological behavior of the composites was studied.

2.7.1 Effect of fiber loading and shear rate on viscosity

Figure 2.14(a) shows the variation of melt viscosity of polystyrene (PS) composites with shear rate and fiber loading at 180 °C. These curves are typical of pseudoplastic materials, which show a decrease in viscosity with increasing shear rate. The reasons for the variation of viscosity with shear rate are well established. All the systems investigated have been found to obey the power law relationship.

$$\eta = K(\gamma)^{n-1}$$

Where n is the power law index and K the consistency index.

In general, the incorporation of fibers in polymer systems increases the viscosity and goes on increasing with fiber content. At low concentration levels, the viscosity is expected to increase rapidly with increasing concentration of the fibers because of the rapidly increasing collisions between particles as they become packed more closely to each other. However, at a critical concentration level, random packing ceases to be possible and further increase in fiber concentration leads to a more orderly anisotropic structure of the fibers in suspension, and these may now slide readily past one another. Hence, above the critical concentration level, further increase in fiber concentration progressively decreases the viscosity of the system until very high concentration levels of fibers are reached. The increase in viscosity is found to be more predominant at lower shear rates where fiber and polymer molecules are not completely oriented. The addition of fiber to a polymer system will perturb the normal flow of the polymer and will

hinder the mobility of chain segments in flow. As the fiber content increases this phenomenon becomes more predominant and hence the viscosity increases further.

2.7.2 Effect of fiber length on viscosity

The variation of melt viscosity of PS-sisal composite with fiber length is given in Figure 2.14 Composites containing 20% fiber and a length of 2, 4 and 6 mm were used to study the effect of fiber length. The fiber length was limited to 6 mm as it was difficult to study the flow behavior of composites containing fibers having a length beyond 6 mm. At all shear rates studied, composites containing 4 mm fibers show the highest viscosity, composites containing 6 mm fibers show the least viscosity and those containing 2 mm fibers show a viscosity value that lies in between the two values. The decrease in viscosity on increasing fiber length is unusual. However, one possible explanation is as follows.

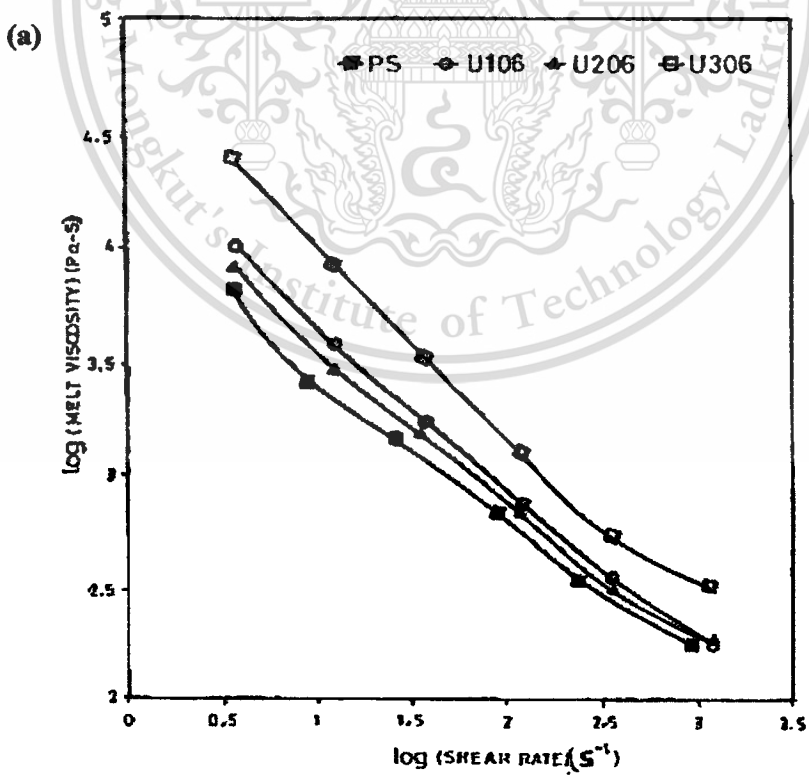

(b)

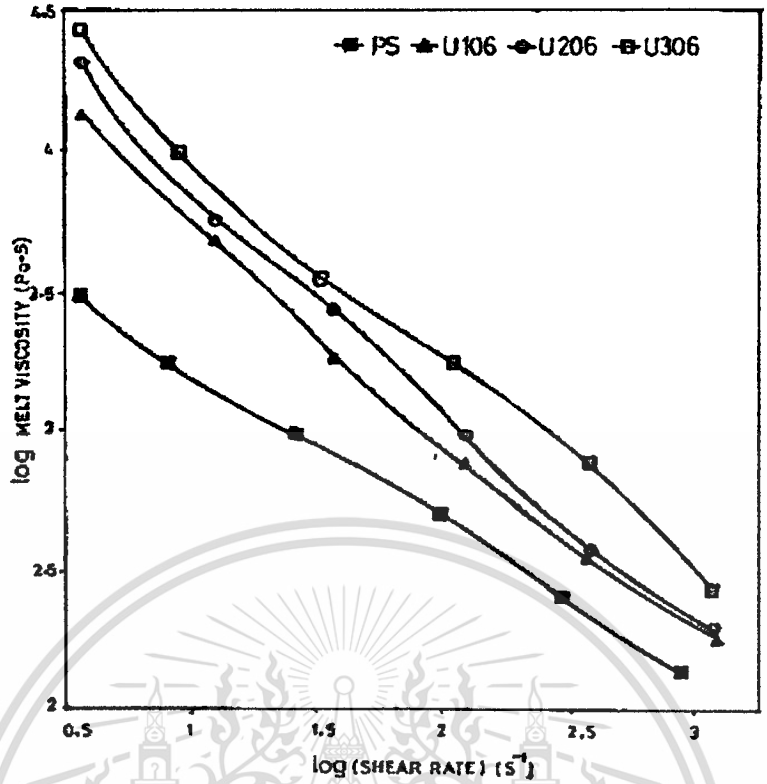

Figure 2.14 Variation of the melt viscosity of PS composites PS, U106, U206, U306 with shear rate at: (a) 180 $^{\circ}C$; and (b) 190 $^{\circ}C$

As discussed earlier, the melt viscosity of the composite is governed mainly by two factors, namely: (i) the fiber orientation that controls the wall-slip; and (ii) fiber–matrix interaction. Another factor that controls the viscosity is the distribution of fiber in the composite. A better distribution of the fiber reduces the viscosity of the composite. In the case of 6 mm fiber composite, the chance of orientation is maximum and leads to the increased wall-slip. The fiber–matrix interaction is lower in this case as the number of fibers is less and this accounts for the lowest viscosity of 6–mm fiber composite. Moreover, the long fibers at higher volume fractions may form themselves into a nematic structure, with a lot of local alignment, and the shorter fibers may rotate more as individuals. The locally aligned structure has less resistance to shearing and leads to an overall lower viscosity in the case of long fiber composites. As the fiber length decreases the chances for fiber orientation decreases and fiber–matrix interaction increases.

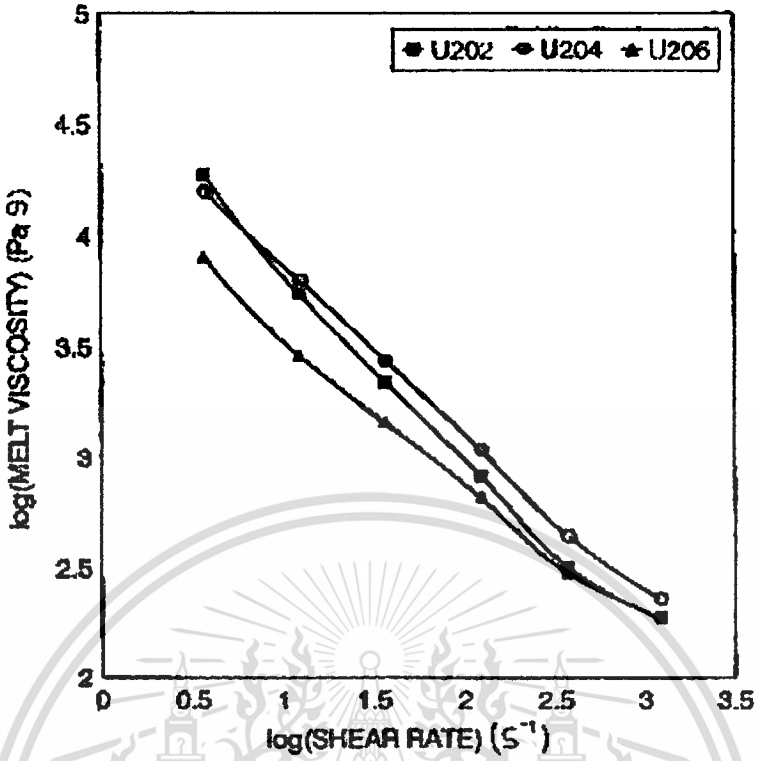

Figure 2.15 Variation of the melt viscosity of PS-composite with fiber length at different shear rates.

2.7.3 Effect of temperature on viscosity

The effect of temperature on the viscosity of polymers is important as the polymers undergo considerable temperature changes during their processing. Generally, the viscosity decreases with temperature at all fiber loading. This is due to the accelerated molecular motion at higher temperature due to the availability of greater free volume and also due to the decreasing entanglement density and weaker intermolecular interactions at higher temperature. Generally, the viscosity decreases with temperature and the same trend is observed with pure PS too. However, PS-sisal composites show a reverse tendency, i.e. the viscosity of the composites increases with temperature. As discussed earlier, the viscosity of the composite is controlled by the fiber–matrix interaction that increases the viscosity, and increased wall slip due to the presence of longitudinally oriented fibers along the wall–melt interface, which decreases the viscosity.

2.8 Injection molding [32-33]

Injection molding is a manufacturing process for producing parts from both thermoplastic and thermosettingplastic materials. Material is fed into a heated barrel, mixed, and forced into a mold cavity where it cools and hardens to the configuration of the mold cavity. After a product is designed, usually by an industrial designer or an engineer, molds are made by a mold maker (or toolmaker) from metal, usually either steel or aluminum, and precision-machined to form the features of the desired part. Injection molding is widely used for manufacturing a variety of parts, from the smallest component to entire body panels of cars. Injection molding is used to create many things such as wire spools, packaging, bottle caps, automotive dashboards, pocket combs, and most other plastic products available today. Injection molding is the most common method of part manufacturing. It is ideal for producing high volumes of the same object. Some advantages of injection molding are high production rates, repeatable high tolerances, the ability to use a wide range of materials, low labor cost, minimal scrap losses, and little need to finish parts after molding. Some disadvantages of this process are expensive equipment investment, potentially high running costs, and the need to design moldable parts. Injection molding machines consist of a material hopper, an injection ram or screw-type plunger, and a heating unit. They are also known as presses, they hold the molds in which the components are shaped. Presses are rated by tonnage, which expresses the amount of clamping force that the machine can exert. This force keeps the mold closed during the injection process. Tonnage can vary from less than 5 tons to 6000 tons, with the higher figures used in comparatively few manufacturing operations. The total clamp force needed is determined by the projected area of the part being molded. This projected area is multiplied by a clamp force of from 20 to 80 kN for each square meter of the projected areas. As a rule of thumb, 60 or 80 MPa can be used for most products. If the plastic material is very stiff, it will require more injection pressure to fill the mold, thus more clamp tonnage to hold the mold closed. The required force can also be determined by the material used and the size of the part, larger parts require higher clamping force.

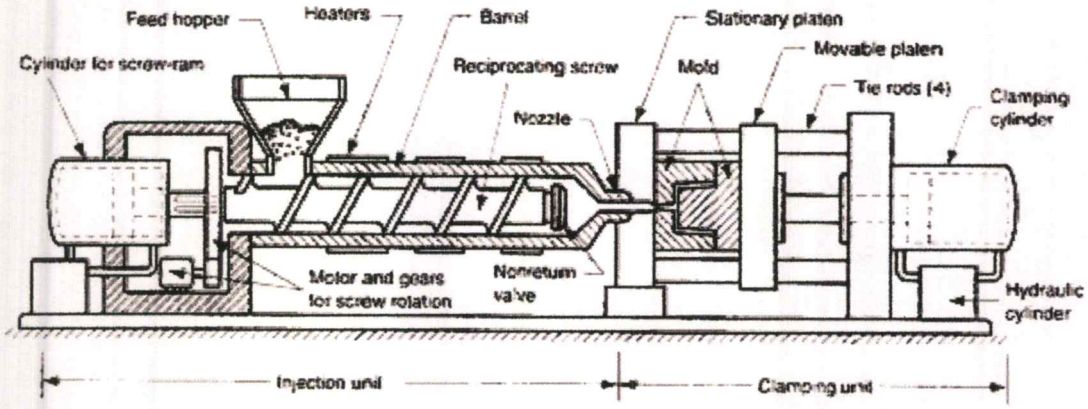

Figure 2.16 Component of injection molding machine [27]

2.8.1 Injection molding process cycle

The process cycle for injection molding is very short, typically between 2 seconds and 2 minutes, and consists of the following four stages: (see Figure2.17)

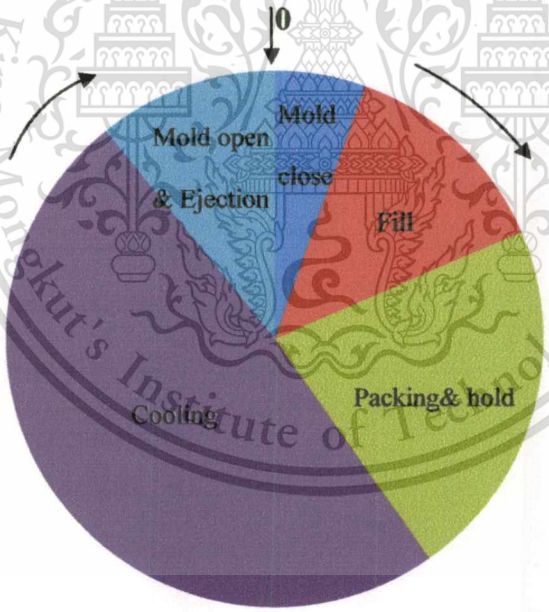

Figure 2.17 The process cycle of injection molding

- **Clamping**– Prior to the injection of the material into the mold, the two halves of the mold must first be securely closed by the clamping unit. Each half of the mold is attached to the injection molding machine and one half is allowed to slide. The electrically or hydraulically powered clamping unit pushes the mold halves together and exerts

sufficient force to keep the mold securely closed while the material is injected. The time required to close and clamp the mold is dependent upon the machine - larger machines (those with greater clamping forces) will require more time. This time can be estimated from the dry cycle time of the machine.

- **Injection** - The raw plastic material, usually in the form of pellets, is fed into the injection molding machine, and advanced towards the mold by the injection unit. During this process, the material is melted by heat and pressure. The molten plastic is then injected into the mold very quickly and the buildup of pressure packs and holds the material. The amount of material that is injected is referred to as the shot. The injection time is difficult to calculate accurately due to the complex and changing flow of the molten plastic into the mold. However, the injection time can be estimated by the shot volume, injection pressure, and injection speed.
- **Cooling** - The molten plastic that is inside the mold begins to cool as soon as it makes contact with the interior mold surfaces. As the plastic cools, it will solidify into the shape of the desired part. However, during cooling some shrinkage of the part may occur. The packing of material in the injection stage allows additional material to flow into the mold and reduce the amount of visible shrinkage. The mold cannot be opened until the required cooling time has elapsed. The cooling time can be estimated from several thermodynamic properties of the plastic and the maximum wall thickness of the part.
- **Ejection** - After sufficient time has passed, the cooled part may be ejected from the mold by the ejection system, which is attached to the rear half of the mold. When the mold is opened, a mechanism is used to push the part out of the mold. Force must be applied to eject the part because during cooling the part shrinks and adheres to the mold. In order to facilitate the ejection of the part, a mold release agent can be sprayed onto the surfaces of the mold cavity prior to injection of the material. The time that is required to open the mold and eject the part can be estimated from the dry cycle time of the machine and should include time for the part to fall free of the mold. Once the part is ejected, the mold can be clamped shut for the next shot to be injected.

2.8.2 Molding defects

Injection molding is a complex technology with possible production problems. They can be caused either by defects in the molds or more often by part processing (molding).

Table 2.1 Molding defects

Molding defect	Alternative names	Descriptions	Causes
Blister	Blistering	Raised or layered zone on surface of the part	Tool or material is too hot, often caused by a lack of cooling around the too or a faulty heater
Burn marks	Air burn/gas burn/dieseling	Black or brown burnt areas on the part located at furthest points from gate or where air is trapped	Tool lacks venting, injection speed is too high
Flash	Burrs	Excess material in thin layer exceeding normal part geometry	Mold is over packed or parting line on the tool is damaged, too much injection speed/material injected, clamping force too low. Can also be caused by dirt and contaminates around tooling surfaces.
Flow marks	Flow lines	Directionally "off tone" wavy lines or patterns	Injection speeds to slow (the plastic has cooled down too much during injection, injection speeds must be set as fast as you can get away with at all times)
Jetting		Deformed part by turbulent flow of material	Poor tool design, gate position or runner. Injection speed set too high.
Polymer degradation		Polymer breakdown from hydrolysis, oxidation etc.	Excess water in the granules, excessive temperatures in barrel

Sink marks	Sinks	Localized depression (In thicker zones)	Holding time/pressure too low, cooling time too short, with sprueless hot runners this can also be caused by the gate temperature being set too high. Excessive material or thick wall thickness
Short shot	Non-fill / Short mold	Partial part	Lack of material, injection speed or pressure too low, mold too cold, lack of gas vents
Weld line	Knit line	Discolored line where two flow fronts meet	Mold/material temperatures set too low (the material is cold when they meet, so they don't bond). Point between injection and transfer (to packing and holding) too early.

2.9 Injection molding process of short-fiber reinforced thermoplastic materials [14, 44]

The interest for injection molded components is the fiber orientation distribution. For example, it may be possible to arrange for the fibers to be oriented parallel to the direction of stress in parts of the component which will be heavily loaded in service. Fiber orientation is controlled by the nature of the flow field during filling of the mold. In general, fibers tend to become aligned parallel to the direction in which the material is becoming elongated (provided the flow is not too turbulent). This is illustrated by the schematic diagram of the flow pattern during injection into a simple rectangular mold, and the corresponding micro-radio-graphs, shown in Figure 2.18. In this case, the fibers are well aligned in the outer layers of the molding, but more randomly oriented towards the core. By predicting the flow behavior under different injection conditions for specific components, a degree of control over the final fiber orientation pattern is often possible.

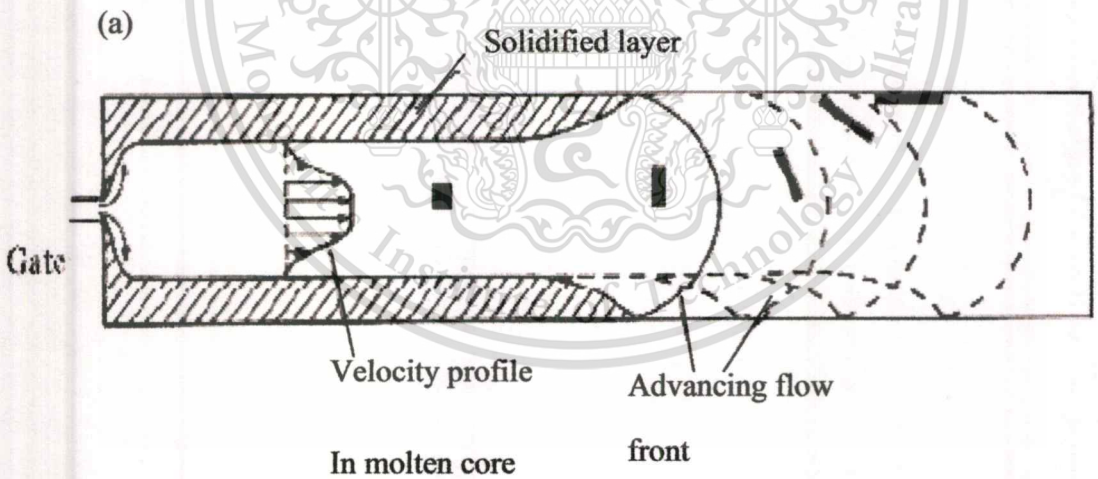

(b)

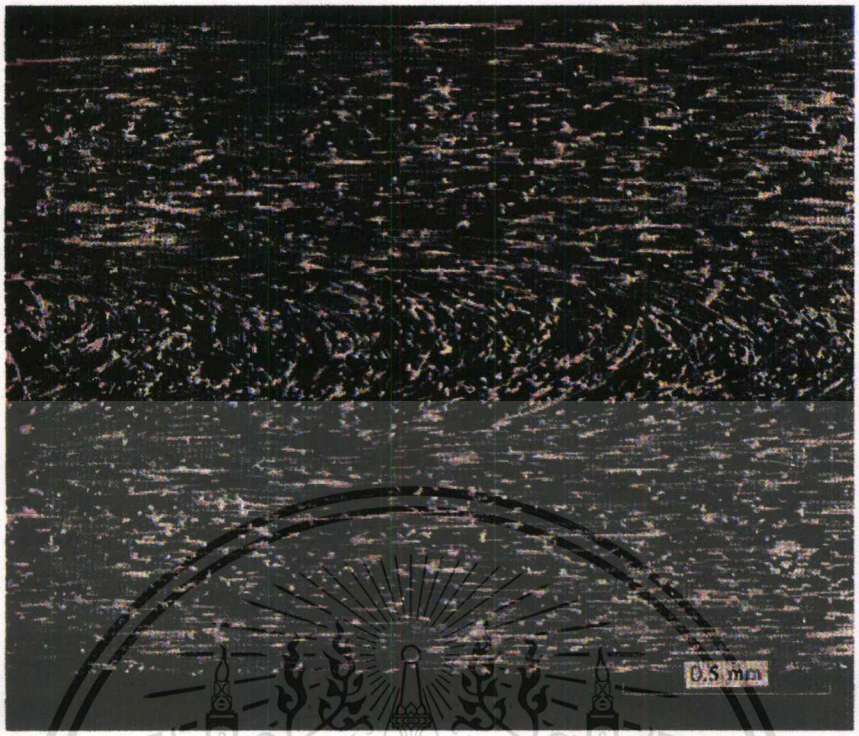

Figure 2.18 (a) Schematic diagram of the mold filling process during injection molding, showing the deformation of an initially square fluid element at successive positions of the advancing flow front. (b) Contact microradiograph of the longitudinal section of a polypropylene/15% glass fiber injection molding.

CHAPTER 3

EXPERIMENTAL PROCEDURES

3.1 Materials

The plastic used in this study was polypropylene (PP). Its commercial name is Moplen, Grade HP500N, homopolymer, supplied by Basell Service Company. The polypropylene used presents a medium-high (12 g/10min) fluidity polypropylene homopolymer. Moplen HP500N is particularly suitable for the production of heavy denier staple, fiber and continuous filament. Moplen HP500N exhibits good process stability and constant, high flow during extrusion. The natural fibers (pineapple fiber) used in this study were obtained from a crop located in the city of Prachuapkhirikhan in the western of Thailand. The compatibilizer (Maleic anhydride grafted polypropylene) or Compoline CO/PP C55 is obtained from Behn Meyer Chemical Co.Ltd. The characteristics of all material used in this study are summarized in Table 3.1.

Table 3.1 Important characteristics of the materials use in this study

Materials	Supplier	Characteristics
Polypropylene (HP500N)	Basell Service Company	MI (g/10 min): 12
Pineapple fiber	Farm in located Prachuapkhirikhan	Fiber diameter: 10 μm Length: 1-3 mm Dry Density: 1.4 kg/cm^3 Elongation at break (%): 4-9 Cellulose content (%): 85-88 Tensile strength(MPa): 450-700
Maleic anhydride grafted polypropylene		MI (g/10 min): 2.5 MAH content: 0.25-0.5 %

3.2 Experimental Procedures

3.2.1 Introduction

The overall experimental procedures in this work were based on injection molding process shown as a flow chart in Figure 3.1. Initially, the pineapple fibers were extracted from its leaf by a mechanical process as shown in Figure 3.2. In this process, the leaves are crushed by a rotating wheel with blunt knives, so that only the fibers remain. The fibers were screened and washed before drying in the sun. Proper drying is important as fiber quality depends largely on reduced moisture content. Dry fibers were combed by a machine. In Figure 3.3 is shown the microstructure of pineapple fiber. The structure was similar to honey comb. The compounding process used mixing twin screw extruder which the temperature was raised from the room temperature to the melting temperature of 190 °C.

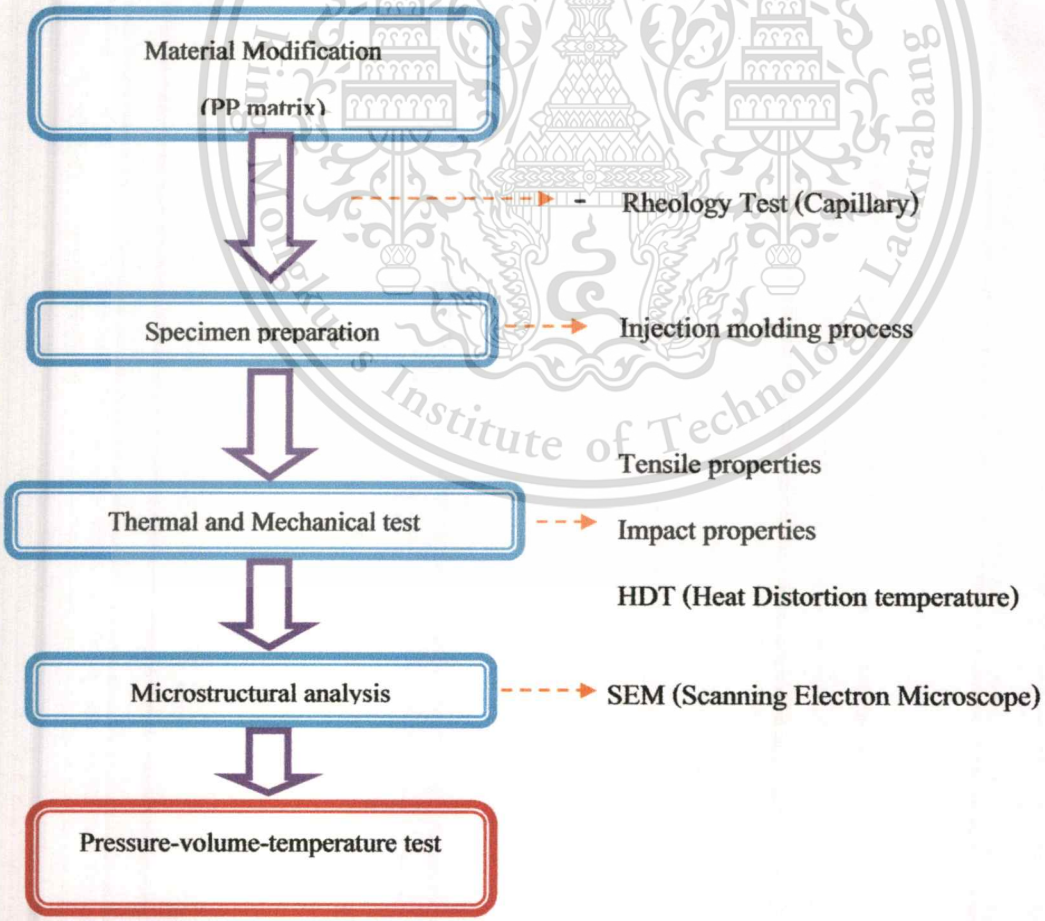

Figure 3.1 Overall experimental procedures

(a) a rotating wheel with blunt knives

(b) screen and wash

(c) Short pineapple fiber

(d) Crusher dry fiber

Figure 3.2 Fiber extraction process

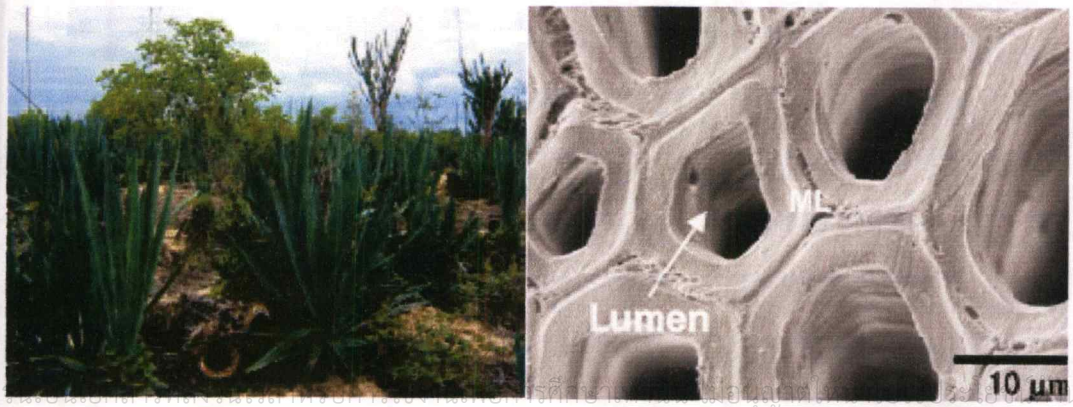

Figure 3.3 Microstructure of pineapple fiber

3.2.2 Effect of compatibilizer on interfacial properties

In this sub-experiment, the compatibilizer was mixed with polypropylene and pineapple fiber by using internal mixer. There were seven mixing conditions designated as conditions A, B, C, D, E, F and G. The details of each condition can be summarized in Table 3.2. Next, the test specimens were prepared by using electric injection molding machine (The FANUC ROBOSHOT S-2000i 100B) and compared mechanical properties of each condition. The interfacial properties between natural fiber and polypropylene matrix were observed using scanning electron microscope. The suitable condition was chosen to mixing in these composites.

Table 3.2 The variation of mixing conditions

Conditions	Percentage of natural fiber	Percentage of compatibilizer
A	10 and 20	0
B		0.5
C		1
D		2
E		5
F		8
G		10

3.3 Testing of Properties

3.3.1 Mechanical properties

3.3.1.1 Tensile Properties

A Universal Testing Machine (Model 55R4502 S/N H3342, Instron Co.) was used to obtain the tensile strength of the specimen at room temperature. Crosshead speeds of 200 mm/min were used for the measurement of the tensile strength. All measurements were performed for five replicates of dumbbell shaped specimens and averaged to obtain the final result. To investigate the morphology of the specimens, their cross-sections were examined with

a Scanning Electron Microscope (SEM). The five pieces of injection specimens were selected to test their tensile properties including ultimate tensile strength and elongation according to the standard test method for determination of tensile properties of the composite material. Standard number ASTM D638

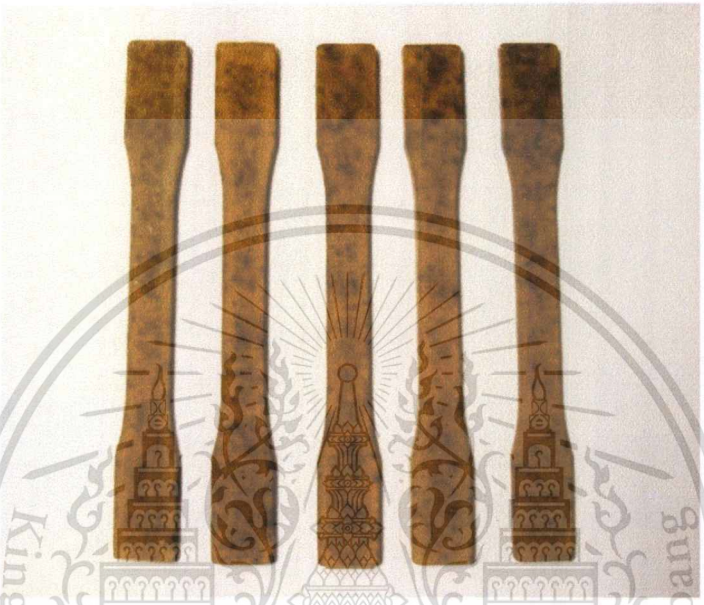

Figure 3.4 Tensile specimens testing

3.3.1.2 Flexural Properties

The five or eight pieces of injection specimens were selected to test with standard ASTM D790. The specimen was prepared to measure 3 data of thickness from 3 positions. The result of flexural test is including Flexural stress, Flexural modulus and Flexural strain

Figure 3.5 Flexural specimens testing

Flexural Stress

$$\sigma_f = 3PL/2bd^2$$

σ_f = Stress (MPa)

P = Maximum Load (N)

L = Support span (mm)

b = Width of beam tested (mm)

d = Depth of beam tested (mm)

Flexural Modulus

$$E_B = L^3m/4bd^3$$

E_B = Maximum Load (N)

L = Support span (mm)

b = Width of beam tested (mm)

d = Depth of beam tested (mm)

m = Slope of the tangent to initial straight-line portion of the load-deflection curve

Flexural Strain

$$\varepsilon_f = 6Dd/L^2$$

ε_f = Strain

D = Maximum Deflection (mm)

L = Support span (mm)

d = Depth of beam tested (mm)

3.3.1.3 Impact Properties

The Izod type was selected to measure the impact properties of the specimen. First, the specimen was prepared to measure with standard ASTM D256 and measure 3 data of thickness from 3 positions. Second, the specimens were notched by ASTM D256 and select five specimens that the data is similar to the others. Finally, the result from impact test is the energy at break and unit is Joule (J).

Figure 3.6 Impact specimens testing

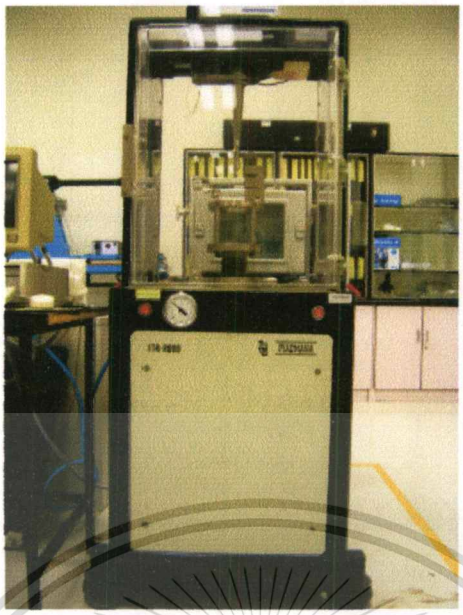

Figure 3.7 Impact testing Machine

3.3.1.4 Heat Distortion Temperature Properties (HDT)

The five or eight pieces of injection specimens were selected to test with standard ASTM D648. The specimen was prepared to measure 3 data of thickness from 3 positions. The result of heat distortion temperature test is including deflection temperature ($°C$).

Figure 3.8 HDT/VICAT specimens testing

Figure 3.9 HDT/VICAT softening temperature tester (Yasuda model HD-PC)

3.3.2 Thermal Properties

3.3.2.1 Thermogravimeteric Analysis (TGA)

The thermal stability of the fibers was evaluated by thermogravimetric analysis (TGA). This experiment was conducted under nitrogen atmosphere, from ambient temperature (25 $°C$) to 900 $°C$ at a heating rate of 20 K/min.

3.3.2.2 Differential scanning calorimetry (DSC)

DSC is used widely for examining polymers to check their composition. Melting points and glass transition temperatures for most polymers are available from standard compilations, and the method can show up possible polymer degradation by the lowering of the expected melting point, T_m, for example. T_m depends on the molecular weight of the polymer, so lower grades will have lower melting points than expected. The percentage crystallinity of a polymer can also be found using DSC. It can be found from the crystallization peak from the DSC graph since the heat of fusion can be calculated from the area under an absorption peak.

This experiment was conducted under nitrogen atmosphere, from 30 $^{\circ}C$ to 230 $^{\circ}C$ at a heating rate of 10 $^{\circ}C$ /min and nitrogen rate of 60 ml/min.

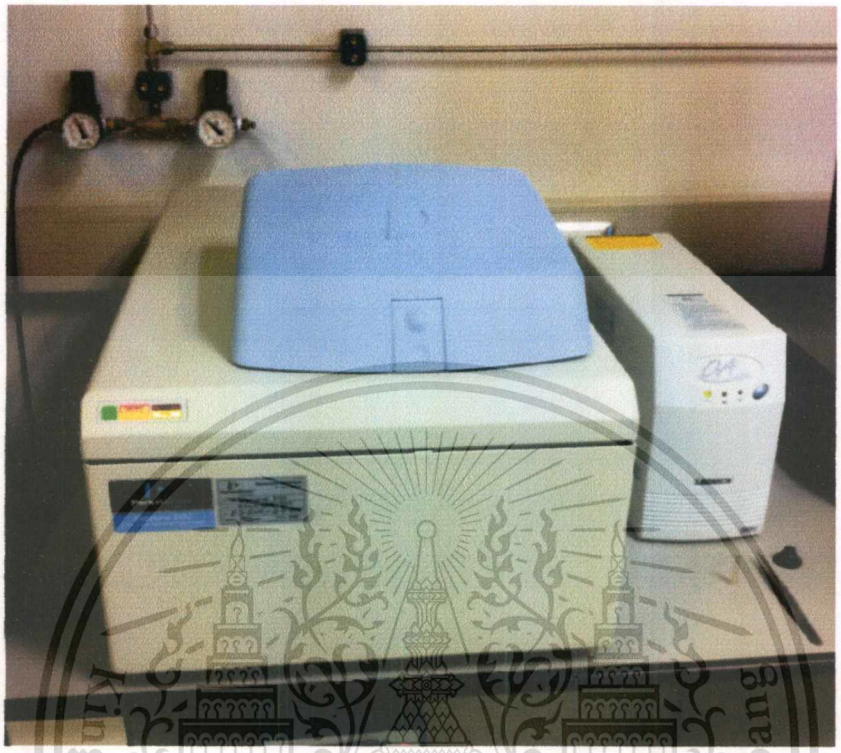

Figure 3.10 Differential Scanning Calorimetry (Perkin Elmer Precisely)

3.3.2.3. Scanning Electron Microscope (SEM)

The morphological characterization of the fibers was done by scanning electron microscopy (SEM). The analysis was performed on gold sputtered samples using secondary electrons, and with a beam voltage of 15-20 kV. This experiment is prepared by fracture in liquid nitrogen and fracture in tensile test. The observed area is top, center and bottom area of specimen that shown in Figure. 3.11.

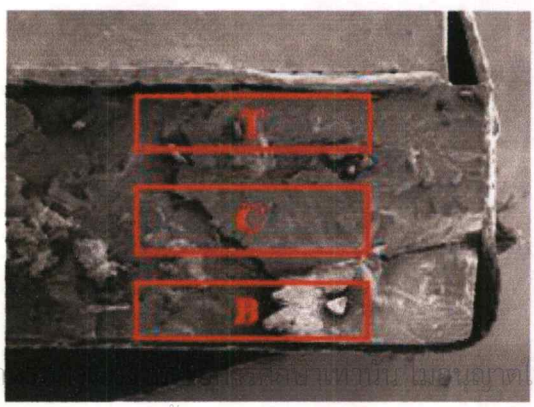

Figure 3.11 Observed area of Scanning Electron Microscope

3.3.3 Rheology Properties

3.3.3.1 Capillary rheometer test

The melt rheological measurements were carried out using an Bohlin instrument capillary rheometer model RH2000 with standard ASTM D 3835. The sample for testing was loaded inside the barrel of the extrusion assembly and forced down into the capillary using a plunger. After giving a residence time of 5 min the melt was extruded through the capillary at predetermined plunger speeds. The initial position of the plunger was kept constant in all the experiments and shear viscosities at different shear rates were obtained from a single charge of the material. The measurements were carried out at three different temperatures (210,220 and 230 °C).

Figure 3.12 Capillary Rheometer RH2000

The shear viscosity (η) was calculated using the equation

$$\eta = \tau / \gamma^{\bullet}$$

$$\tau_w = \frac{RP_c}{2L}$$

$$\gamma^{\bullet} = \frac{4Q}{\pi R^3}$$

Where: τ_w = wall shear stress

$\gamma^{\bullet}_w$ = wall shear strain

R = Diameter of capillary die

L = Length of capillary die

P_c = Pressure

Q = Flow volume

Moreover, the rheological measurement with orifice die can be calculated extensional viscosity (η_ε) using the equation

$$\eta_\varepsilon = \sigma / \varepsilon^{\bullet}$$

$$\sigma_w = \frac{3(n+1)P_o}{8}$$

$$\varepsilon^{\bullet}_w = \frac{4\eta \dot{\gamma}^2}{3(n+1)P_o}$$

Where: σ_w = wall shear stress

$\dot{\varepsilon}_w$ = wall shear strain

Analysis of the relationship between chemical structure and flow properties of polymer using two parameter including Newtonian viscosity and power law index from two mathematic model.

Cross model $$\eta = \frac{\eta_o}{1+\left(\eta_o \dot{\gamma}/\tau^*\right)^{1-n}}$$

Power law model $$\eta = K\dot{\gamma}^{n-1}$$

Where: $\dot{\gamma}$ = shear rate

η = shear viscosity

η_o = Newtonian viscosity

τ^* = stress at non-Newtonian point

K = constant

3.3.3.2 Melt flow index test (MFI)

The melt flow index measurements were carried out using Lloyd Instrument model Davenport MFI-10 with standard ASTM D 1238. The melt flow index is experiment at temperature 230 $^{\circ}C$. The sample for testing is including pure polypropylene (HP500N), 5 wt% fiber and 10 wt% fiber. Cut off time is setting about 30 second and pre-heat is 6 minutes.

Figure 3.13 Davenport MFI-10 melt flow indexer

3.3.3.3 Pressure- volume- temperature (PVT) tests

The Pressure- volume- temperature measurements were carried out using an Bohlin instrument capillary rheometer model RH7 in Figure 3.14. The sample for testing was loaded inside the barrel of the extrusion assembly and forced down into the capillary using a plunger. After giving a residence time of 6 min the melt was extruded through the capillary at 2 mm/min of plunger speeds. The initial position of the plunger was kept constant at 25 cm^3 in all the experiments and PVT die was installed after the volume reaches the initial position. The pressure at different volume was obtained from this instrument. The measurements were carried out at different temperatures from 120 $°C$ to 220 $°C$. The results were calculated using Charles's law equation.

Charles's law equation

$$PV = RT$$

Where P = pressure

V = volume

R = gas constant

T = temperature

At constant pressure, which can be written as;

$$V \propto T$$

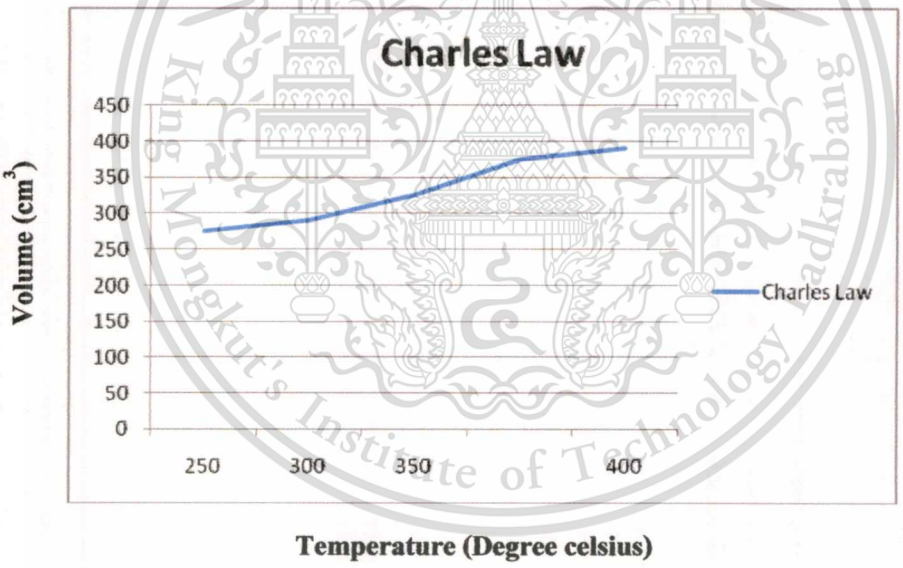

Figure 3.14 Bohlin instrument capillary rheometer model RH7

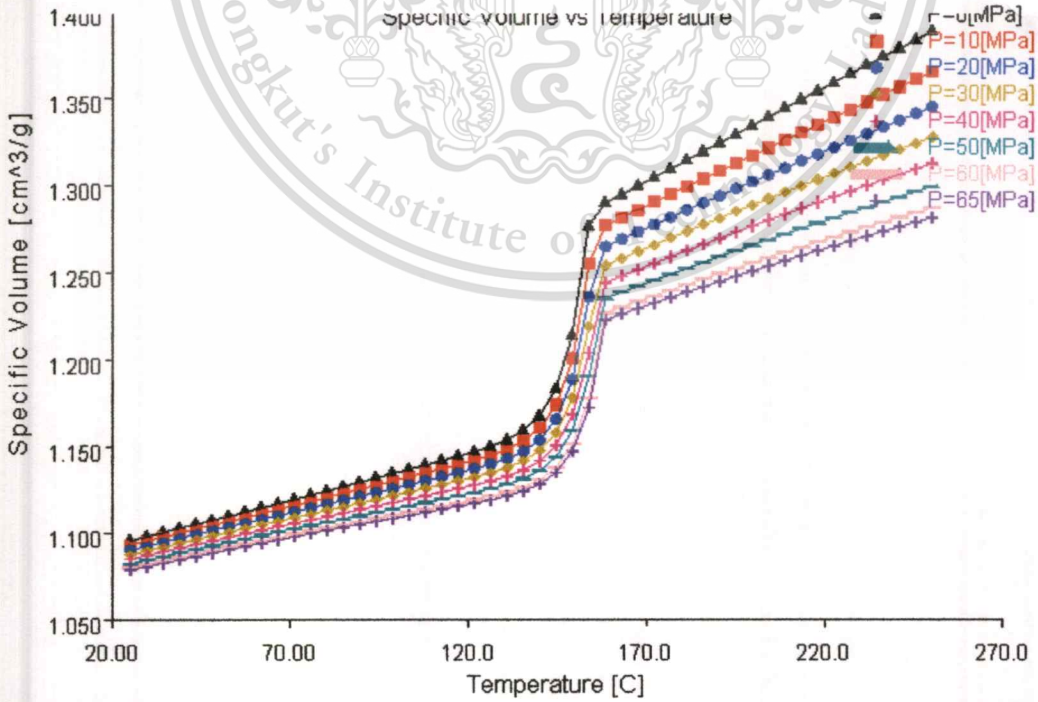

Figure 3.15 Pressure-Volume-Temperature Graph

3.3.3.4 Fourier Transform Infared Spectroscopy (FTIR)

Fourier transform infrared spectroscopy (FTIR) is a technique which is used to obtain an infrared spectrum of absorption, emission, photoconductivity or Raman scattering of a solid, liquid or gas. An FTIR spectrometer simultaneously collects spectral data in a wide spectral rang. The instrument using in this experiment is Perkin Elmer precisely model spectrum 100 as shown in Figure. 3.16. The sample for testing is including pure polypropylene (HP500N), pure maleic anhydride graft polypropylene, 5 wt% fiber with and without compatibilizer and 10 wt% fiber with and without compabilizer.

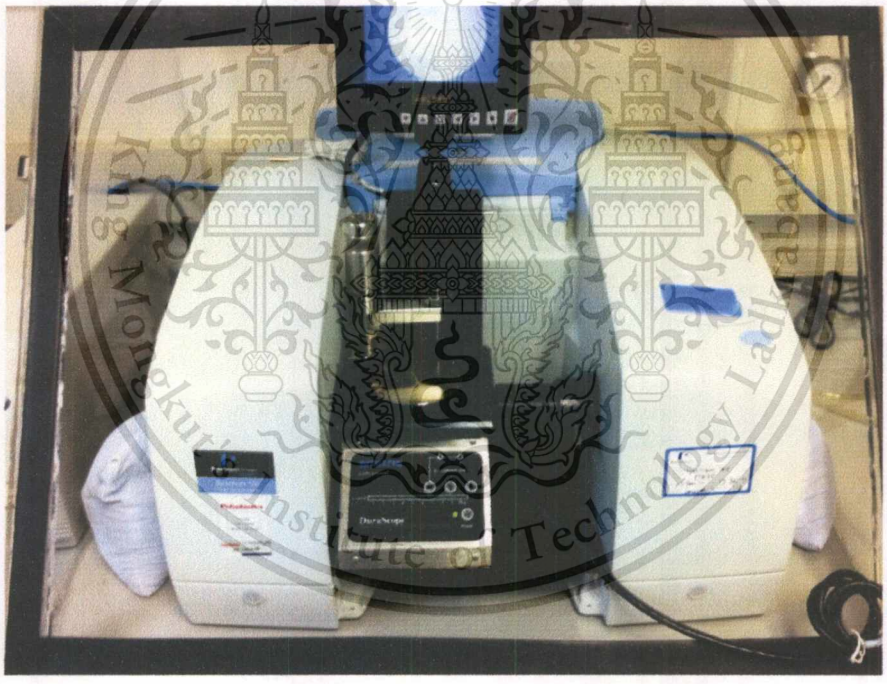

Figure 3.16 Fourier Tranform Infared Spectrometer

3.3.3.5 Contact Angle

The contact angle is the angle at which a liquid/vapor interface meets a solid surface. The contact angle is specific for any given system and is determined by the interactions across the three interfaces. Most often the concept is illustrated with a small liquid

droplet resting on a flat horizontal solid surface. The shape of the droplet is determined by the Young's relation. The contact angle plays the role of a boundary condition. Contact angle is measured using a contact angle goniometer.

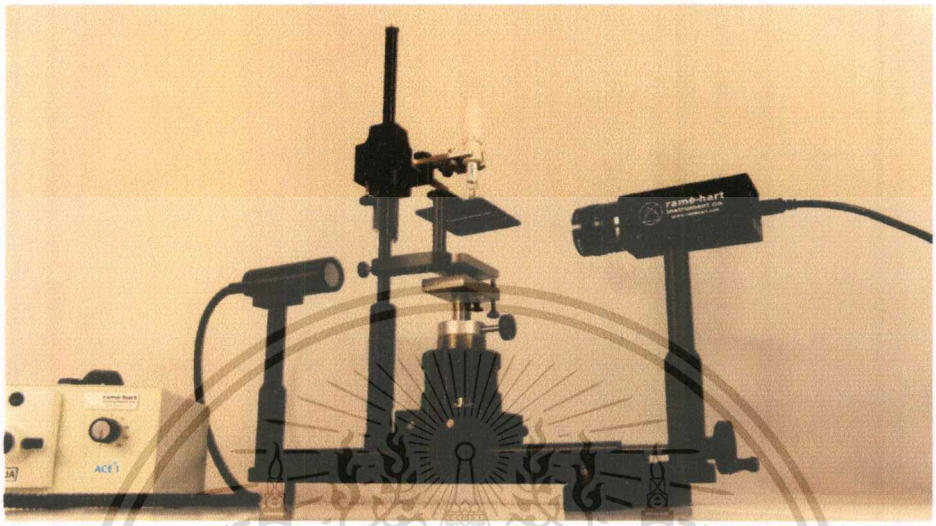

Figure 3.17 Rame-hart Instrument model 500 advanced

CHAPTER 4

EXPERIMENTAL RESULTS AND DISCUSSIONS

4.1 Processing Condition

4.1.1 Effect of natural fiber on Rheology properties

4.1.1.1 Effect of fiber loading

In the case of composites containing hydrophobic fiber, it is evident that the increase of fiber content is associated with lower water uptake. On the other hand, in the case of hydrophilic fibers, their moisture absorption show that the kinetics of absorption and the moisture content at equilibrium distinctly increase with increasing fiber content

Figure 4.1 shows the variation of fiber loading at low shear rate and Figure 4.2 shows the variation of fiber loading at high shear rate between 100 and 1000 (1/s). It is clear from the figure that the shear viscosity increase with increasing fiber content. The increasing of fiber content is effet to the shear viscosity because the fiber was against the flow.

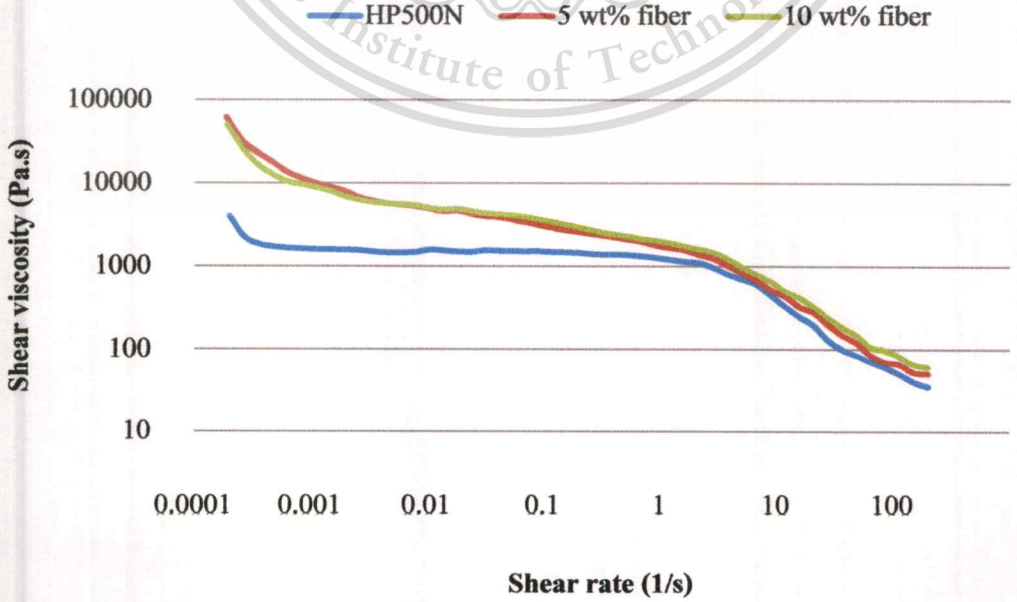

Figure 4.1 Shear viscosity of variation fiber content at low shear rate

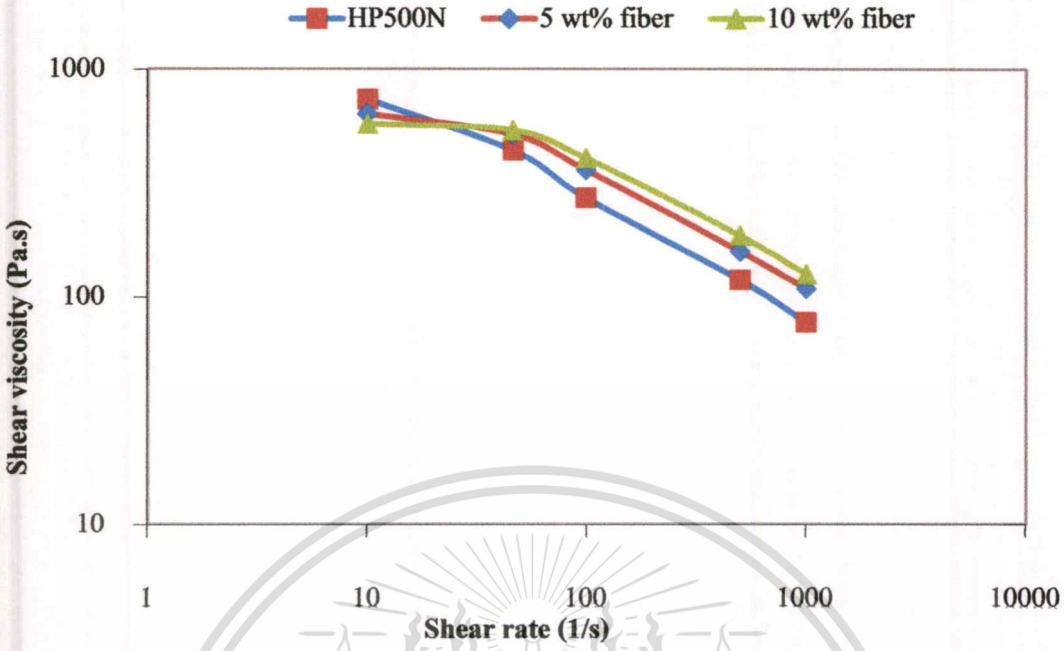

Figure 4.2 Shear viscosity of variation fiber content at high shear rate

4.1.1.2 Effect of temperature

The shear viscosity of pineapple fiber composites with low shear rate and high shear rate at different temperatures are given in Figure 4.3 and Figure 4.4.

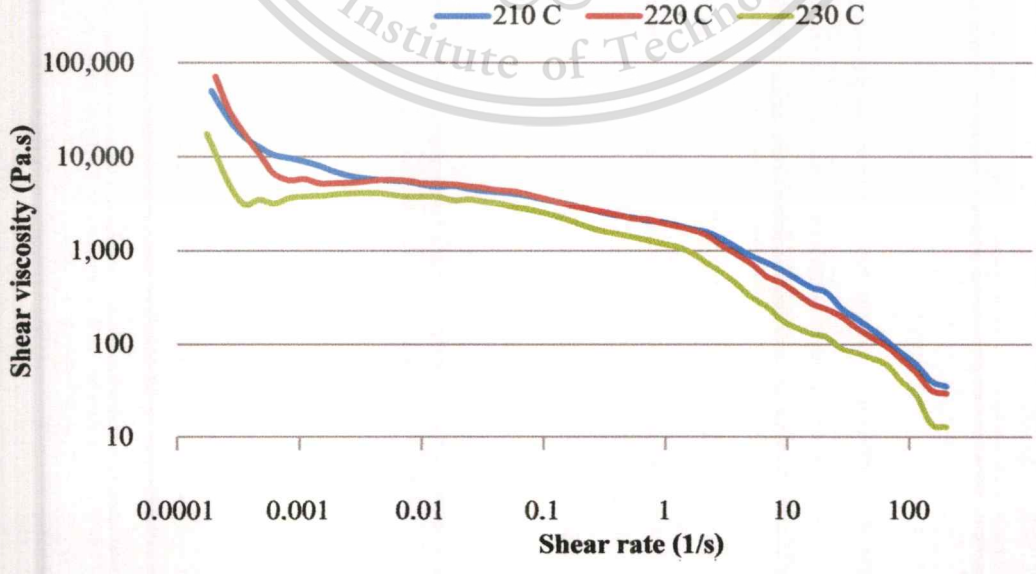

Figure 4.3 Shear viscosity of temperature variation at low shear rate

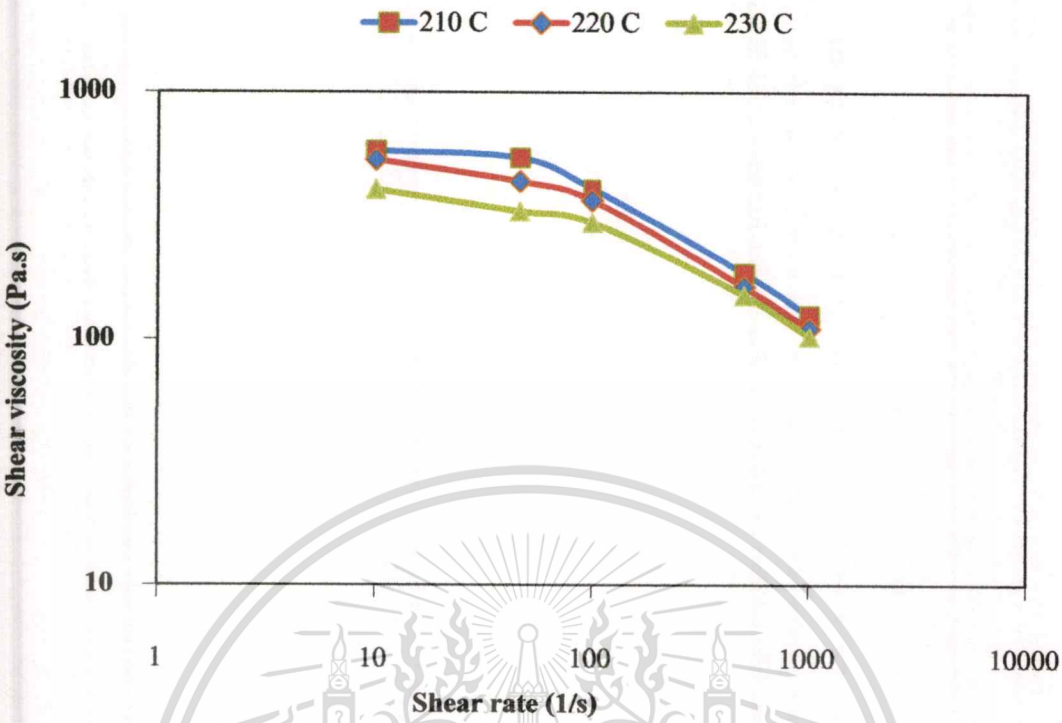

Figure 4.4 Shear viscosity of temperature variation at high shear rate

From the Figure 4.4, it is clear that shear viscosity decreases with increasing temperature. At higher temperature, the molecular motion is accelerated due to the availability of greater free volume and also due to decreasing entanglement density and weaker intermolecular interactions at higher temperature.

4.1.1.3 Effect of compatibilizer

The enhanced bonding in maleic anhydride modified polypropylene (PP-g-MA) treated fiber composite is attributed to the esterification reaction between pineapple fiber hydroxyl groups and anhydride part of PP-g-MA which causes a reduction in interfacial tension and an increase in interfacial adhesion between PP and the fiber. A hypothetical model of the interphase between PP-g-MA with cellulose-OH group of sisal fiber is given in Figure 4.5.

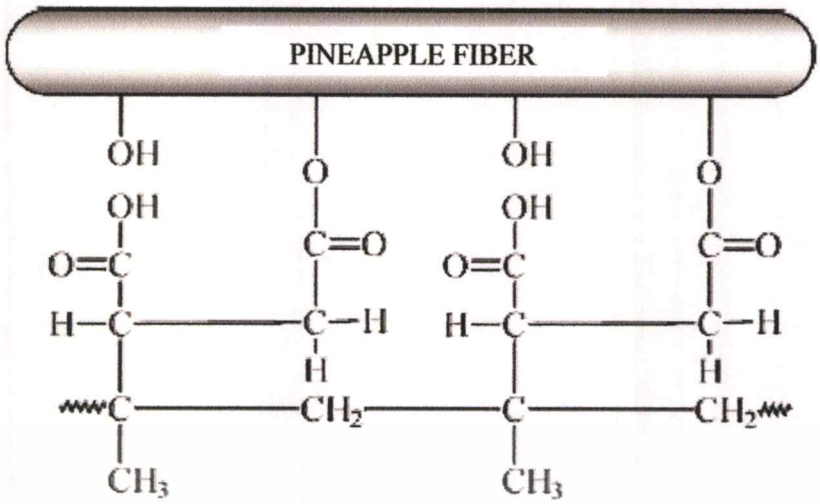

Figure 4.5 Hypothetical model the interphase between PP-g-MA with cellulose-OH group of pineapple fiber. [30]

4.1.2 Effect of natural fiber on Melt flow index test

In Table 4.1 is shown melt flow index of pineapple fiber composite at different fiber content. The melt flow index of pure polymer, 5wt% fiber and 10wt% fiber are 12, 10.13 and 6.84 g/10 min. The melt flow index was decrease when increasing fiber content. Because polypropylene is melt first and the characteristic of pineapple fiber is against the flow. Thus, MFI was decrease.

Table 4.1 MFI values of pineapple fiber composite at 230 °C

Sample	MFI (g/10 min)
Polypropylene HP500N (pure polymer)	12.00
5 wt% Fiber	10.13 ± 0.68
10 wt% Fiber	6.84 ± 0.085

4.1.3 Effect of natural fiber on Pressure volume temperature (PVT) test

The specific volume of 5 wt% of pineapple fiber composite is found that when increase temperature the specific volume (cm^3/g) is gradually increase until temperature reach 200°C and

then sharply increase. When increasing pressure, specific volume is decreased. Moreover, the trend of 10 wt% of pineapple fiber composite is similar to 5 wt%. This result is follow to Charles's law equation

$$PV = RT$$

From equation, specific volume is direct variation with temperature but it is reverse variation with pressure. This result is proved with Charles's law equation. The comparison of pure polypropylene, 5 wt% and 10 wt% of pineapple fiber composite is shown in Figure.4.6. The specific volume of pure polypropylene (HP500N) is higher than 5wt% and 10wt% because the density of pineapple fiber in 10wt% is highest. When the temperature is exceed 190 °C, the composites material is leak because this experiment is using rheology instrument that adapt for PVT test. So, the weight of material is loss and effect to PVT result. Figure.4.7 shows PVT test during temperature 120°C and 190°C. The different of specific volume of Pure polypropylene (HP500N) is higher than 5 wt% fiber composites. As a result, the adding fiber content is improve the different of specific volume. This result is related to the result of heat distorting temperature. This experiment cannot observe temperature in range of cooling process because the limit of load of Bohlin instrument capillary rheometer model RH7 is not exceeding 50 kN. So, this instrument is improper in PVT testing because result of pressure is insufficient for injection molding process.

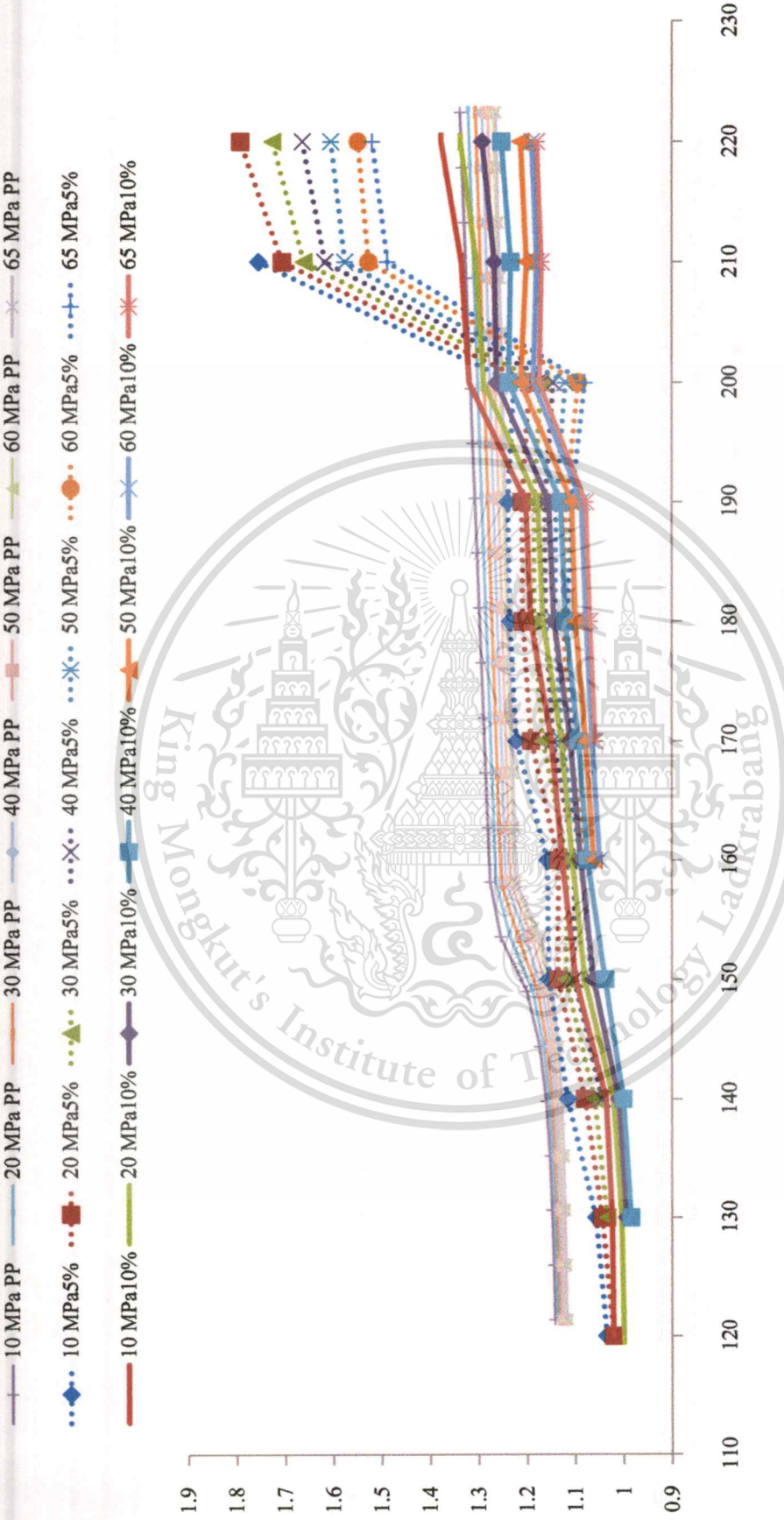

Figure 4.6 Comparision of Pressure-volume-temperature of Polypropylene HP500N, 5 wt% Fiber and 10 wt% fiber

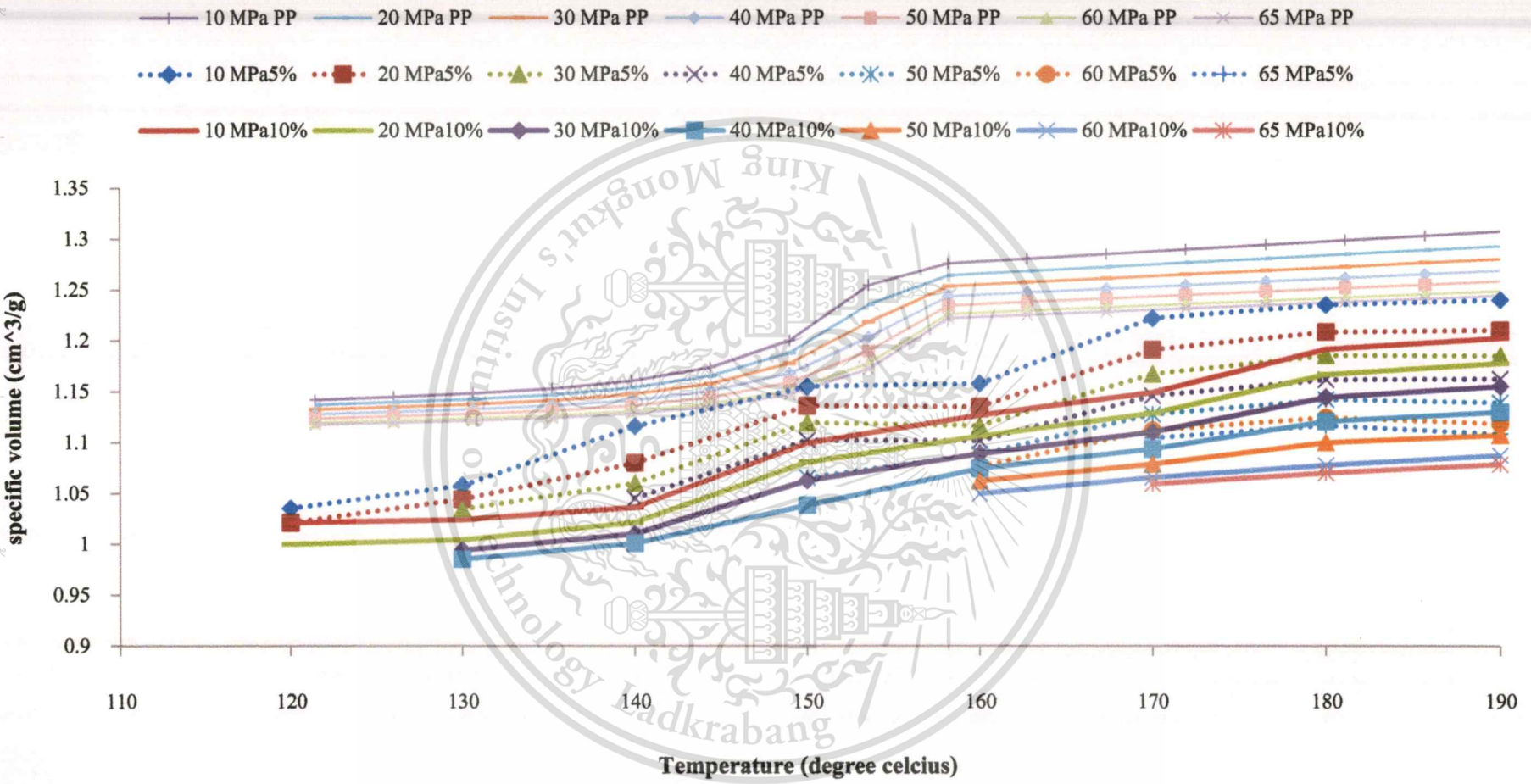

Figure 4.7 Comparision of Pressure-volume-temperature of Polypropylene HP500N, 5 wt% Fiber and 10 wt% fiber during 120°C and 190°C

4.1.4 Effect of natural fiber on Processing temperature

4.1.4.1 Thermogravimeteric Analysis (TGA) of pineapple fiber

Pure pineapple fiber, pure polypropylene, natural fiber composite without compatibilizer and natural fiber composite with compatibilizer are prepared for analysis in this method. The results of the thermogravimetric analysis of pure pineapple fiber are shown in Figure.4.8. One may note that following a small low temperature loss of weight between 85°C and 156°C, the onset of the fiber thermal degradation does not occur until 288.8°C. The low temperature weight loss of 20.90% can be attributed to water in the form of absorbed moisture or combined water. Figure.4.9 shows the thermogravimetric analysis curves for pure polypropylene, natural fiber composite without compatibilizer in the temperature range of 30-900°C. The curve of 5 wt% fiber and 10 wt% fiber composite without compatibilizer sample show that the weight loss between 200°C and 400°C are 3.56% and 8.52% respectively. As a result, the thermal stability of treated composites is higher than that of untreated fiber composites. The improved thermal stability of treated fiber composites is associated with the superior thermal stability of treated fibers. Another factor that contributes to the higher thermal stability of treated composites is the improved fiber/matrix interactions, which produce additional intermolecular bonding between fiber and matrix.

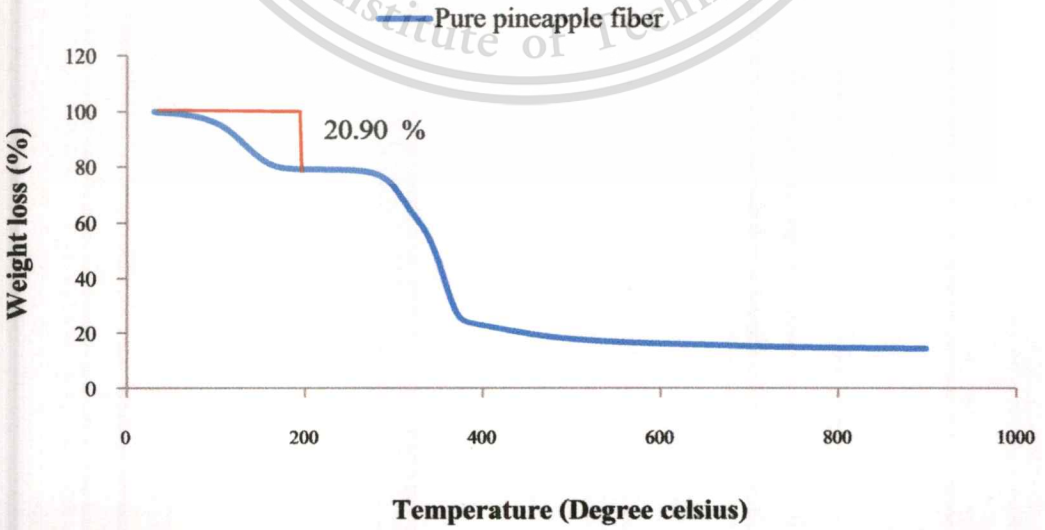

Figure 4.8 The thermogravimetric analysis curves for pure pineapple fiber in the temperature range of 30-900°C.

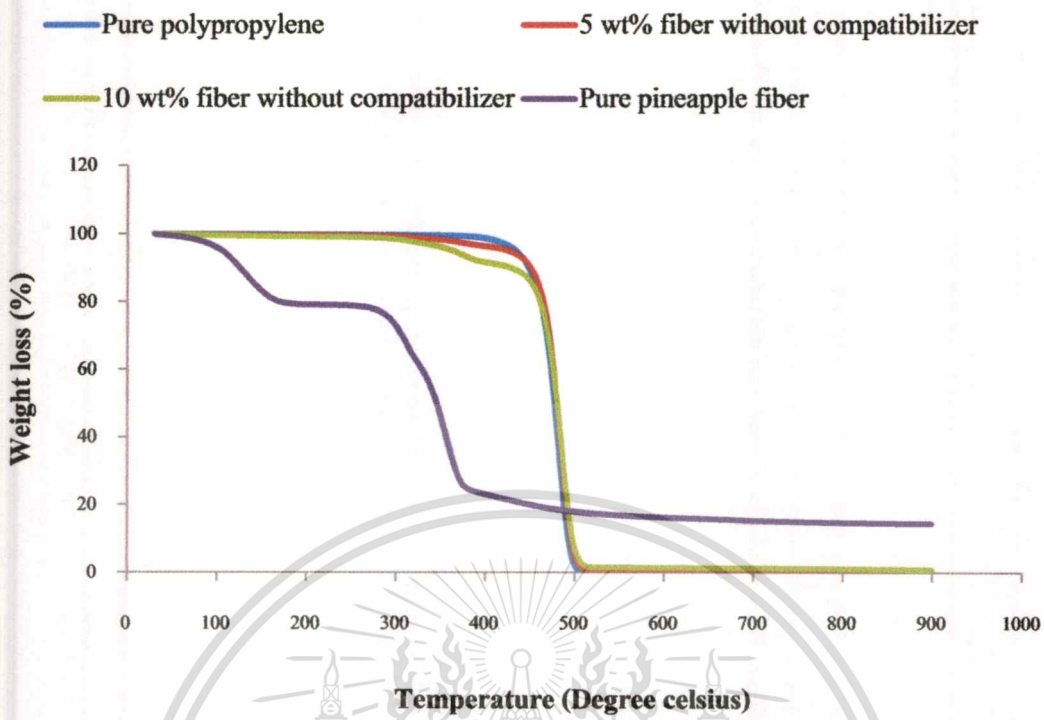

Figure 4.9 The thermogravimetric analysis curves for pure polypropylene, 5 wt% fiber without compatibilizer and 10 wt% fiber without compatibilizer in the temperature range of 30-900°C.

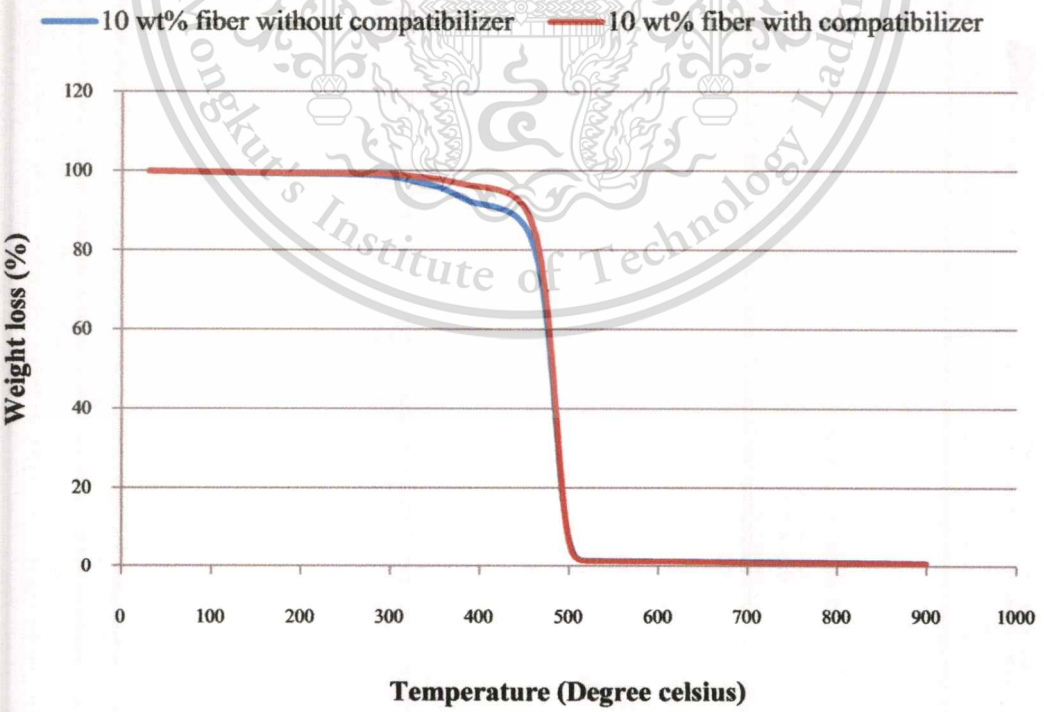

Figure 4.10 *The thermogravimetric analysis curves for 10 wt% fiber without compatibilizer and* 10 wt% fiber with compatibilizer in the temperature range of 30-900°C.

4.1.4.2 Differential scanning calorimetry

The effect of fibers on the thermal properties of PP has also been analyzed in non-isothermal DSC experiments. Thermal parameters such as melting temperature (T_m), crystallization temperature (T_c) were analyzed by non-isothermal crystallization experiments. The results are reported in Table.4.2. Melting temperature and crystallization temperature of pure polymer is approximately 165.93°C and 109.76°C respectively.

Table 4.2 *DSC* properties of fiber percentage with various percentage of compatibilizer

Samples	Melting Temperature (T_m)	Crystallization Temperature (T_C)
Pure polypropylene	165.93	109.76
5 wt% without compatibilizer	165.43	115.08
5 wt% with 5 wt% compatibilizer	165.30	120.11
10 wt% without compatibilizer	165.05	116.87
10 wt% with 5 wt% compatibilizer	164.92	120.49

Melting temperature and crystallization temperature of 5 wt% without compatibilizer is approximately 165.43°C and 115.08°C respectively. Melting temperature and crystallization temperature of 10 wt% without compatibilizer is approximately 165.05°C and 116.87°C respectively. As a result from Table.4.2, melting temperature at end point is decrease when increasing the fiber content but crystallization temperature is increase as see in Figure.4.11 and Figure.4.12. In addition, crystallization temperature is also increase when increasing percentage of compatibilizer as see in Figure.4.13 and Figure.4.14. The fiber surface modification by chemical treatments the compatibility between the fiber and PP matrix is increased favoring interaction between the fiber and PP. It is clear from Table.4.2 that the crystallinity of pure PP is increased by the addition of pineapple fiber. As the amount of pineapple fiber increases, crystallinity too increases because the fiber surface acts as nucleation sites for the crystallization

and the partial crystalline growth of PP. In the second scanning, the graph of endothermic is the same as the first scanning that mean the properties of this composite is thermoplastic. This composite can recycle.

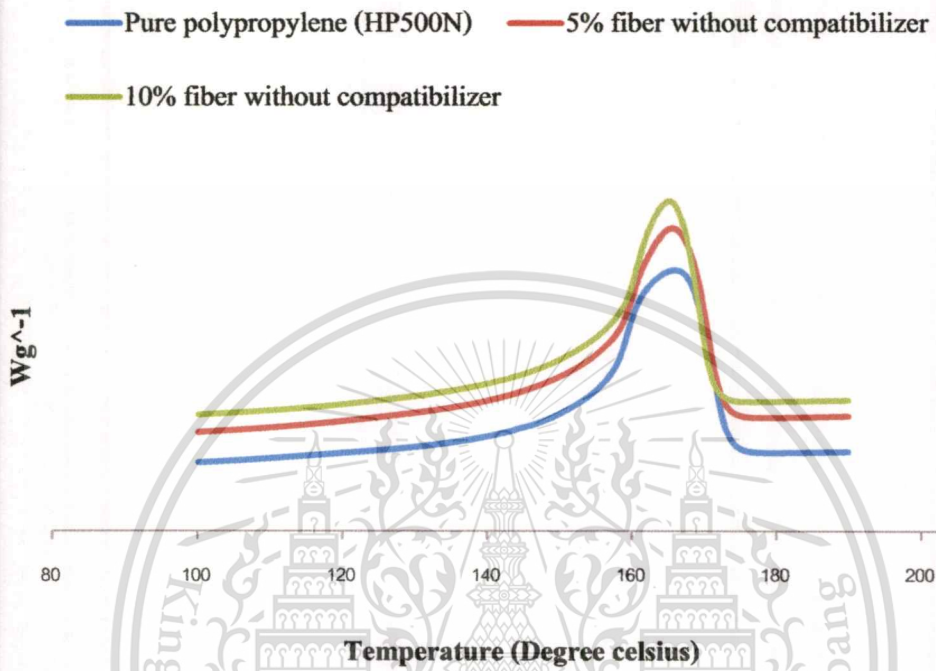

Figure 4.11 Melting Temperature with various fiber content

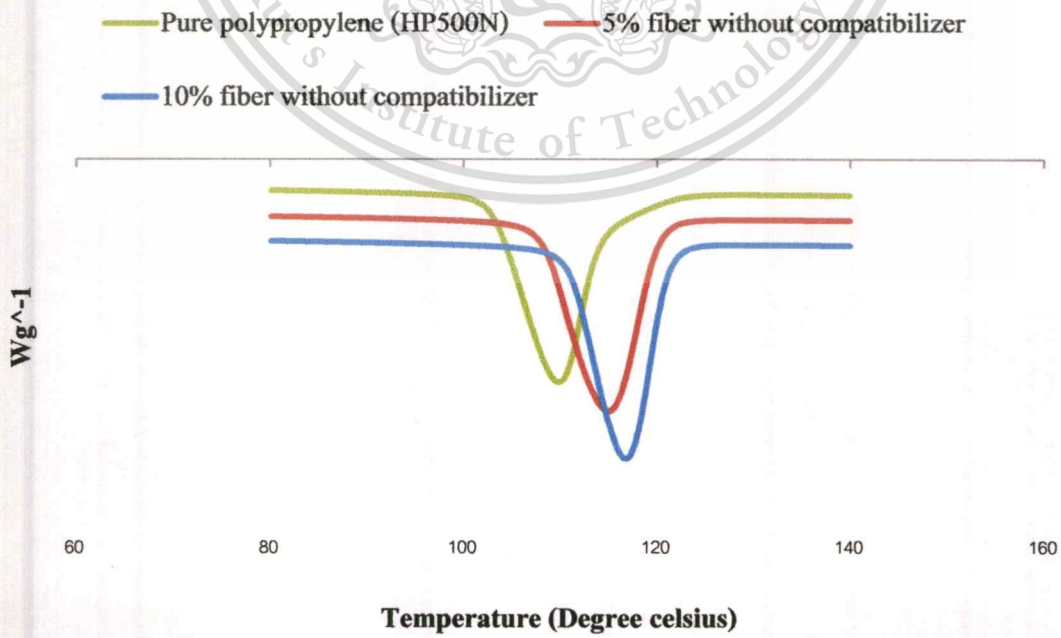

Figure 4.12 Crytallization Temperature with various fiber content

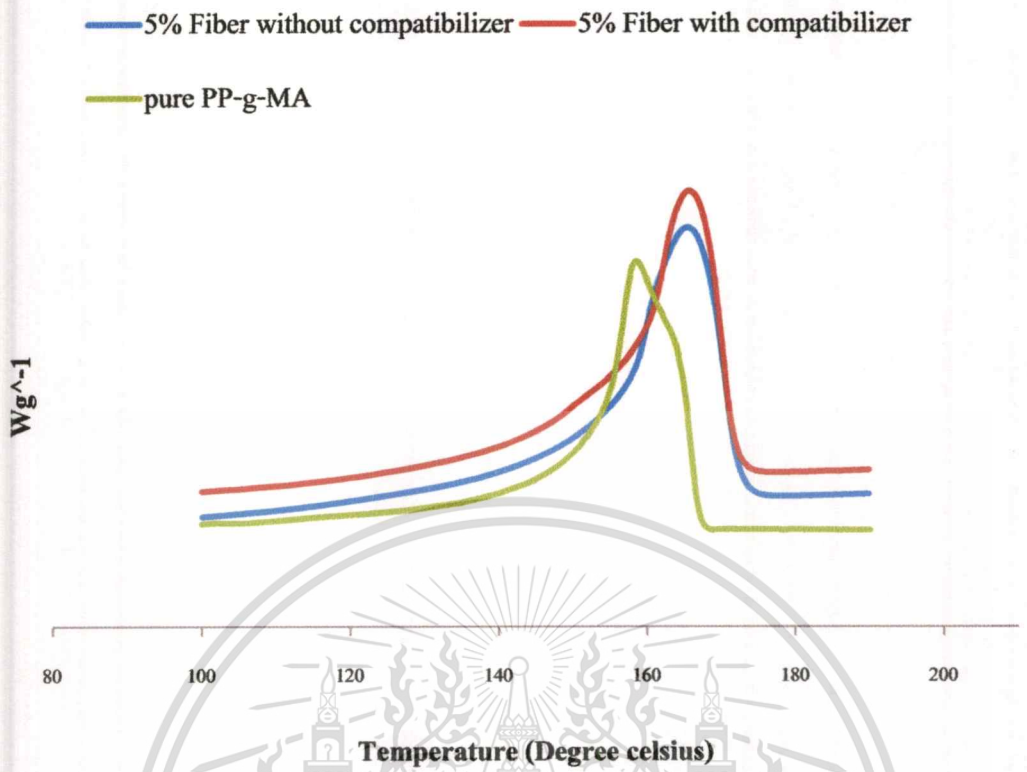

Figure 4.13 Melting Temperature with various percentage of compatibilizer

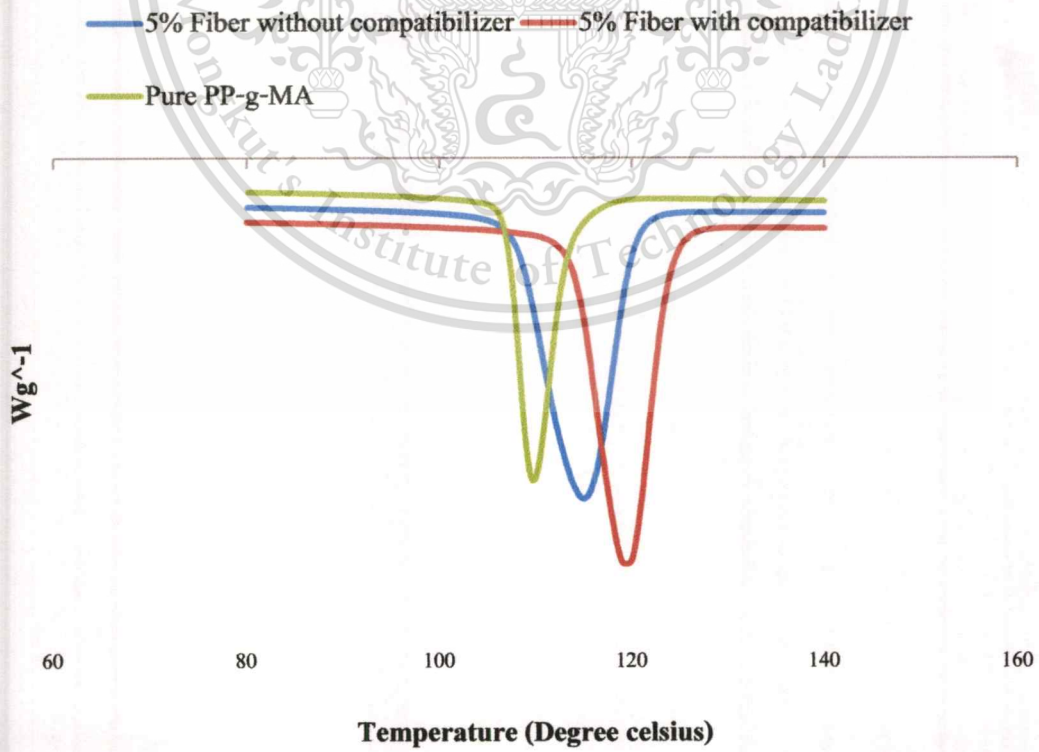

Figure 4.14 Crytallization Temperature with various percentage of compatibilizer

4.1.4.3 Contact Angle measurements

Consider a liquid drop on a solid surface. If the liquid is very strongly attracted to the solid surface, the droplet will completely spread out on the solid surface and the contact angle will be close to 0°. Less strongly hydrophilic solids will have a contact angle up to 90°. On many highly hydrophilic surfaces, water droplets will exhibit contact angles of 0° to 30°. If the solid surface is hydrophobic, the contact angle will be larger than 90°. On highly hydrophobic surfaces the surfaces have water contact angles as high as 120° on low energy materials. As a result from Table. 4.3, contact angle is decrease when increasing fiber content or compatibilizer. Contact angle is decrease that means the liquid is very strongly attracted to the solid surface and work of adhesion is also increase see in Figure.4.15 and Figure.4.16.

Table 4.3 Contact angle of fiber percentage with various percentage of compatibilizer

	Angle (Degree)	Work of Adhesion (mJ/m^2)
Polypropylene (HP500N)	*81.42 ± 2.30*	*83.66 ± 2.86*
5 wt% Fiber without compatibilizer	48.56 ± 0.45	121.01 ± 0.43
10 wt% Fiber without compatibilizer	42.64 ± 3.40	126.27 ± 2.95
5 wt% Fiber with 5 wt% compatibilizer	44.78 ± 1.84	124.45 ± 1.64
10 wt% Fiber with 5 wt% compatibilizer	42.50 ± 2.94	126.42 ± 2.48

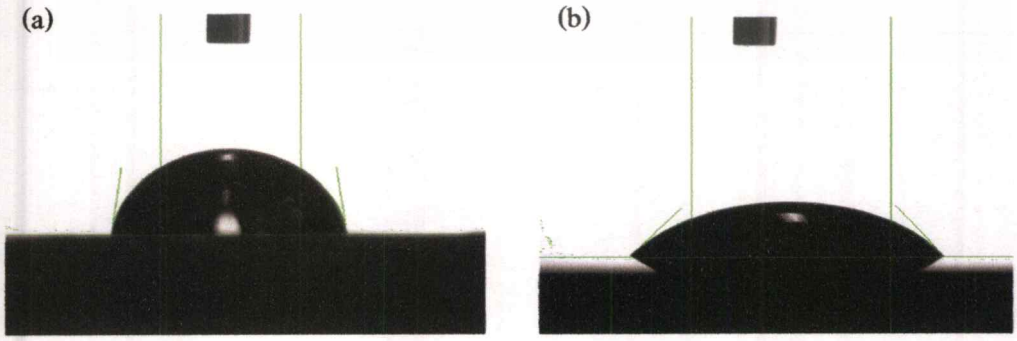

(c)

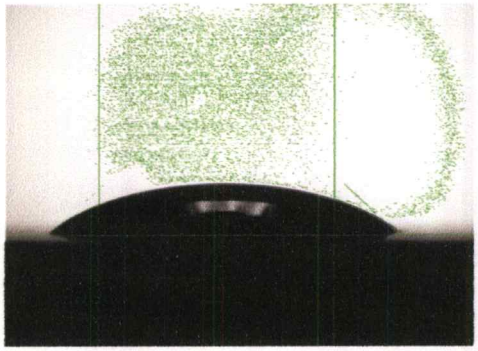

Figure 4.15 (a) Contact angle of pure polypropylene (b) 5% fiber without compatibilizer (c) 10% fiber without compatibilizer

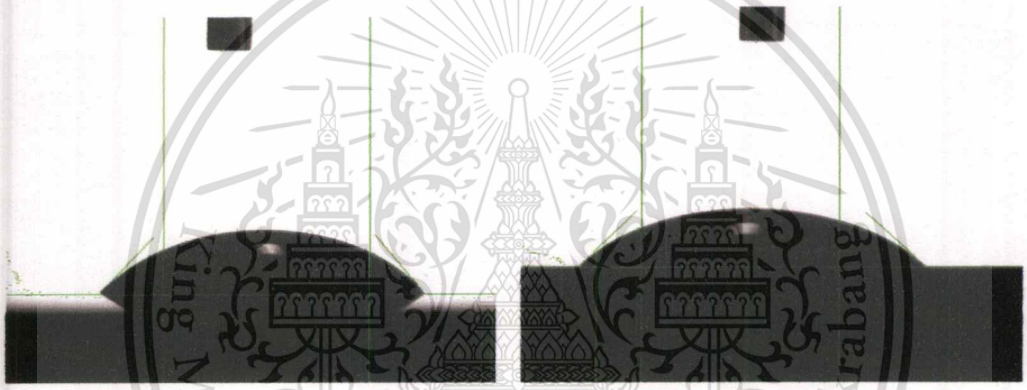

(a) 5% fiber without compatibilizer (b) 5% fiber with compatibilizer

Figure 4.16 Dynamic contact angles (θ) of water drop on the surface of PP/fiber composties

4.1.4.4 Fourier Transform Infrared Spectroscopy analysis (FTIR)

These natural fiber composites were characterized by FTIR analysis. This analysis was able to reveal the main differences of the pure polypropylene, 5 wt% fiber without compatibilizer, 5 wt% fiber with compatibilizer, 10 wt% fiber without compatibilizer and 10 wt% fiber with compatibilizer. In addition, the changes and appearance of new bands could provide information about the efficiency of chemical modification. In Figure 4.17 show the differences between band pure polypropylene and added fiber content. The main change of added fiber

content in comparison to pure polypropylene is related to the appearing of band at 1738 cm^{-1}, this band is proceeding from wide C=O carbonyl peak. This peak is appear because the effect of natural fiber and compatibilizer (PP-g-MA). In Figure 4.18 show the appearing of brand of 5 wt% fiber with compatibilizer. Band at 2700-3000 cm^{-1} show the proceeding from C-H from cellulose and at 1300-1040 cm^{-1} from C-O alcohol. As a result from Figure.4.17, the appearance of band of increased fiber content and increased compatibilizer is similar to pure polypropylene that means the natural fiber is wrapped with polypropylene.

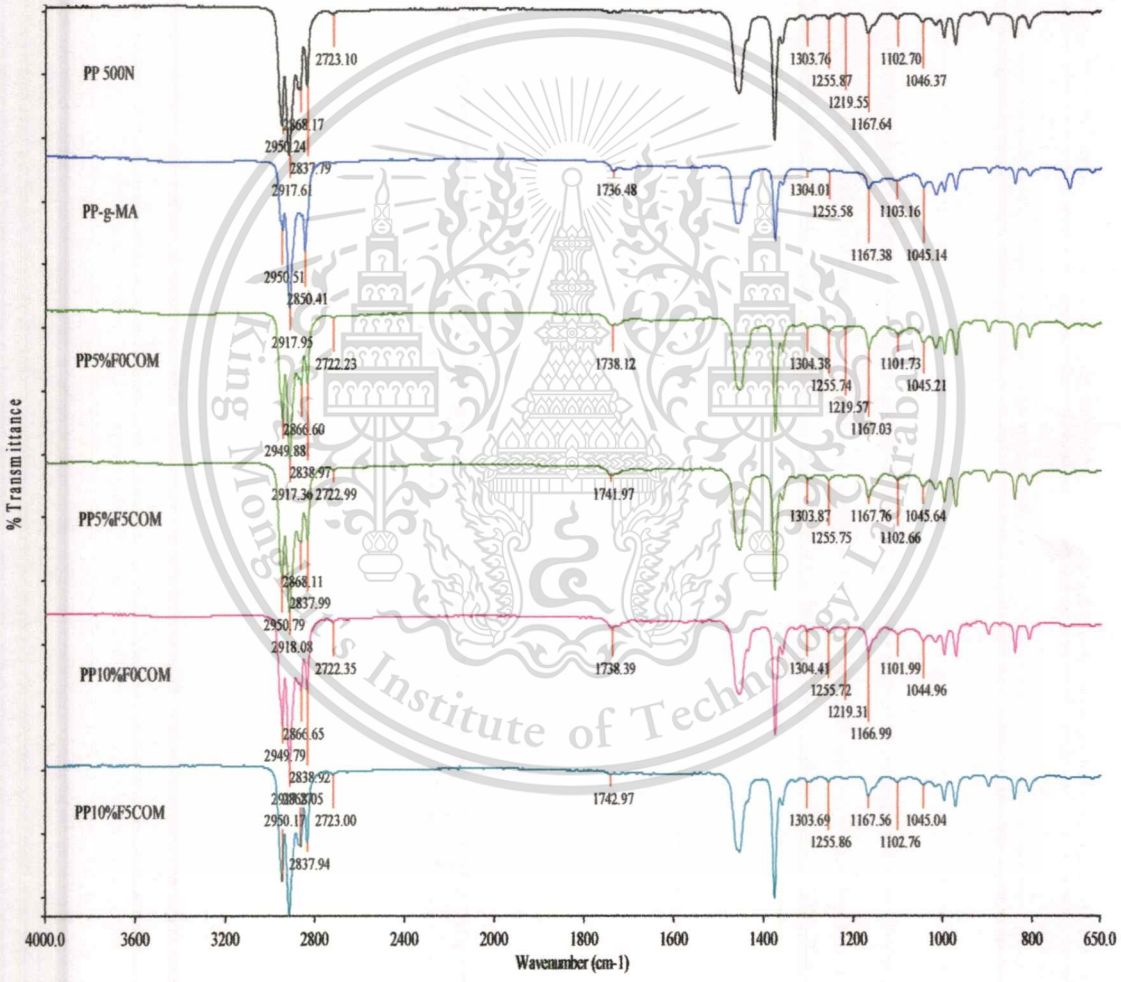

Figure 4.17 The Comparison of pure polypropylene, pure compatibilizer and natural fiber composite with/without compatibilizer.

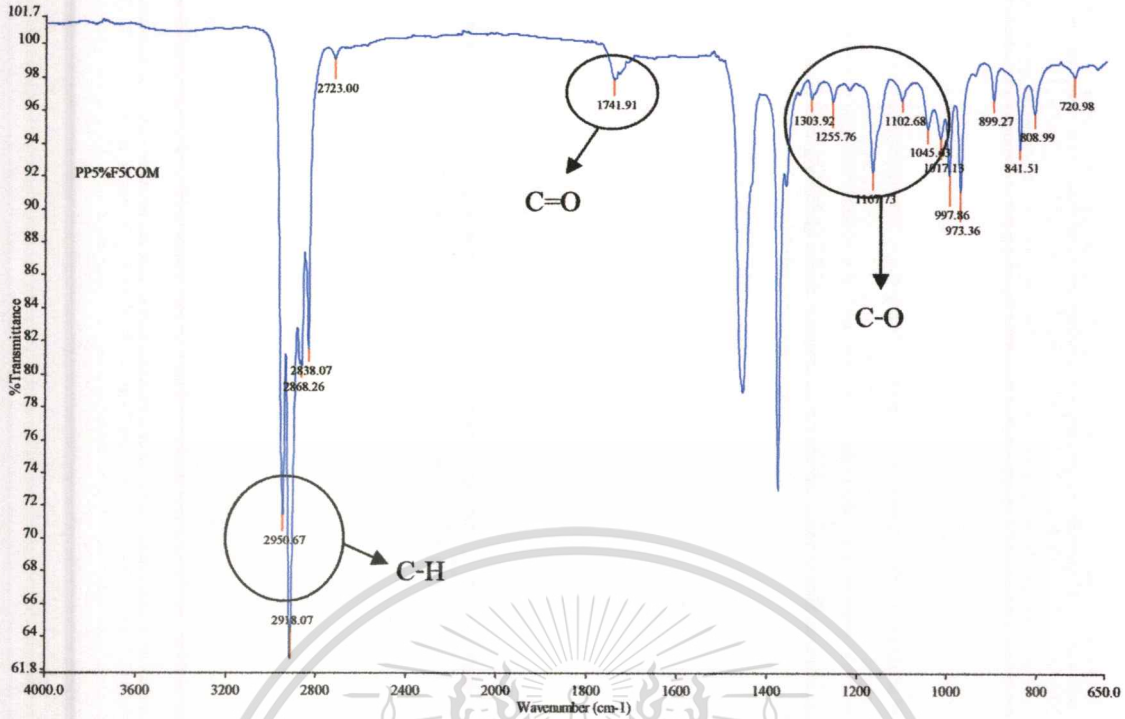

Figure 4.18 FTIR spectra of PP+5 wt% fiber with 5 wt% compatibilizer (650-4000 cm^{-1}).

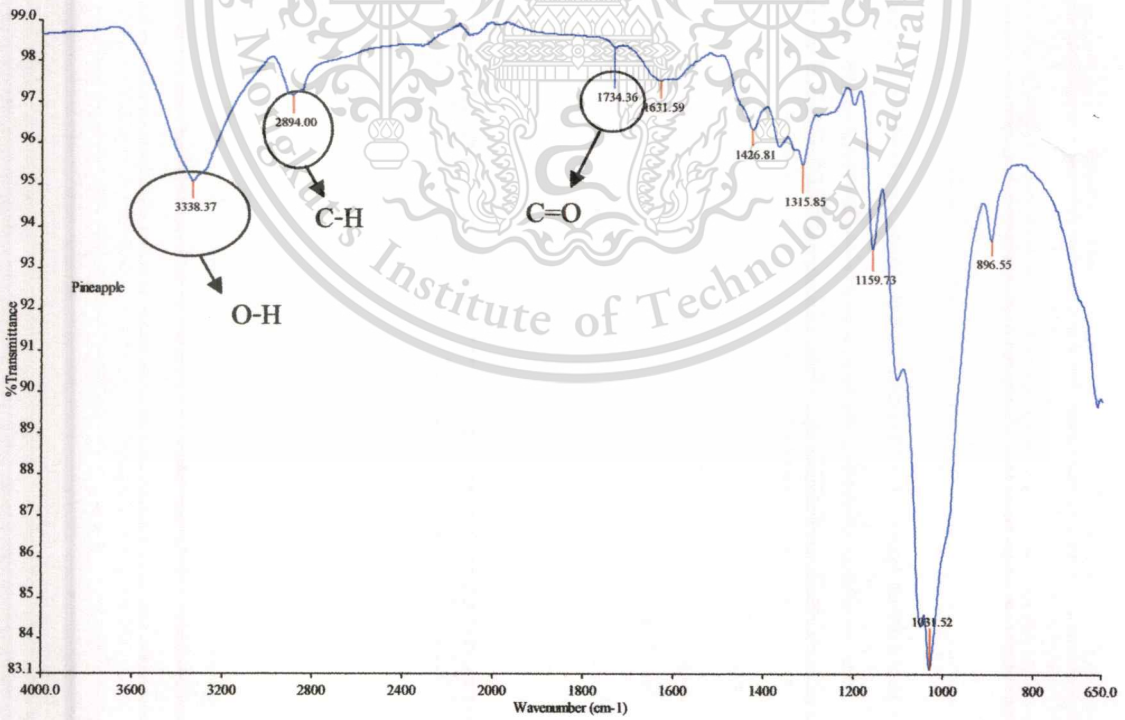

Figure 4.19 FTIR spectra of pineapple fiber (650-4000 cm^{-1}).

4.2 Morphology and Microstructure Analysis

4.2.1 Effect of natural fiber on natural fiber distribution

The natural fiber distribution in these composite are shown in the Figure 4.20. Unmodified fiber composites are shown in Figure 4.20(a), and as can be observed, there is hardly any adhesion at the fiber/matrix interface since the fibers are pulled out from the polymer matrix without leaving any sign and the fibers themselves show a very clean. There are any voids on the fracture surface. On the other hand, Figure 4.20(b) having 5wt% of PP-g-MA show better fracture surface than unmodified fiber composites. There are hardly any void and without fiber pull out.

Figure 4.20 Natural fiber distribution of: (a) unmodified and (b) 5wt% of PP-g-MA

4.2.2 Effect of compatibilizer percentage on Morphological structure

The SEM micrographs of the tensile strength surface of 10 wt% fiber composites with and without PP-g-MA are shown as in Figure 4.21. The tensile strength surfaces determined are perpendicular to the flow direction. In Figure 4.21(a) shows the clean surface of pineapple fiber a composite, which implies that no adhesion exists between pineapple fiber and PP matrix. Hole are created in the PP matrix as the fiber pullout and visible in Figure 4.21(a). Tensile fracture occurred in PP by the pulling of chains and the formation of voids in the bulk polymer

material. Figure 4.21(b) exhibits the fracture of pineapple fiber reinforced PP composite having 1wt% of PP-g-MA which reflects the improved fiber-matrix interaction at interface. Moreover, in the case of the 5wt% of PP-g-MA (Figure 4.21(c)) a considerable improvement of the adhesion at the interface is observed and there hardly any voids on the fracture surface which indicates that the fibers are so well trapped by the polymer that fiber pull-out considerably decreases. As a result, it can conclude that the optimum amount of PP-g-MA in this type is 5 wt%, the interaction between the fiber and PP matrix is highest.

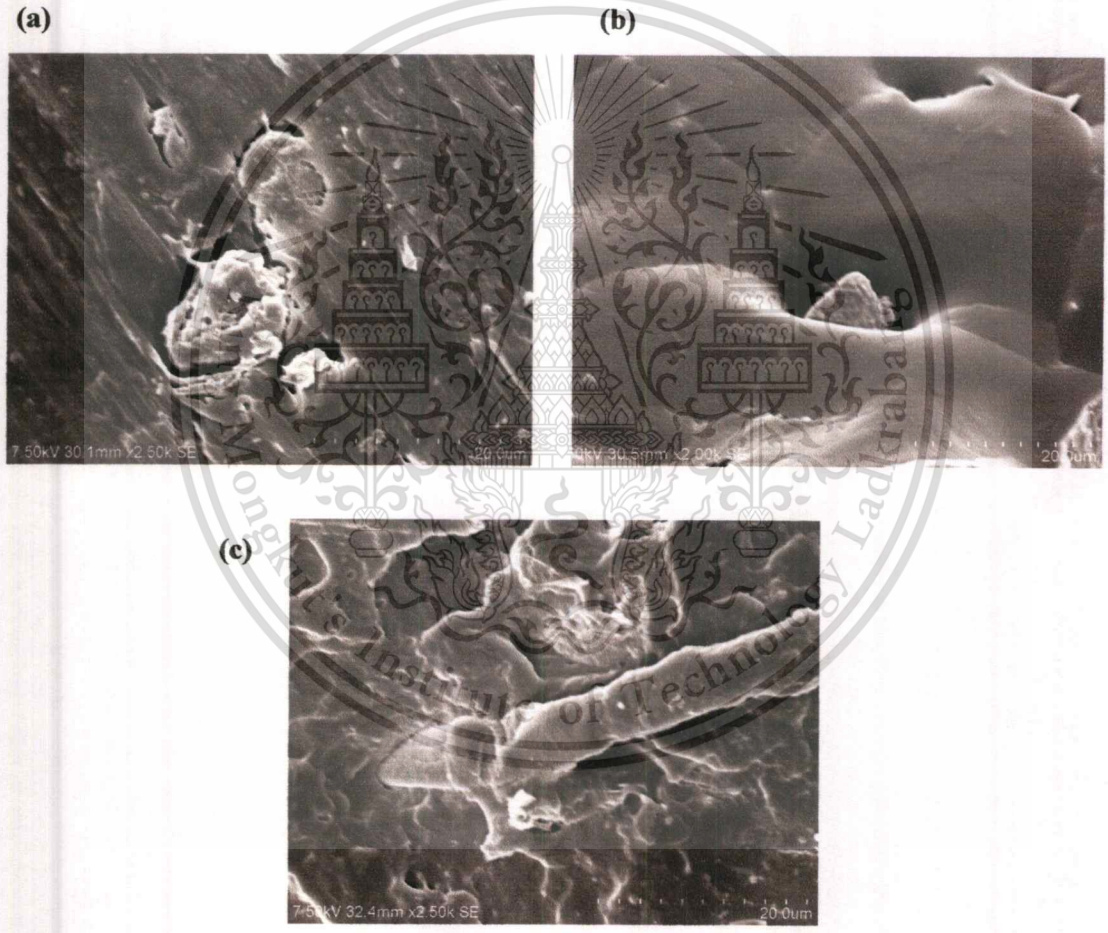

Figure 4.21 (a) shows SEM of tensile fractured surface of unmodified pineapple fiber reinforce PP composite. (b) SEM of tensile fractured surface of 1wt% PP-g-MA modified pineapple fiber reinforced PP composite. (c) SEM of tensile fractured surface of 5wt% PP-g-MA modified pineapple fiber reinforced PP composite.

4.3 Effect of natural fiber on Mechanical properties and Service thermal properties

4.3.1 Effect of natural fiber on Mechanical properties

4.3.1.1 Effect of compatibilizer on Mechanical properties

Pineapple fiber reinforced PP composites were successfully developed with and without PP-g-MA by using internal mixer. Values of tensile strength of unmodified and PP-g-MA modified pineapple fiber reinforced PP composites are listed in Table 4.4. From this table, the tensile strength of 5 wt% PP-g-MA added composite is highest as compared to other pineapple fiber reinforced PP composites. The tensile strength is increased as S-curve like. The improvement in the tensile strength is attributed to the increased adhesion between pineapple fiber and PP that facilitates more stress transfer through bonding to the pineapple fiber. This adhesion is due to the presence of PP-g-MA, which reacted with the hydroxyl group present in the pineapple fiber surface. On the other hand, the addition of PP-g-MA increased the resistance to pullout the fiber from PP matrix[15].

Table 4.4 Tensile properties of fiber percentage with various percentage of compatibilizer

Percentage of compatibilizer	Tensile strength (MPa)	
	10% fiber	20% fiber
0%	21.74 ± 1.42	18.80 ± 1.04
0.5%	25.17 ± 0.78	19.61 ± 1.46
1%	24.68 ± 0.24	19.43 ± 0.57
5%	25.38 ± 0.40	22.25 ± 0.66
10%	24.78 ± 1.28	21.34 ±1.11

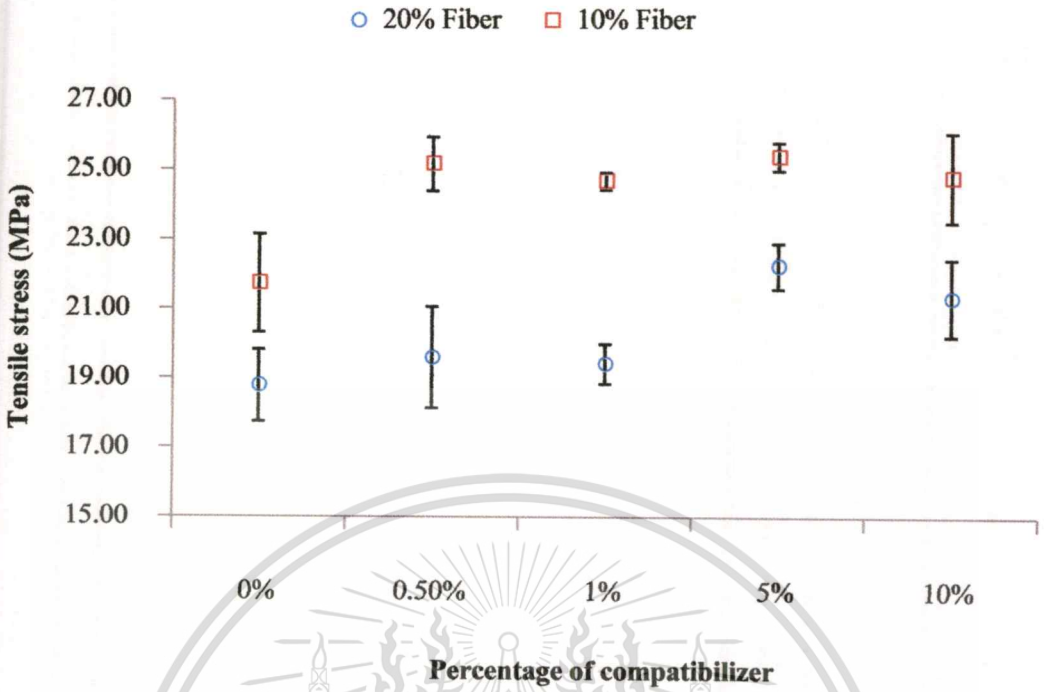

Figure 4.22 Tensile strength with various percentage of compatibilizer

The pure PP-g-MA has lower tensile strength as compared to PP. The acid anhydride groups of PP-g-MA coupling agent form chemical bond with the hydroxyl groups of the lingo-cellulosic fiber. The hydroxyl and carboxylic acid groups of the natural fiber are the active sites for absorption of water, which also lead to weak interfacial bonding. The anhydride rings of PP-g-MA are covalently linked with the hydroxyl groups of the pineapple fibers to form ester linkage. The PP-g-MA modified pineapple fiber surface increased the wet ability with PP matrix. PP's long chains in PP-g-MA are compatible with the PP matrix, which lowers the surface tension of the fibers and increases its wet ability with the PP matrix [15].

4.3.1.2 Effect of natural fiber on Tensile properties

In addition, the tensile strengths and Young's modulus of the pure polymer and composites were shown in the Figure 4.23 and 4.24, respectively. The specific of tensile strength and modulus are

also listed in Table 4.5. Pure polymer displayed the highest (28.17 MPa) tensile strength while 10 wt% fiber composite showed the lowest (about 27.27 MPa).

Table 4.5 The specific tensile strength and modulus of various fiber percentages with PP-g-MA

Conditions	Tensile strength (MPa)	Elongation (%)	Young Modulus (GPa)
Polypropylene HP500N (pure polymer)	28.17 ± 0.33	24.01 ± 4.34	1.31 ± 0.02
5 wt% natural fiber	27.95 ± 0.19	8.83 ± 1.09	1.51 ±0.03
10 wt% natural fiber	27.27 ± 0.21	6.55 ± 0.37	1.67 ± 0.02

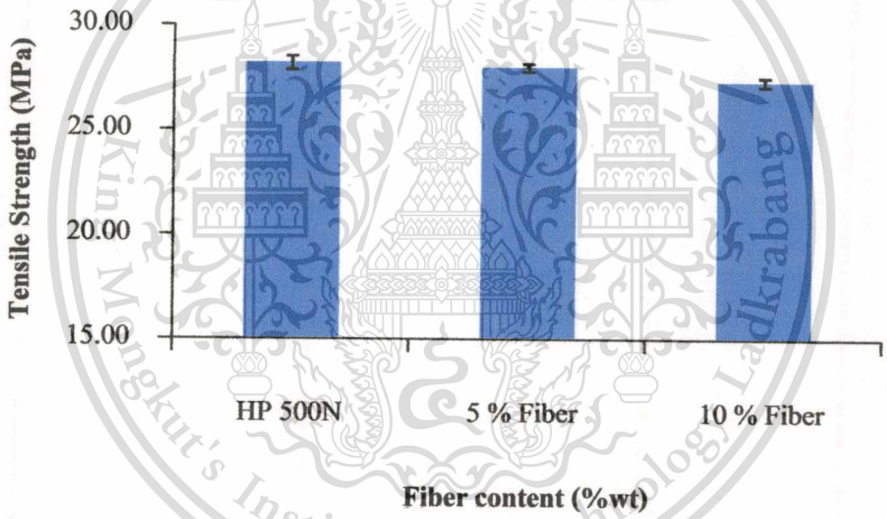

Figure 4.23 Tensile strength of natural fiber composites as a function of natural fiber contents

The results show a decrease in the percentage elongation with increasing fiber weight fraction. Figure 4.24 shows the measured tensile modulus of the natural fiber composites. The tensile modulus of the pure polymer was low (1.31 GPa) in contrast to added 10 wt% of fiber composites which registered about 1.67 GPa. The results show an increase in the tensile modulus with increasing fiber weight fraction. With increasing amount of pineapple fibers, the tensile strength and percentage of elongation of the PP/pineapple fiber composites decreases, as would be expected. Concerning the plant characteristics the mechanical behavior of the pineapple fiber is dependent on its plant source, age, type of processing (mechanism of fiber extraction) as well as

the fiber microstructure. Two major reasons for decreased in tensile strength are the weakest part of the composites and the interfacial interaction between PP and pineapple fiber is weak. Therefore, the tensile strength of the pineapple fiber composites decreases with increasing wt% of pineapple fiber.

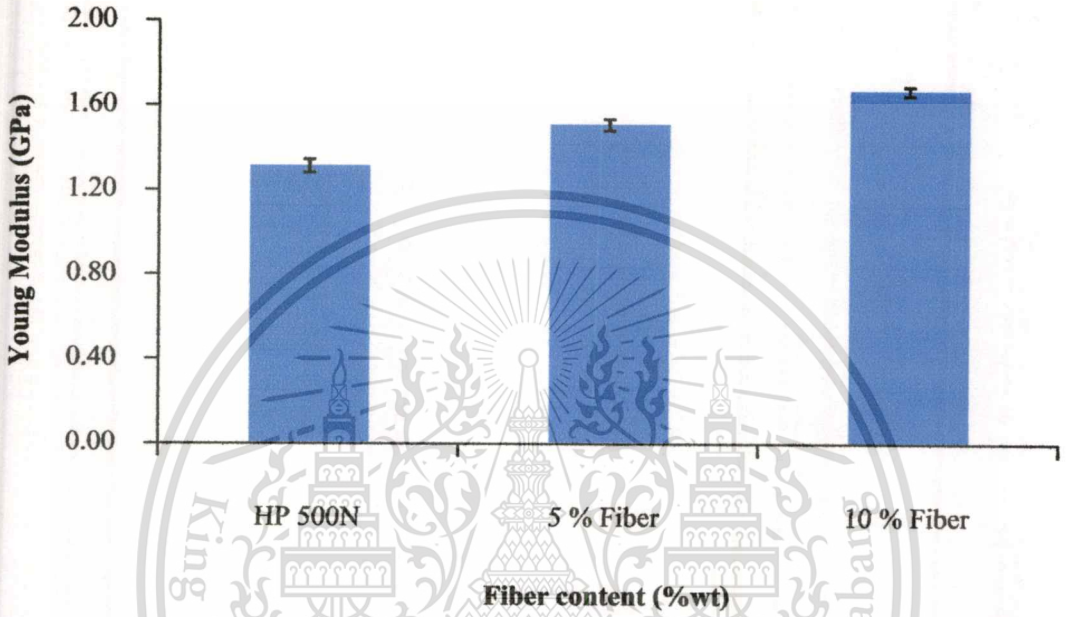

Figure 4.24 Young's modulus of natural fiber composites as a function of natural fiber contents

4.3.1.3 Effect of natural fiber on Flexural properties

Even though these composites material trend to decreasing in tensile strength when increasing amount of fiber whereas flexural strength and flexural modulus are increased. The flexural strength and modulus of PP matrix with pineapple fiber were shown in Figure 4.25 and 4.26, respectively. The specific of flexural strength and modulus are also listed in Table 4.6. The flexural strength and modulus of composites is increased from 42.19 MPa to 46.41 MPa and from 1.30 GPa to 1.60 GPa when increased fiber content. Based on this result for the PP matrix with pineapple fiber composites, it can be inferred that these composite is better as the viewpoint of the enhancement of the flexural strength. This mean the compression is better than the tension in flexural testing.

Table 4.6 The specific flexural strength and modulus of various fiber percentages with PP-g-MA.

Conditions	Flexural strength (MPa)	Flexural Modulus (GPa)
Polypropylene HP500N (pure polymer)	42.19 ± 0.26	1.30 ± 0.01
5 wt% natural fibers	45.12 ± 0.36	1.45 ± 0.03
10 wt% natural fibers	46.41 ± 0.35	1.60 ± 0.03

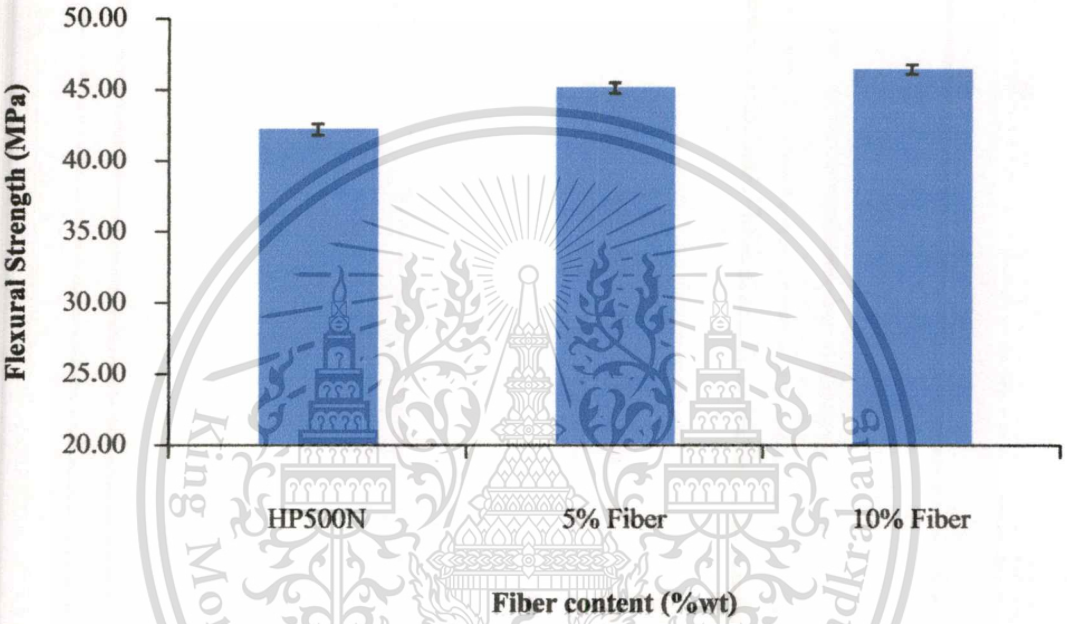

Figure 4.25 Flexural strength of natural fiber composites as a function of natural fiber contents

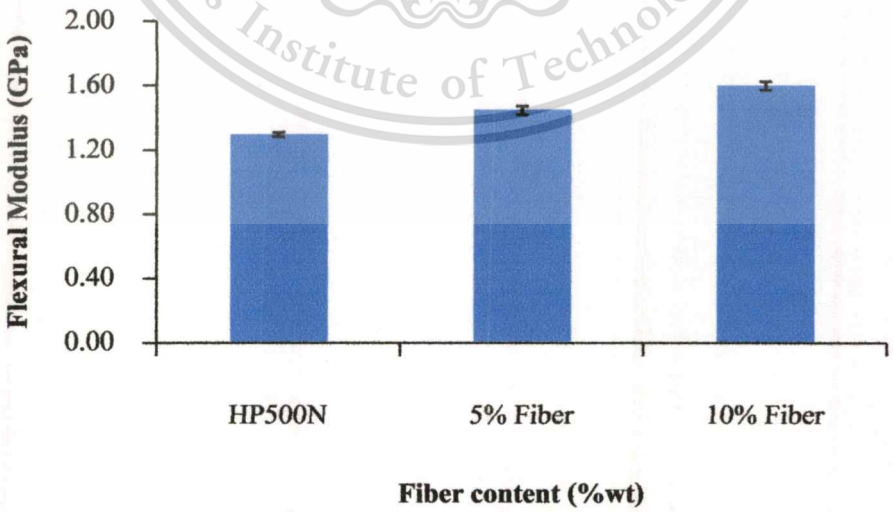

Figure 4.26 Flexural modulus of natural fiber composites as a function of natural fiber contents

4.3.1.4 Effect of natural fiber on Impact properties

Figure 4.27 represents the Izod impact strength (energy absorbed/cross-sectional thickness) results of the composites. The natural fiber composites tested displayed high impact strengths (> 25 J/m^2) compared to pure polymer of polypropylene (17.53 J/m^2). The impact response of fiber composites is highly influenced by the interfacial bond strength, the matrix and fiber properties. Impact energy is dissipated by debonding, fiber and/or matrix fracture and fiber pull out. Fiber fracture dissipates less energy compared to fiber pull out. The former is common in composites with strong interfacial. In this result, the increasing of impact properties is depending on the displacement of energy absorption. Figure 4.28(a) show the absorption displacement of pure polypropylene shorter than Figure 4.28(b) which filled with natural fiber. So, the increasing of fiber content is effect to the absorption displacement.

Table 4.7 The specific impact strength of various fiber percentages with PP-g-MA

Conditions	Impact strength (J/m^2)
Polypropylene HP500N (pure polymer)	17.53 ± 0.28
5 wt% natural fibers	25.58 ± 1.62
10 wt% natural fibers	26.61 ± 0.95

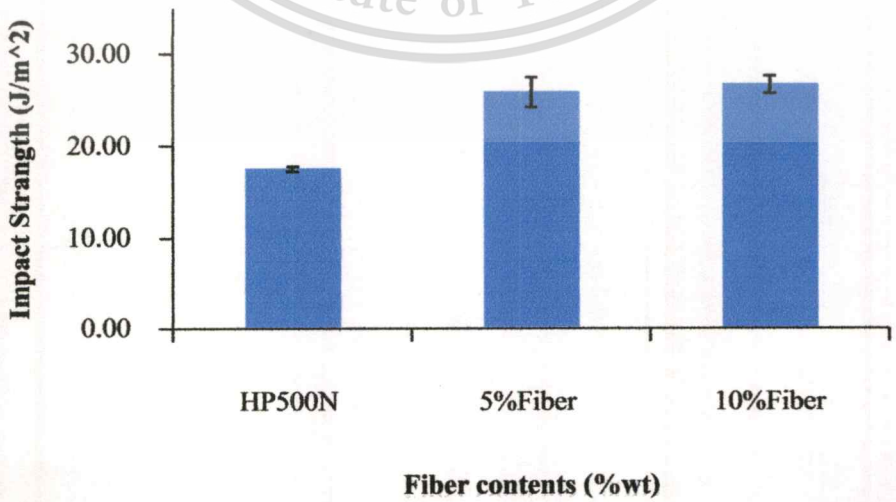

Figure 4.27 Impact strength of natural fiber composites as a function of natural fiber contents

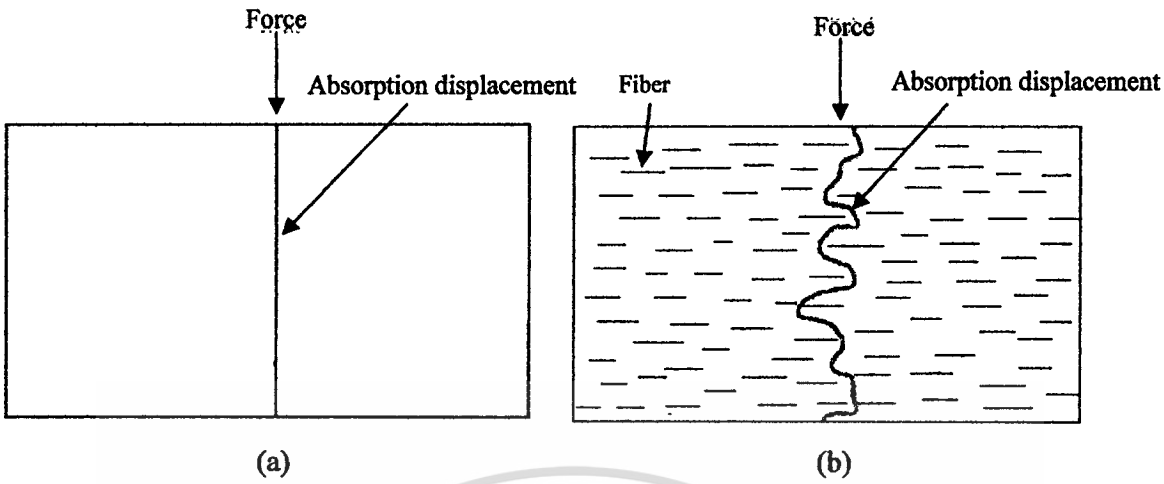

Figure 4.28 (a) Absorption displacement of pure polymer (b) Absorption displacement of composites

4.3.2 Effect of natural fiber on Service thermal properties

4.3.2.1 Effect of natural fiber on Heat Distortion Temperature

Table 4.8 represents the heat distortion temperature of a vary fiber content. Heat distortion temperature of pure polypropylene, 5 wt% and 10 wt% are 61.5°C, 63.02°C and 65.82°C, respectively. This could be found that the natural fiber can resist loading as same as effect on the impact strength and flexural strength results. It could be concluded that amount of fiber content effect on service temperature of these composite system.

Table 4.8 Heat distortion temperature with various fiber content

Sample	HDT (°C) 18.5 kg.f/cm^2
PP (pure)	61.58 ± 0.54
5 wt% fiber	63.02 ± 0.41
10 wt% fiber	65.82 ± 0.75

CHAPTER 5

CONCLUSION AND SUGGESTIONS

5.1 Conclusion

All factors that effect to the properties of natural fiber composite are density, fiber distribution, fiber length distribution and adhesion surface. But the main factor that influenced all the properties of pineapple fiber composite was adhesion surface. Pineapple fiber have moisture content about 20.90% and a small low temperature loss of weight between 85 and 156 °C that observed by TGA test. The curve of 5 wt% fiber and 10 wt% fiber composite without compatibilizer sample show that the weight loss between 200°C and 400°C are 3.56% and 8.52% respectively. As a result, the thermal stability of treated composites is higher than that of untreated fiber composites. This composite was treatment with compatibilizer (maleic anhydride graft polypropylene). So, the surface adhesion between matrix and natural fiber increase which is observed in the SEM micrograph and the mechanical properties also increased. The mechanical properties depend on the weakest part of the composites and it has the void between matrix and natural fiber. The tensile strength of pure polymer displayed the highest (28.18 MPa) tensile strength while 5 wt% and 10 wt% fiber composite showed 27.95 MPa and 27.29 MPa, respectively. The tensile strength of the composites decreases with increasing amount of fibers. The increasing amount of fiber is also increasing the void because the inner structure of pineapple fiber was similar to honey comb structure. However, the flexural strength and modulus of composites is increased from 42.21 MPa to 46.41MPa and from 1.30 GPa to 1.60 GPa when increased fiber content. The flexural strength of composites increases with increasing amount of fiber. This composite is better to enhancement of the flexural strength. In the impact properties, the natural fiber composites tested displayed high impact strengths (> 25 J/m^2) compared to pure polymer of polypropylene (17.57 J/m^2). The impact properties is highly influenced by the

interfacial bond strength, the matrix and fiber properties. The increasing of fiber content is effect to increasing the displacement of the energy absorption due to microscopic voids in the pineapple fiber.

The natural fiber distribution in these natural fiber thermoplastics composite, unmodified fiber composites is hardly any adhesion at the fiber/matrix interface since the fibers are pulled out from the polymer matrix without leaving any sign and the fibers themselves. There are many voids on the fracture surface. On the other hand, 5 wt% of PP-g-MA shows better fracture surface than unmodified fiber composites. There are hardly any void and without fiber full out. The tensile strength properties of 0 wt%, 1 wt% and 5 wt% of PP-g-MA are 21.7 MPa, 24.26 MPa and 25.20 MPa respectively. As a result, it can conclude that with increasing amount of PP-g-MA, the interaction between the fiber and PP matrix is also increase. If added too much, the result may be poor.

The effect of fibers on the thermal properties of polypropylene has also been analyzed in non-isothermal DSC experiment. Melting temperature at end point is decrease when increasing the fiber content but crystallization temperature is increase. In addition, crystallization temperature is also increase when increasing percentage of compatibilizer. The fiber surface modification by chemical treatments the compatibility between the fiber and PP matrix is increased favoring interaction between the fiber and polypropylene. It is clear that the crystallinity of pure polypropylene is increased by the addition of pineapple fiber. As the amount of pineapple fiber increases, crystallinity too increases because the fiber surface acts as nucleation sites for the crystallization and the partial crystalline growth of polypropylene. Heat distortion temperature of pure polypropylene, 5 wt% and 10 wt% are 61.5°C, 63.02°C and 65.82°C, respectively. This could be found that the natural fiber can resist loading as same as effect on the impact strength and flexural strength results. It could be concluded that amount of fiber content effect on service temperature of these composite system. In the case of contact angle of this composite is decrease when increasing fiber content or compatibilizer. Contact angle is decrease that means the liquid is very strongly attracted to the solid surface and work of adhesion is also increase. In the case of rheology properties of this composite, the effect of fiber content in

rheology properties is shown that the shear viscosity increase with increasing fiber content. On the other hand, the shear viscosity was decrease with increase temperature. In the pressure volume temperature (PVT) test, the trend of specific volume of 5 wt% and 10 wt% of pineapple fiber composite is found that the specific volume (cm^3/g) is gradually increase until temperature reach 200°C and then sharply increase. The specific volume of 5 wt% is higher than 10 wt% because the density of pineapple fiber in 10 wt% is higher.

Table 5.1 Summary of Pineapple fiber thermoplastic composites properties

	Properties	**Natural fiber composite (compared to PP HP500N)**
Mechanical	Tensile strength	↓ (3.2%)
	Flexural strength	↑ (10%)
	Impact strength	↑ (42.3%)
	Contact angle	↑
Thermal	Melting temperature	↓
	Crystallization temperature	↑
	Heat distortion temperature	↑
Rheology	Shear viscosity (various fiber content)	↑
	Shear viscosity (various temperature)	↓

5.2 Suggestions

Although this work was finished, it was only the first step of pineapple fiber composite towards plastic injection molding process. There are some suggestions to the work for further study towards plastic injection molding for pineapple fiber composite as follow:

5.2.1 In the case of mixing condition of natural fiber and polypropylene matrix, most natural fiber is not split but combine into a group because natural fiber is sensitive to moisture. So, it has a void inside during mixing process. The best process should be get rid of moisture content in natural fiber before mixing.

5.2.2 Another suggestion is on the data of pressure volume temperature. This experiment cannot observe temperature in range of cooling process because the limit of load of Bohlin instrument capillary rheometer model RH7 is hot exceed 50 kN. So, this instrument is improper in PVT testing because result of pressure is insufficient for plastic injection molding process.

5.2.3 Together the above suggestion, if all the temperature of pressure-volume-temperature test are collected. It can used as the database of this composite in simulation process of mold flow program.

5.2.4 The data of rheology can finding the curve fitting that using as the database in mold flow program.

REFERENCES

[1] T.Q. Li, M.P. Wolcott. "Rheology of HDPE-wood composites. I. Steady state shear and extensional flow". **Composites: Part A.** 35 (2004) : 303-311.

[2] F.G. Torres, M.L. Cubillas. "Study of the interfacial properties of natural fibre reinforced polyethylene". **Polymer Testing.** 24 (2005) : 694-698.

[3] Alireza Ashori, Amir Nourbakhsh. "Characteristics of wood-fiber plastic composites made of recycled materials". **Waste Management.** 23 (2009) : 1291-1295.

[4] L. Dobircau, P.A. Sreekumar, R. Sauah, N. Leblanc, C. Terrie, R. Gattin, J.M. Saiter. "Wheat flour thermoplastic matrix reinforced by waste cotton fibre". **Composites: Part A.** 40 (2009) : 329-334.

[5] J.R.M. d'Almeida, R.C.M.P. Aquino, S.N. Monteiro. "Tensile mechanical properties, morphological aspects and chemical characterization of piassava (Attalea funifera) fibers". **Composites: Part A.** 37 (2006) : 1473-1479.

[6] K. Murali Mohan Rao, K. Mohana Rao. "Extraction and tensile properties of natural fibers: Vakka, date and bamboo". **Composite Structures.** 77 (2007) : 288-295.

[7] Flavio de Andrade Silva, Nikhilesh Chawla, Romildo Dias de Toledo Filho. "Tensile behavior of high performance natural (sisal) fibers". **Composites Science and Technology.** 68 (2008) : 3438-3443.

REFERENCES (CONT.)

[8] M.A. Lopez-Manchado, M. Arroyo. "Thermal and dynamic mechanical properties of *polypropylene and short organic fiber composites*". **Polymer.** 41 (2000) : 7761-7767.

[9] Paul Wambua, Jan Ivens, Ignaas Verpoest. "Natural fibres: can they replace glass in *fibre reinforced plastics?*". **Composites Science and Technology.** 63 (2003) : 1259-1264.

[10] Sam-jung Kim, Jin-Bok Moon, Gue-Hyun Kim, Chang-Sik Ha. "Mechanical *properties of polypropylene/natural fiber composites: Comparison of wood* fiber and cotton fiber". **Polymer testing.** 27 (2008) : 801-806.

[11] Plamen G. Malchev, Ciprian T. David, Stephen J. Picken, Alexandros D. Gotsis. "*Mechanical properties of short fiber einforced thermoplastic blends*". **Polymer.** 46 (2005) : 3895-3905.

[12] J.L. Thomason. "The influence of fibre length and concentration on the properties of *glass fibre reinforced polypropylene: 7. Interface strength and fibre strain in* injection moulded long fibre PP at high fibre content". **Composites: Part A.** 38 (2007) : 210-216.

[13] J.L. Thomason. "*The influence of fibre length and concentration on the properties of* glass fibre reinforced polypropylene: 5. Injection moulded long and short fibre PP". **Composites: Part A.** 33 (2002) : 1641-1652.

REFERENCES (CONT.)

[14] Nick Tucker, and Kevin Lindsey. 2002. **An Introduction to Automotive Composites.** UK : *Rapra Technology Limited.*

[15] U.K.Dwivedi, Navin Chand. "Influence of MA-g-PP on abrasive wear behavior of chopped sisal fibre reinforced polypropylene composites". **Journal of Materials *Processing Technology.*** *209 (2009) : 5371-5375.*

[16] K.C.M. Nair, R.P. Kumar, S. Thomas, S.C. Schit, K. Ramamurthy. "Rheological behavior of short sisal fiber-reinforced polystyrene composites". **Composites: *Part A.*** *31 (2000) : 1231-1240.*

[17] D. Hull, T. W. Clyne. 1996. **An Introduction to Composite Materials.** 2nd ed. Cambridge Solid State Science Series.

[18] *Caroline Baillie. 2004.* ***Green composites Polymer composites and the environment.*** 1st ed. Cambridge England : Woodhead Publishing Limited.

[19] The university of Southern Mississippi, "**Ziegler-Natta vinyl polymerization**", [online]. Available: http://pslc.ws/macrog/ziegler.htm. 2005.

[20] The university of Southern Mississippi, "**Metallocene catalysis polymerization**", [online]. Available: http://pslc.ws/macrog/mcene.htm. 2005.

[21] Nutman RJ. "Agave fibres Pt. I. Morphology, histology, length and fineness: frading problems". **Empire J Exp Agr.** 1936 : 75-95.

REFERENCES (CONT.)

[22] Gram HE. "Durability of natural fibers in concrete". **Swedish Cement and Concrete Research Institute**, *Research Fo. 1983 : 225.*

[23] F.O. Anderegg, **Industrial Engineering Chemistry**, 1939 : 31,37

[24] Arsenault, "The strengthening of Al alloy 6061 by fiber and platelet SiC". **Material science and Engineering.** *1984 : 71-81.*

[25] Penning fon, D. (1979) **Ph.D thesis**, University of Liverpool.

[26] C. Albano, J. Reyes, M. Ichazo, J. Gonzalez, M. Brito, D. Moronta. "Analysisi of the *mechanical, thermal and morphological behavior of polypropylene compounds with* sisal fibre and wood flour, irradiated with gamma rays". **Polymer Degradation and Stability.** 76 (2002) : 191-203.

[27] *Bryce, Douglas M.* ***"Plastic injection Molding : Manufacturing Process Fundamentals"***. SME 1996.

[28] K.L. Fung, X.S. Xing, R.K.Y. Li, S.C. Tjong, Y.-W. Mai. "An investigation on the *processing of sisal fibre reinforced polypropylene composites*". ***Composites*** **Science and Technology.** 63 (2003) : 1255-1258.

[29] Jayamol George, R. Janardhan, J. S. Anand, S. S. Bhagawan, Sabu Thomas. "Melt *rheological behavior of short pineapple fibre reinforced low density polyethylene* composites". **POLYMER Volume 37.** 24 (1996) : 5421-5431.

REFERENCES (CONT.)

[30] P.V. Joseph, Marcelo S. Rabello, L.H.C. Mattoso, Kuruvilla Joseph, Sabu Thomas. "*Environmental effects on the degradation behavior of sisal fibre reinforced* polypropylene composites". **Composites Science and Technology.** 62 (2002) : 1357-1372.

[31] C.P.L. Chow, X.S. Xing, R.K.Y. Li. "Moisture absorption studies of sisal fibre reinforced polypropylene composites". **Composites Science and Technology.** 67 (2007) : 306-313.

[32] *Dr. Wuttipong Rungseesantivanon. 2009.* ***Seminar on Plastics-Datasheets-Applications.*** Bangkok : MTEC, Thailand Science Park.

[33] Dr. Wuttipong Rungseesantivanon. 2009. **Seminar on Plastics Injection Technology.** *Bangkok : MTEC, Thailand Science Park.*

[34] Joseph K, Thomas S, Pavithran C. "Effect of chemical treatment on the tensile properties of short sisal fibre-reinforced polyethylene composites". **Polymer.** 37 (1996) : 5139-5149.

[35] Bledzki AK, Gasssan J. "Composites reinforced with cellulose based fibres". **Prog Polym Sci.** 24 (1999) : 221-274.

REFERENCES (CONT.)

[36] Joseph PJ, Joseph K, Thomas S. "Effect of processing variables on the mechanical properties of sisal-fiber-reinforced polypropylene composites". **Composites Science and Technology**. 59 (1999) : 1625-1640.

[37] M. Sepehr, G. Ausias, P.J. Carreau. "Rheological properties of short fiber filled polypropylene in transient shear flow". **J. Non-Newtonian Fluid Mech.** 123 (2004) : 19-32.

[38] Milton Ohring. 1995. **Engineering materials science.** United States of America : Academic Press Limited.

[39] Yongli Mi, Xiaoya Chen, Qipeng Guo. "Bamboo Fiber-reinforced Polypropylene Composites: Crystallization and Interfacial Morphology". **J Appl Polym Sci.** 64 (1997) : 1267-1273.

[40] Scott A. Eastman, Alan J. Lesser, Thomas J. McCarthy. "Bamboo is a Suitable Template for Polymerizations". **J Appl Polym Sci.** 109 (2008) : 3961-3967.

[41] Wanjun Liu, Kelby Thayer, Manjusri Misra, Lawrence T. Drzal, Amar K. Mohanty. "Processing and Physical Properties of Native Grass Reinforced Biocomposites". **Polymer engineering and science.** 47 (2007) : 969-976.

[42] G. M. Mamoor, Nida Qamar, Umer Mehnood, M. S. Kamal. "Effect of short glass fiber on mechanical and rheological properties of PMMA/SBR vulcanizate". **Chemical Engineering Research Bulletin.** 13 (2009) : 51-54.

REFERENCES (CONT.)

[43] Richard P. Wool, Xiuzhi Susan Sun. 2005. **Bio-Based Polymers and Composites.** *United States of America : Elsevier Science & Technology Books.*

[44] James M. Margolis. 2006. **Engineering Plastics Handbook.** United States of America : The McGraw-Hill Companies.

[45] *Anatole A. Klyosov. 2007.* ***Wood-Plastic composites.*** *New Jersey : John Wiley & Sons, Inc., Publication.*

[46] Mark. Bikales. Overberger. Menges. 1985. **Encyclopedia of polymer science and *engineering*.** *2nd ed. Vol.01. New York : A wiley-interscience publication.*

[47] J. Catherine, G. Robert, E. Marielle, J. Appl. Polym.Sci. 61 (1996).57.

[48] Maier, Clive; Calafut, Teresa (1998). Polypropylene: the definitive user's guide and databook. William Andrew. P. 14.

[49] Weizhi Wang, Longxiang Tang, Baojun Qu. "Mechanical properties and morphological structures of short glass fiber reinforced PP/EPDM composite". ***European Polymer Journal.*** 39 (2003) : 2129-2134.

[50] S. Mukhopadhyay, R. Srikanta. "Effect of ageing of sisal fibres on properties of sisal-Polypropylene composites". **Polymer Degradation and Stability.** 93 (2008) : 2048-2051.

REFERENCES (CONT.)

[51] Adriana R. Martin, Maria Alice Martins, Odilon R.R.F. da Silva, Luiz H.C. Mattoso. "Studies on the thermal properties of sisal fiber and its constituents". **Thermochimica Acta**. 506 (2003) : 14-19.

[52] K.C. Manikandan Nair, Sabu Thomas, G. Groeninckx. "Thermal and dynamic mechanical analysis of polystyrene composites reinforced with short sisal fibres". ***Composites Science and Technology***. 61 (2001) : 2519-2529.

[53] P.V. Joseph, K. Joseph, S. Thomas, C.K.S. Pillai, V.S. Prasad, G. Groeninckx, Mariana Sarkissova. "The thermal and crystallization studies of short sisal fibre reinforced polypropylene composites". **Composites: Part A**. 34 (2003) : 253-266.

[54] Yan Li, Yiu-Wing Mai, Lin Ye. "Sisal fibre and its composites: a review of recent developments". **Composites Science and Technology**. 60 (2000) : 2037-2055.

[55] Yan-Hong Feng, Da-Wei Zhang, Jin-Ping Qu, He-Zhi He, Bai-Ping Xu. "Rheological properties of sisal fiber/poly(butylenes succinate) composites". **Polymer Testing**. 30 2011) : 124-130.

REFERENCES (CONT.)

[56] A. Bourmaud, C. Baley. "Investigations on the recycling of hemp and sisal fibre reinforced polypropylene composites". **Polymer Degradation and Stability**. 92 (2007) : 1034-1045.

Appendices

APPENDIX A

MATERIAL AND PROCESSING INFORMATION

Appendix A-1: Product information of Polypropylene HP500N

Appendix A-1: Product information of Polypropylene HP500N

Product Data and Technical Information

Email this page Print this page

Name	*Moplen*
Grade	HP500N
Resin type	Polypropylene, Homopolymer
Description	*Moplen* HP500N is a homopolymer used for gereral purpose injection moulding applications. It exhibits good flow and stiffness. *Moplen* HP500N is suitable for food contact.
Availability	Europe, Africa-Middle East

Technical data	
Density	0.9 g/cm³
Melt flow rate (MFR)	12 g/10 min (230°C/2.16kg)
Melt volume flow rate	16 cm³/10min (230°C/2.16kg)
Tensile Modulus	1550 MPa
Tensile Stress at Yield	35 MPa
Tensile Strain at Break	>50 %
Tensile Strain at Yield	10 %
Charpy unnotched impact strength	30 kJ/m² (0 °C)
Charpy unnotched impact strength	110 kJ/m² (23 °C)
Charpy notched impact strength	3 kJ/m² (23 °C)
Heat deflection temperature B (0.45 MPa) Unannealed	95 °C
Vicat softening temperature A/50	153 °C
Vicat softening temperature B/50	85 °C

Figure A-1 Scanned image of product information of polypropylene used in this study

Appendix A-2: Product information of Compoline CO/PP C55

Product information

Compolines CO/PP C05 and CO/PP C55 are polypropylenes modified with maleic anhydride. The physical form is colourless pellets with very light smell of maleic derivates.
Together with the natural compatibility with polypropylene, EPR and EPDM rubbers, the grafted groups result in excellent compatibility properties of **Compoline** with all the polar polymers (polyethylene copolymers such EVA or EMA/EBA, polyamides, polyesters, polycarbonate, polyurethane, etc...) and with all the inorganic fillers (aluminium or magnesium hydroxide, calcium carbonate, kaolin and silicate in general, talc, glass fibres, etc...).
Compoline CO/PP C05 and CO/PP C55 differ in the flexural modulus: CO/PP C55, less stiff, is recommended for HFFR compounds containing more amount of fillers.

Table 1 **Typical values of COMPOLINE CO/PP C05 and CO/PP C55**

	CO/PP C05	CO/PP C55	Unit	Method
Flexural Modulus	1250	1000	MPa	ISO 1133
Melt flow index (230° C, 2.16 Kg)	5	2.5	g/10min	ISO 1133
Melting point	168(1)	165(1)	°C	I.T.M.(3)
Graft level	High(2)	Medium(2)	%	I.T.M.(3)

Notes
1. The value was determined on the base polymer
2. Low: 0,05-0,25; Medium: 0,25-0,5; High: 0,5-1,0; Very high: >1,0
3. Internal test method

Figure A-2 Scanned image of product information of compatibilizer used in this study

APPENDIX B

PINEAPPLE FIBER THERMOPLASTIC COMPOSITE

Appendix B-1: Mechanical properties data of pineapple fiber composites

Appendix B-2: Thermal properties data of pineapple fiber composites

Appendix B-3: Rheology properties data of pineapple fiber composites

Appendix B-1: Mechanical properties data of Pineapple fiber composites

Table B-1.1 The tensile strength of pineapple fiber composites prepared at different fiber content

	Tensile strength (MPa)		
Samples	HP500N	5 wt% fiber	10 wt% fiber
1	28.86	28.52	27.72
2	28.3	28.73	27.52
3	28.09	28.35	27.27
4	28.05	28.37	27.31
5	27.62	28.42	27.18
6	28.21	28.44	27.02
7	27.95	28.27	27.13
8	28.01	28.28	27.36
9	28.42	28.21	27.08
10	28.19	28.02	27.15
AVG	28.17	27.95	27.27
SD	0.33	0.19	0.21

Table B-2.2 The percentage of elongation of pineapple fiber composites prepared at different fiber content

	Elongation (%)		
Samples	HP500N	5 wt% fiber	10 wt% fiber
1	34.45	9.08	7.04
2	24.12	8.18	6.09
3	18.12	9.08	6.96
4	21.22	8.98	6.83
5	20.7	7.73	6.35
6	23.7	11.25	6.4
7	25.4	7.18	6.38
8	22.76	8.55	6.02
9	23.7	9.03	6.95
10	25.89	9.2	6.43
AVG	24.01	8.83	6.55
SD	4.34	1.09	0.37

Table B-1.3 The Young modulus of pineapple fiber composites prepared at different fiber content

	Young Modulus (GPa)		
Samples	HP500N	5 wt% fiber	10 wt% fiber
1	1.31	1.46	1.69
2	1.36	1.54	1.70
3	1.30	1.52	1.67
4	1.30	1.51	1.66
5	1.30	1.53	1.67
6	1.32	1.48	1.66
7	1.31	1.54	1.65
8	1.31	1.50	1.69
9	1.3	1.50	1.63
10	1.3	1.50	1.64
AVG	1.31	1.51	1.67
SD	0.02	0.03	0.02

Table B-1.4 The flexural strength of pineapple fiber composite prepared at different fiber content

	Flexural strength (MPa)		
Samples	HP500N	5 wt% fiber	10 wt% fiber
1	42.42	45.24	46.77
2	42.45	44.63	46.47
3	41.77	45.68	45.73
4	42.35	45.09	46.52
5	42.28	45.37	46.45
6	42.12	44.74	46.26
7	41.84	45.07	46.70
AVG	42.19	45.12	46.41
SD	0.26	0.36	0.35

Table B-1.5 The flexural modulus of pineapple fiber composite prepared at different fiber content

	Flexural modulus (GPa)		
Samples	HP500N	5 wt% fiber	10 wt% fiber
1	1.30	1.44	1.63
2	1.31	1.42	1.59
3	1.28	1.49	1.59
4	1.30	1.47	1.61
5	1.32	1.45	1.58
6	1.31	1.42	1.56
7	1.31	1.44	1.64
AVG	1.30	1.45	1.60
SD	0.01	0.03	0.03

Table B-1.6 The Impact strength of pineapple fiber composite prepared at different fiber content

	Impact strength (J/m^2)		
Samples	HP500N	5 wt% fiber	10 wt% fiber
1	17.95	27.97	26.95
2	17.32	24.45	27.55
3	17.61	24.76	25.14
4	17.15	23.73	27.50
5	17.62	26.98	25.86
AVG	17.53	25.58	26.61
SD	0.28	1.62	0.95

Table B-1.7 The tensile strength of 10 wt% fiber with various percentage of compatibilizer

	Tensile strength (MPa) of 10% fiber				
	Percentage of compatibilizer				
	0	0.5	1	5	10
1	19.57	26.08	24.83	24.76	26.83
2	22.30	25.69	24.85	25.64	24.08
3	23.24	24.47	24.31	25.2	23.46
4	21.21	25.35	24.86	25.71	24.56
5	22.42	24.28	24.56	25.62	24.98
AVG	21.75	25.17	24.68	25.39	24.78
SD	1.42	0.78	0.24	0.4	1.28

Table B-1.8 The tensile strength of 20 wt% fiber with various percentage of compatibilizer

	Tensile strength (MPa) of 20% fiber				
	Percentage of compatibilizer				
	0	0.5	1	5	10
1	18.23	19.45	19.60	22.24	22.60
2	19.76	21.41	19.32	23.34	20.20
3	20.00	19.89	18.50	22.01	22.46
4	17.57	19.96	19.89	21.57	20.72
5	18.43	17.35	19.86	22.11	20.74
AVG	18.80	19.61	19.43	22.25	21.34
SD	1.04	1.46	0.57	0.66	1.11

Table B-1.9 The contact angle of fiber with various percentage of compatibilizer

		L	R	Mean	Work of Adhesion (mJ/m^2)
Polypropylene (HP500N)	1	78.5	80.6	79.5	86.02
	2	82.2	81.9	82.1	82.84
	3	82.7	82.8	82.8	81.96
	4	84.5	83.6	84.1	80.31
	5	79.3	77.9	78.6	87.18
			AVG	81.42	83.66
			SD	2.30	2.86
5% Fiber 0% PP-g-MA	1	47.6	48.8	48.2	121.31
	2	47.8	50.4	49.1	120.46
	3	47.1	50.1	48.8	120.88
	4	46.9	50.5	48.7	120.82
	5	46.2	49.7	48	121.55
			AVG	48.56	121.00
			SD	0.45	0.43
10% Fiber 0% PP-g-MA	1	42.1	42.9	42.5	126.47
	2	39.5	40.2	39.9	128.69
	3	44.7	47.4	46	123.34
	4	46.8	45.4	46.1	123.25
	5	38.4	39	38.7	129.61
			AVG	42.64	126.27
			SD	3.40	2.95

5% Fiber 5% PP-g-MA	1	45	43	44	125.19
	2	43.7	44.8	44.2	124.95
	3	47.1	48.2	47.7	121.84
	4	43.6	42.1	42.8	126.18
	5	44.1	46.3	45.2	124.09
			AVG	44.78	124.45
			SD	1.84	1.64

10% Fiber 5% PP-g-MA	1	44.5	46.3	45.4	123.93
	2	36.7	38.9	37.8	130.34
	3	41.9	43.3	42.6	126.36
	4	41.4	42.9	42.2	126.76
	5	43	46.1	44.5	124.72
			AVG	42.5	126.42
			SD	2.94	2.48

Appendix B-2: Thermal properties data of Pineapple fiber composites

Table B-2.1 The heat distortion temperature of pineapple fiber composite prepared with different fiber content

	Heat distortion temperature (°C)		
	Polypropylene (HP500N)	5 wt% fiber	10 wt% fiber
1	61.3	63.1	66.4
2	61.0	63.3	66.3
3	62.1	63.3	64.9
4	61.3	62.3	65.1
5	62.2	63.1	66.4
AVG	61.58	63.02	65.82
SD	0.54	0.41	0.75

Appendix B-3: Rheology properties data of Pineapple fiber composites

Table B-3.1 The shear viscosity versus shear rate at low shear rate of temperature 210 °C with various fiber content

HP500N		5 wt% fiber		10 wt% fiber	
Shear rate (1/s)	Shear viscosity (Pa.s)	Shear rate (1/s)	Shear viscosity (Pa.s)	Shear rate (1/s)	Shear viscosity (Pa.s)
0.000198	4014	0.000185	6.18E+04	0.000188	5.05E+04
0.000264	2274	0.000255	3.20E+04	0.000263	2.49E+04
0.00035	1851	0.000352	2.28E+04	0.000352	1.63E+04
0.000471	1713	0.000463	1.77E+04	0.00047	1.26E+04
0.000619	1651	0.000618	1.35E+04	0.000622	1.05E+04
0.000815	1618	0.000816	1.16E+04	0.000818	9702
0.001085	1597	0.001082	9991	0.001091	8924
0.001439	1583	0.001438	9011	0.001442	8038
0.001912	1573	0.001913	8089	0.001905	6984
0.002528	1550	0.002531	6790	0.002525	6326
0.003355	1502	0.003355	6106	0.003358	5917
0.004448	1465	0.004447	5712	0.004445	5690
0.005889	1443	0.005888	5515	0.005897	5555
0.00781	1472	0.007813	5287	0.007811	5413
0.01036	1566	0.01035	4913	0.01035	5018
0.01373	1541	0.01372	4545	0.01373	4791
0.0182	1500	0.01823	4623	0.01822	4890
0.02413	1482	0.02412	4216	0.02412	4579
0.03202	1548	0.03196	3989	0.03195	4318
0.04245	1528	0.04236	3871	0.04232	4184
0.05616	1505	0.05615	3564	0.05622	4039
0.07461	1502	0.07423	3315	0.07422	3829

0.09879	1499	0.09893	3055	0.099	3543
0.131	1467	0.1305	2814	0.1306	3284
0.1735	1454	0.1732	2639	0.1732	3051
0.2299	1419	0.2296	2478	0.2298	2786
0.3055	1385	0.3045	2362	0.3048	2554
0.4046	1373	0.4043	2209	0.4046	2391
0.5362	1358	0.5363	2071	0.5362	2249
0.711	1314	0.7109	1949	0.7109	2105
0.9427	1258	0.9422	1762	0.9423	2016
1.25	1186	1.25	1650	1.249	1872
1.657	1126	1.657	1545	1.656	1706
2.196	1090	2.196	1355	2.197	1580
2.912	949	2.912	1223	2.913	1450
3.859	798	3.86	998	3.858	1192
5.116	705	5.115	828.2	5.118	945
6.783	598	6.785	670.2	6.782	794
8.993	450	8.992	519.4	8.995	638
11.92	331.7	11.92	435.2	11.92	498
15.81	250	15.8	328	15.81	420
20.96	195.7	20.95	281	20.97	327
27.79	130	27.78	198	27.77	241.7
36.81	102	36.83	150	36.82	187.4
48.82	84.5	48.83	123	48.81	147.4
64.72	68	64.71	85	64.74	107
85.81	60	85.79	70	85.8	98
113.8	52	113.7	65	113.8	82
150.8	39	150.8	52	150.8	65
199.9	35	199.9	50	199.9	60

Table B-3.2 The shear viscosity versus shear rate at high shear rate of temperature 210 °C with various fiber content

HP500N		5 wt% fiber		10 wt% fiber	
Shear rate (1/s)	Shear viscosity (Pa.s)	Shear rate (1/s)	Shear viscosity (Pa.s)	Shear rate (1/s)	Shear viscosity (Pa.s)
9.96	734.37	9.94	636.62	9.96	576.27
46.04	439.12	46.03	516.74	45.98	539.72
98.88	271.36	98.90	360.07	98.87	406.78
499.92	118.22	499.93	157.90	499.92	185.07
1000.21	77.13	1000.21	108.25	1000.22	125.06

Table B-3.3 The shear viscosity versus shear rate at low shear rate of 10 wt% fiber with different temperature

210°C		220°C		230°C	
Shear rate (1/s)	Shear viscosity (Pa.s)	Shear rate (1/s)	Shear viscosity (Pa.s)	Shear rate (1/s)	Shear viscosity (Pa.s)
0.000188	5.05E+04	0.000202	7.12E+04	0.000174	1.77E+04
0.000263	2.49E+04	0.000266	3.02E+04	0.000267	5000
0.000352	1.63E+04	0.000361	1.67E+04	0.000351	3137
0.00047	1.26E+04	0.000471	1.05E+04	0.000468	3496
0.000622	1.05E+04	0.000607	6741	0.000617	3198
0.000818	9702	0.000819	5632	0.000825	3653
0.001091	8924	0.001088	5808	0.001092	3794
0.001442	8038	0.001442	5211	0.001436	3832
0.001905	6984	0.001908	5230	0.0019	3978
0.002525	6326	0.002519	5255	0.002526	4065
0.003358	5917	0.003353	5445	0.003357	4095

0.004445	5690	0.004448	5649	0.004448	4091
0.005897	5555	0.005894	5671	0.005898	3909
0.007811	5413	0.007814	5508	0.007812	3771
0.01035	5018	0.01036	5192	0.01036	3768
0.01373	4791	0.01372	5148	0.01374	3745
0.01822	4890	0.01821	5056	0.01819	3441
0.02412	4579	0.02413	4842	0.02416	3523
0.03195	4318	0.03194	4656	0.03201	3347
0.04232	4184	0.0423	4392	0.04246	3179
0.05622	4039	0.0564	4256	0.05622	2954
0.07422	3829	0.07447	3949	0.07469	2759
0.099	3543	0.09889	3598	0.09861	2551
0.1306	3284	0.1311	3304	0.1313	2304
0.1732	3051	0.174	3014	0.1737	2053
0.2298	2786	0.2301	2781	0.2304	1803
0.3048	2554	0.3055	2606	0.3056	1628
0.4046	2391	0.4047	2407	0.4044	1507
0.5362	2249	0.5362	2229	0.5363	1396
0.7109	2105	0.7112	2148	0.7109	1288
0.9423	2016	0.9424	1977	0.9426	1190
1.249	1872	1.249	1821	1.25	1095
1.656	1706	1.657	1662	1.657	937
2.197	1580	2.197	1441	2.196	735.5
2.913	1336	2.912	1127	2.912	582
3.858	1068	3.86	910.7	3.86	439.2
5.118	874	5.117	716.3	5.116	315.4
6.782	746.7	6.782	528	6.785	250
8.995	619.3	8.992	450	8.995	180
11.92	500	11.93	350	11.92	150
15.81	402.9	15.81	270	15.8	130
20.97	356.1	20.95	235.6	20.95	120

27.77	241.7	27.77	196.9	27.78	90
36.82	187.4	36.82	150	36.82	80
48.81	147.4	48.82	119.3	48.82	70
64.74	110	64.72	94.45	64.74	60
85.8	80	85.8	68.39	85.8	40
113.8	60	113.8	48.84	113.8	27.84
150.8	40	150.8	31.68	150.8	13.78
199.9	35	199.9	29.22	199.9	12.8

Table B-3.4 The shear viscosity versus shear rate at high shear rate of 10 wt% fiber with different temperature

210°C		220°C		230°C	
Shear rate (1/s)	Shear viscosity (Pa.s)	Shear rate (1/s)	Shear viscosity (Pa.s)	Shear rate (1/s)	Shear viscosity (Pa.s)
9.96	576.27	9.96	529.95	9.96	402.18
45.98	539.72	45.97	434.47	45.97	329.15
98.87	406.78	98.87	364.42	98.82	296.16
499.92	185.07	499.91	162.74	499.91	150.69
1000.22	125.06	1000.13	110.68	1000.21	102.38

Table B-3.5 The melt flow index of pineapple fiber composites at different fiber content under temperature 230°C

	Melt flow index at 230°C (g/10 min)		
	HP500N	5 wt% fiber	10 wt% fiber
1	12	10.56	6.96
2	12	9.36	6.72
3	12	10.92	6.84
4	12	9.48	6.84
5	12	10.32	6.84
AVG	12	10.13	6.84
SD	0	0.68	0.085

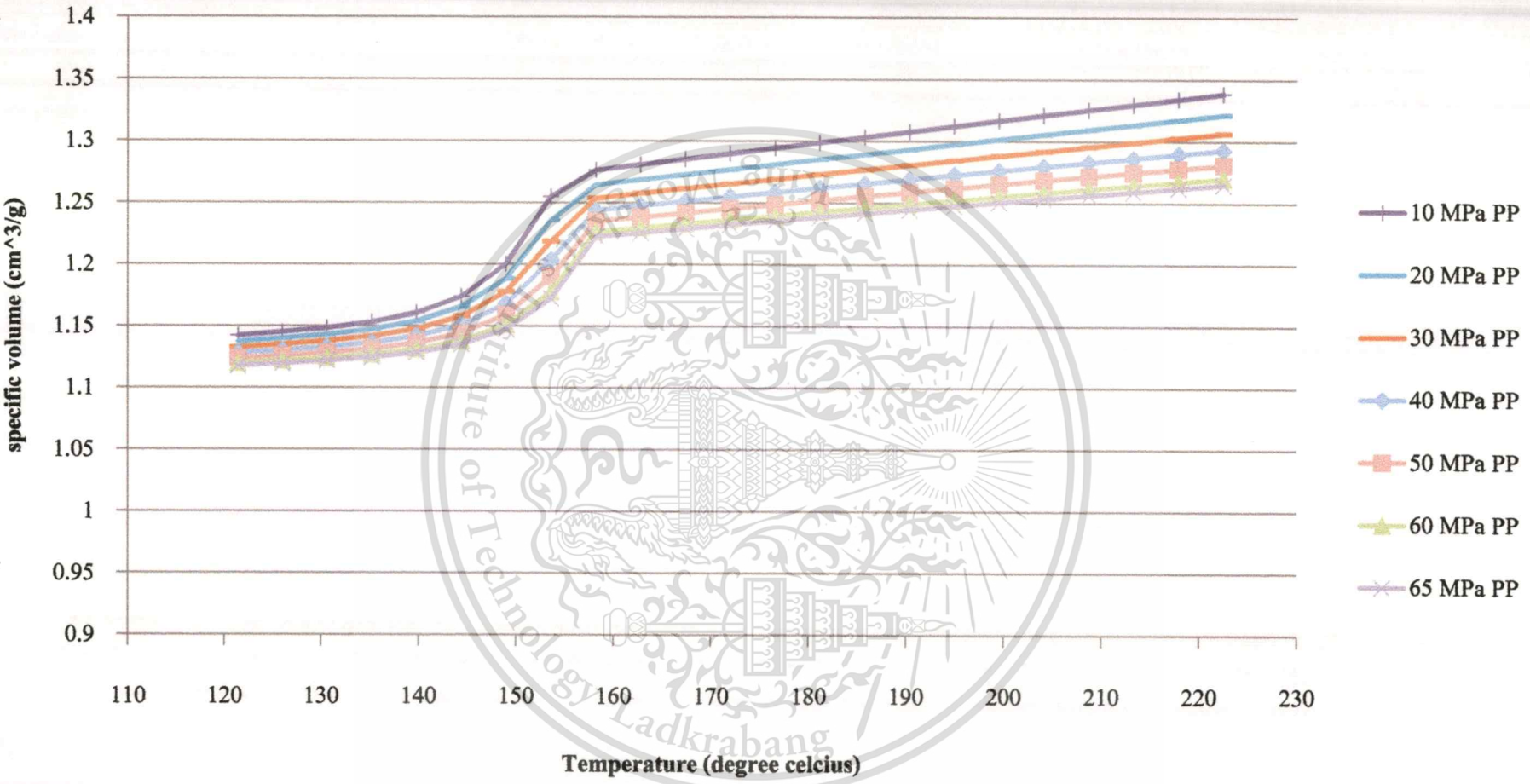

Figure B-3.1 Pressure-volume-temperature of Polypropylene (HP500N)

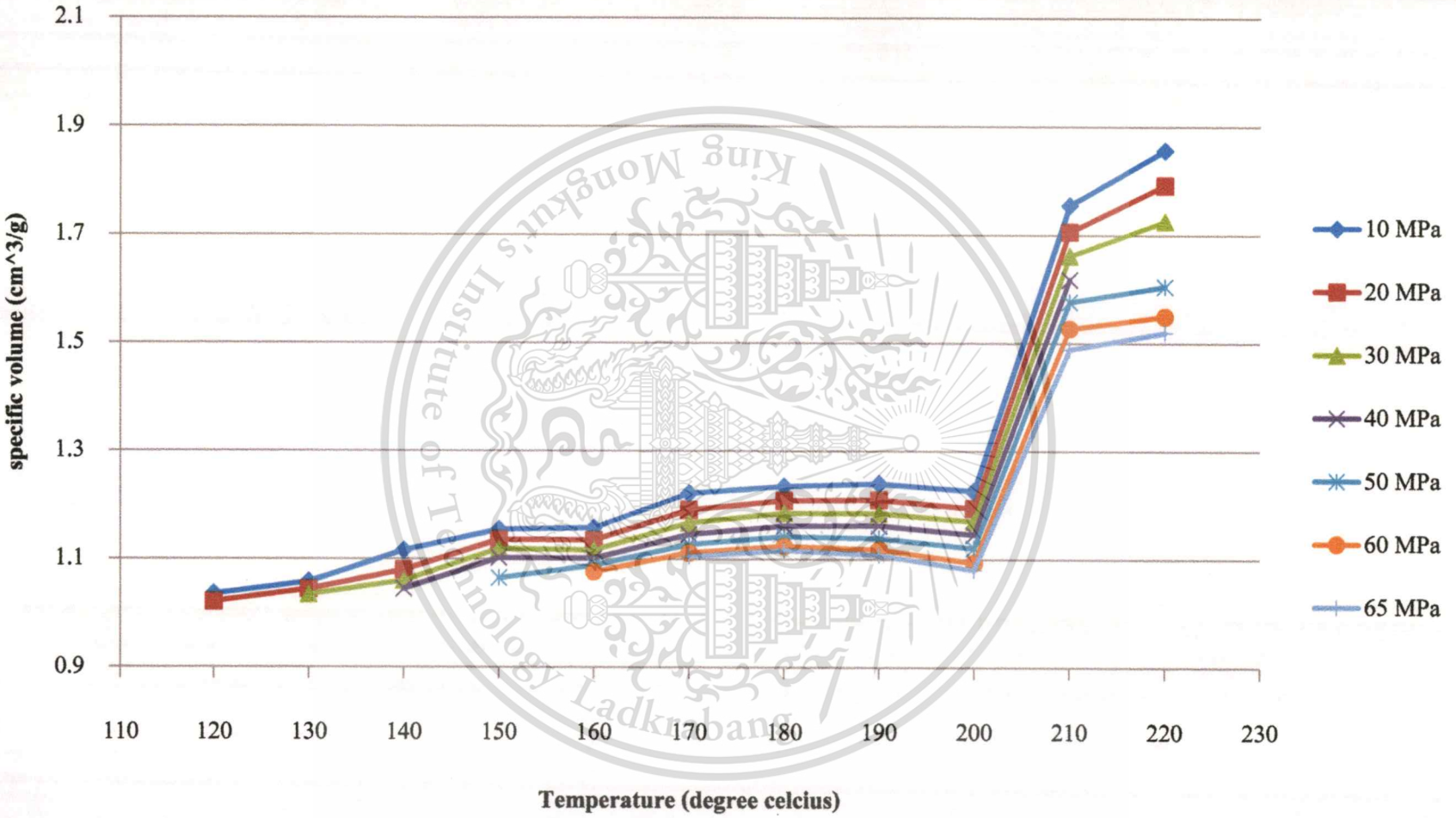

Figure B-3.2 Pressure-volume-temperature of 5 wt% Fiber

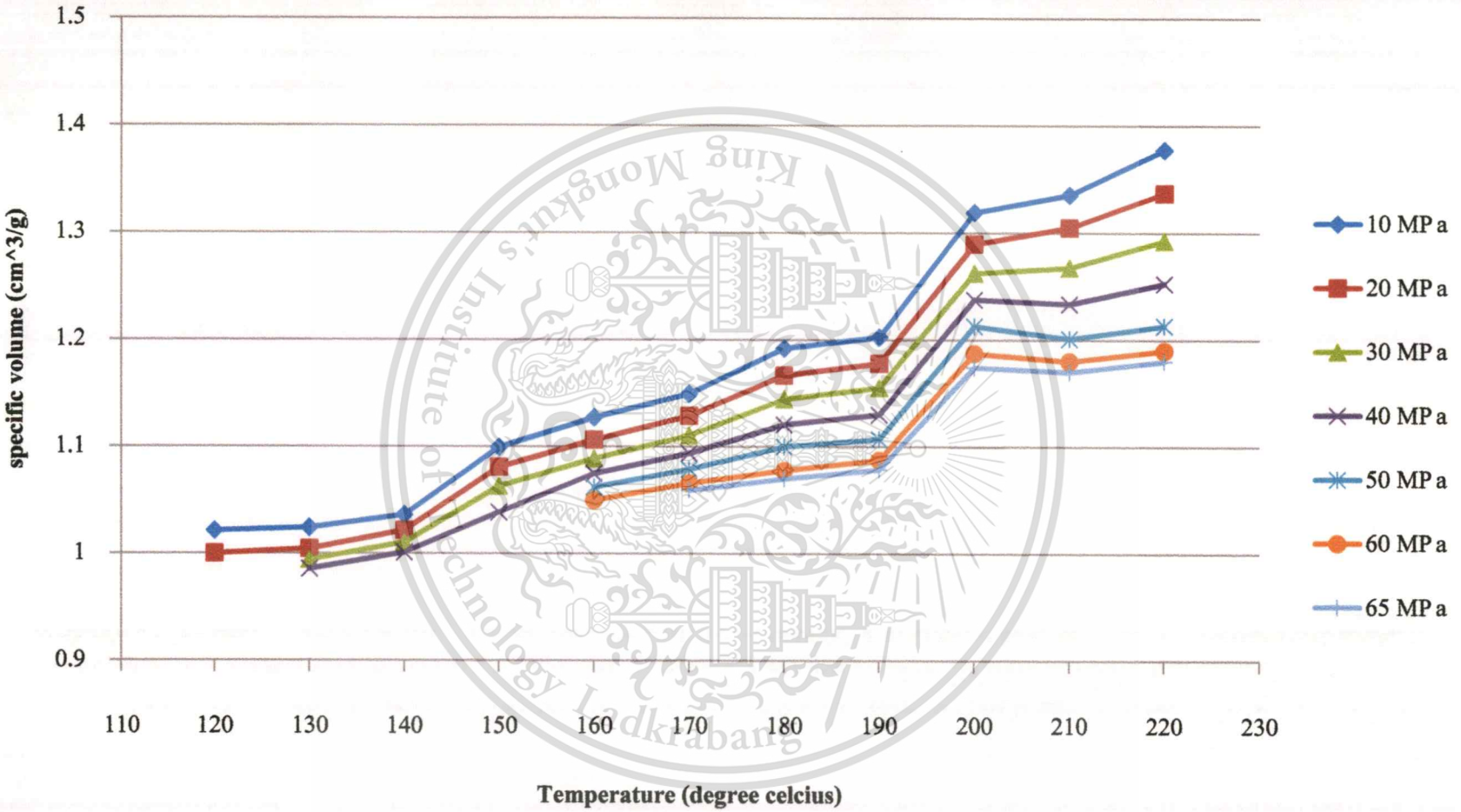

Figure B-3.3 Pressure-volume-temperature of 10 wt% Fiber

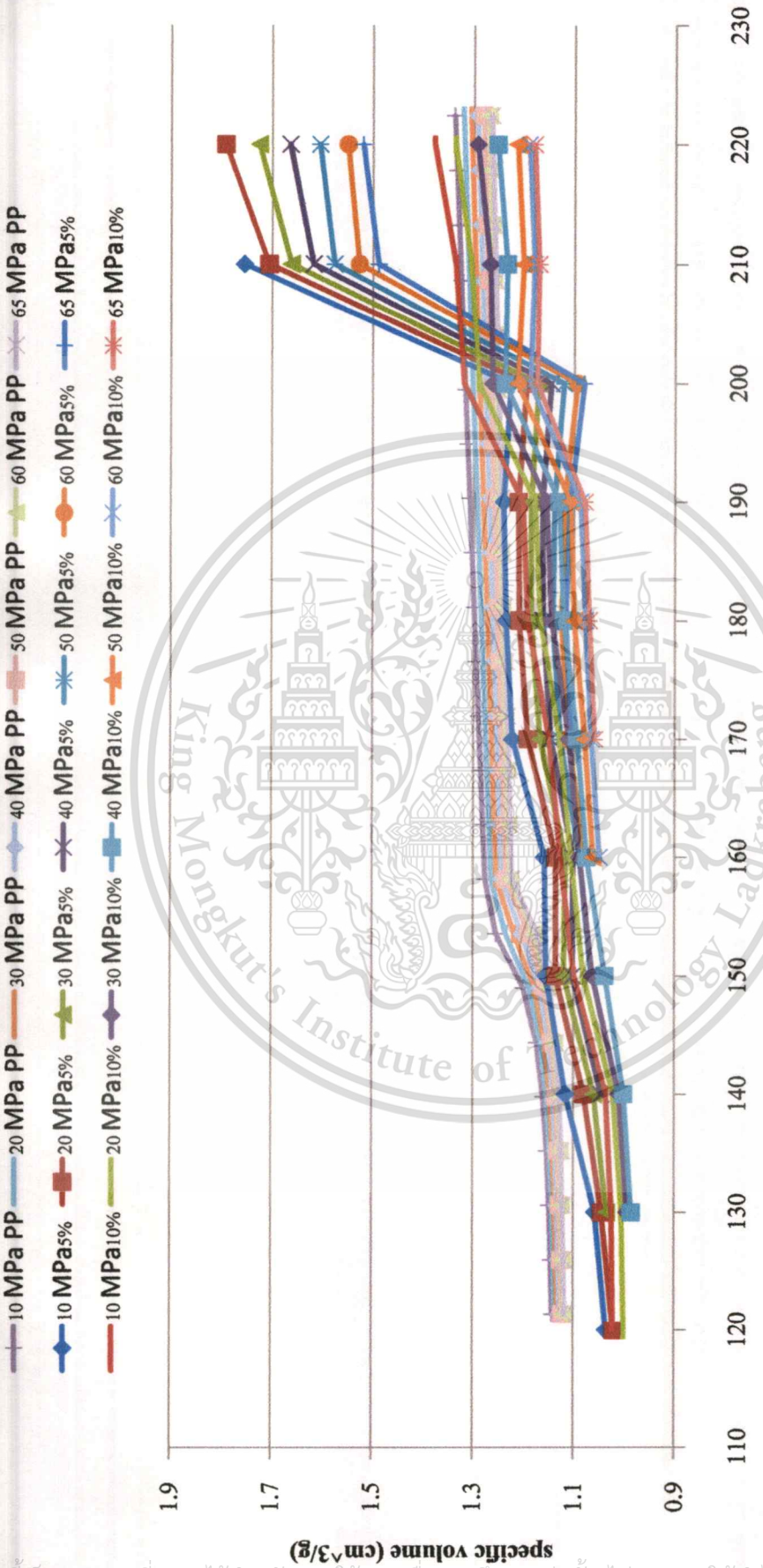

Figure B-3.4 Comparision of Pressure-volume-temperature of Polypropylene HP500N, 5 wt% Fiber and 10 wt% fiber

BIOGRAPHY

Name: Mr. Ratchaphon Tangnopphapaton

Date of Birth: April 01, 1986

Place of Birth: Nakornratchasima, Thailand

Education:

2004-2008	B. Eng. in Mechanical Engineering (2nd class honour), Department of Mechanical Engineering, Sirindhorn International Institute of Technology (SIIT), Thammasat University.
2008-2011	M. Eng. in Automotive Engineering (International program), International College, King Mongkut's Institute of Technology Ladkrabang (KMITL)

Honour and Scholarships:

2007	Received SIIT scholarship award for academic excellence and good conduct
2008	Received B. Eng. with the 2nd class honour in Mechanical Engineering
2008-2011	Full scholarship for study in the master degree from National Science and Technology Development Agency (NSTDA)

Publications:

1. R. Tangnopphapaton, S. Areerat, W. Rungseesantivanon, T. Saito, I. Satoh, N. Prakymoramas, B. Hararak, D. Thanomjitr. "Mechanical Properties of Natural fiber Thermoplastic composite (PP Matrix)". Proceeding of the 9th Asian workshop on Polymer Processing 2010, Alloy & Blend & Composite, Hanoi, Vietnam, December 7-10, 2010. pp 304-307.